Department of Physics and Astronomy

Heidelberg University

Master thesis

in Physics

submitted by

Maya Hager

born in Munich

2023

RESTORING NATURALNESS

TO

COMPOSITE HIGGS MODELS

This Master thesis has been carried out by Maya Hager

at the

Max-Planck Institut für Kernphysik

under the supervision of

Dr. Florian Goertz

ZUSAMMENGESETZTE HIGGS–MODELLE: WIEDERHERSTELLUNG DER NATÜRLICHKEIT

Zusammengesetze Higgs Modelle eröffnen eine Möglichkeit, das Hierarchie Problem zu lösen, da das Higgs nicht mehr als elementares Teilchen, sondern als Bindungszustand einer neuen starken Interaktion betrachtet wird. Es entsteht als pseudo–Nambu–Goldstone Boson einer spontanen Symmetriebrechung. Demzufolge besitzt das Higgs kein tree–level Potential und die radiative Korrekturen zur Higgs Masse werden bei der Kompositätsskala abgeschnitten. In den letzten Jahren haben ausbleibende experimentelle Beobachtungen anderer Bindungszuständen dazu geführt, dass die Kompositätsskala höher und höher erwartet wird, was ein *kleines Hierarchie Problem* verursacht. Diese zusätzlichen Bindungszustände sind eine universelle Vorhersage von zusammengesetzten Higgs Modellen und vom leichtesten neuen Zustand wird erwartet, dass er die Quantenzahlen des Top besitzt. In dieser Arbeit zeigen wir, wie exotische Fermionen die Natürlichkeit von zusammengesetzten Higgs Modellen wiederherstellen können und für den leichtesten neuen Bindungszustand andere Quantenzahlen vorhersagen. Die Exoten heben den quadratischen Beitrag des Tops zum Higgs Potential auf, and treten natürlicherweise in zusammengesetzten grossen vereinheitlichten Theorien auf. Wir stellen ein Modell–Bau Rezept vor, das es ermöglicht den Mechanismus in andere Modelle miteinzubauen. In den zwei beispielhaft untersuchten Restklassen besitzt der leichteste Bindungszustand die Baryonenzahl $B = 2/3$, was zu einem komplizierten Zerfall mit sechs finalen Teilchen führt, eine Signatur nach der am LHC bisher noch nicht gezielt gesucht wurde.

RESTORING NATURALNESS TO COMPOSITE HIGGS MODELS

Composite Higgs models offer a solution to the hierarchy problem, as the Higgs is no longer an elementary particle, but instead a bound state of some new strong interaction and it arises as a pseudo–Nambu–Goldstone boson of a spontaneous symmetry breaking. Consequently, there is no tree–level potential and the radiative corrections to the Higgs mass are cut off around the compositeness scale. However, in recent years the compositeness scale has been pushed higher and higher, reintroducing a *little hierarchy problem*, which stems from the non–observation of additional composite resonances with top–like quantum numbers at colliders, an ubiquitous prediction of composite Higgs models. In this work we show how exotic fermions can restore naturalness to composite Higgs models and furthermore predict a lightest composite resonance that differs with respect to generic composite Higgs models. The quadratic contribution of the exotic fermions to the scalar potential cancels the quadratic top contribution and the exotics arise naturally in composite Grand Unified Theories. We give a model–building recipe of how the cancellation mechanism can be included in other models. Two exemplary cosets are analysed in which the lightest partner carries baryon number $B = 2/3$, leading to a complicated six–particle final state, a signature not yet explored at the LHC.

Contents

List of Abbreviations

AdS/CFT	**A**nti–**d**e–**S**itter / **C**onformal **F**ield **T**heory
BC	**B**oundary **C**onditions
BR	**B**ranching **R**atio
BSM	**B**eyond–**S**tandard–**M**odel
CCWZ	**C**allan–**C**oleman–**W**ess–**Z**umino
CH	**C**omposite **H**iggs
CHM	**C**omposite **H**iggs **M**odels
dof	**d**egree **o**f **f**reedom
EFT	**E**ffective **F**ield **T**heory
EW	**E**lectro**W**eak
EWSB	**E**lectro**W**eak **S**ymmetry **B**reaking
FCNC	**F**lavour **C**hanging **N**eutral **C**urrents
GHGUT	**G**auge–**H**iggs **G**rand **U**nified **T**heory
GUT	**G**rand **U**nified **T**heory
IR	**I**nfra**R**ed
KK	**K**aluza–**K**lein
LH	**L**eft–**H**anded
LHC	**L**arge **H**adron **C**ollider
LQ	**L**epto**Q**uark
NGB	**N**ambu–**G**oldstone–**B**oson
PC	**P**artial **C**ompositeness
pNGB	**p**seudo–**N**ambu–**G**oldstone–**B**oson
QCD	**Q**uantum **C**hromo**D**ynamics
QFT	**Q**uantum **F**ield **T**heory
RH	**R**ight–**H**anded
SM	**S**tandard **M**odel
SSB	**S**pontaneos **S**ymmetry **B**reaking
SUSY	**SU**per–**SY**mmetry
UV	**U**ltra**V**iolet
vev	**V**acuum **E**xpectation **V**alue
VL	**V**ector–**L**ike

List of Symbols

$\mathcal{L}$	Lagrangian density	$[ET/L^4]$
f	SSB scale	$[(ET)/L^2]^{1/2}$
v	vev of physical Higgs field	$[(ET)/L^2]^{1/2}$
v_{SM}	vev of SM Higgs field	$[(ET)/L^2]^{1/2}$
m_E	elementary Dirac mass	$[L]^{-1}$
m_*	resonance mass scale	$[L]^{-1}$
g_*	coupling in strong sector	$[ET]^{-1/2}$
λ	linear mixing between elementary and composite sector	$[ET]^{-1/2}$
ω_R	right–handed mirror fermion	$[ET/L^3]^{1/2}$
θ_L	left–handed mirror fermion	$[ET/L^3]^{1/2}$

Chapter 1

Introduction

The Standard Model (SM) of particle physics has been immensely successful in describing nature how we see it. With the confirmation of the existence of the Higgs boson in 2012 ([1, 2]) the last puzzle piece seemed to fall into place. Still, there are many unresolved issues that simply cannot be explained within the SM, such as the nature of dark matter and dark energy, the origin of the observed baryon asymmetry, the flavour hierarchy and several more. In this thesis we will focus on different aspects, which are the unexplained hierarchy found within the Higgs sector of the SM, as well as the idea of unification of the SM gauge groups. The former arises when looking at the scales in nature

$$\begin{aligned} M_{\text{Pl}} &\sim 10^{19}\ \text{GeV} \\ M_{\text{GUT}} &\sim 10^{15}\ \text{GeV} \\ M_{\text{Higgs}} &\sim 125\ \text{GeV}\ . \end{aligned}$$

There is a clear separation between the Higgs mass M_{Higgs}, and the Planck scale M_{Pl} at which gravity can no longer be treated perturbatively. If the SM gauge groups unify, there are still many orders of magnitude between M_{Higgs} and the expected unification scale M_{GUT}. Examining the SM, out of all present parameters, the Higgs mass m_H is the only fundamental parameter that features an energy scale instead of being dimensionless. In contrast, the Quantum Chromodynamics (QCD) scale Λ_{QCD} emerges from the condensation of the strong sector, when the strong coupling $\alpha_s \approx 1$. The measured Higgs mass is a combination of a bare mass term, and radiative corrections due to quantum fluctuations. The fermionic one-loop contribution to m_H^2 can be seen in Fig. 1.1. Of course, there are additional radiative corrections from gauge bosons and the Higgs boson itself, but due to its large Yukawa y_t the top predominates. It can be calculated to be (see e.g. [3])

$$\delta m_H^2 \propto \frac{y_t^2}{16\pi^2}\Lambda_{\text{UV}}^2 \tag{1.1}$$

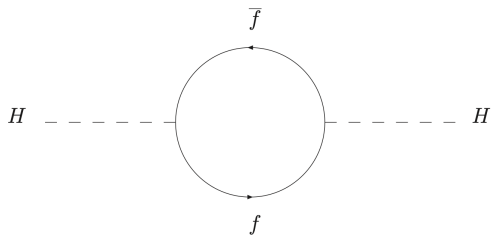

FIGURE 1.1: Quadratically divergent fermionic one-loop corrections to the Higgs mass. Diagram taken from [3]

which is quadratically divergent. Here, Λ_{UV} is the ultraviolet scale until which the theory is assumed to be valid, i.e. the scale at which new physics is expected. By the same logic by which operators with dimension $d > 4$ are expected to be suppressed by $\Lambda_{\text{UV}}^{4-d}$, which in turn means that all non–SM effects are highly suppressed at low energies, the only $d = 2$ term should be enhanced by Λ_{UV}^2. Then, if the SM holds up to Planck–scale energies, the corrections to the Higgs mass will be of the order of 10^{36} GeV^2. To achieve $m_H = 125$ GeV, the bare mass term of the Higgs has to cancel δm_H^2 with a precision of 10^{32}, which leads to the *hierarchy problem*.

To solve the hierarchy problem, new physics is required that goes beyond the standard model (BSM), and usually lies around the TeV scale, since the scale should be as low as possible to improve the hierarchy between Higgs mass and new mass scale. In most models a TeV scale is the lowest scale that does not lead to conflict with experimental predictions. Furthermore, the BSM theory has to respect additional symmetries, such as baryon and lepton number, since corresponding problematic $d > 4$ operators are no longer sufficiently suppressed, as can be argued if e.g. $\Lambda_{\text{UV}} \sim M_{\text{Pl}}$.

One such idea are composite Higgs models (CHM) ([4–9]), which are inspired by QCD and electroweak symmetry breaking (EWSB). The Higgs, which is a bound state, arises as a Nambu–Goldstone–Boson (NGB) of some spontaneous symmetry breaking (SSB) $G \to H$. In addition, G is broken explicitly which leads to the Higgs becoming a pseudo–Nambu–Goldstone boson (pNGB) and acquiring both mass and potential. The SM is then seen as a low–energy effective field theory (EFT), valid up to the compositeness scale. If the Higgs is such a bound state, the scale of new physics, i.e. the compositeness scale, has to be $\sim$ TeV to address the hierarchy problem.

In CHMs, the lure of unification increases, since $M_{\text{GUT}} \gg M_{\text{Higgs}}$ no longer poses the same hierarchy problem as before. Grand Unified Theories (GUTs) unify all three gauge groups of the SM into one symmetry group G_{GUT}, such as $SU(5)$ or $SO(10)$, therefore bringing us closer to a complete description of nature. GUTs can be made part of CHMs if G is enlarged to fit G_{GUT}. There are two possible descriptions of such a model. One are the four–dimensional composite dynamics that have been mentioned so far and we refer to them as composite GUTs. Another possibility are five–dimensional holographic models, which feature a warped extra dimension. One such example is the holographic $SU(6)$ Gauge–Higgs GUT (GHGUT) by [10], which will be in the focus of this thesis, where the Higgs is the fifth component of the same five–dimensional gauge field as the SM gauge bosons. Due to the duality between weakly coupled five–dimensional theories and strongly–coupled four dimensional theories the GHGUT model can be treated as a composite GUT. More on the equivalence will be explained in Sec. 2.3.3, and a holographic dictionary will be given.

CHMs are not without fault, and often they predict additional particles that should have already been observed at the Large Hadron Collider (LHC). Additionally, the interaction behaviour of a composite Higgs differs from the SM expectation and the bounds stemming from non–observations of these fields and effects push most models to higher and higher tuning, therefore reintroducing a *little hierarchy problem*. It is very much a matter of taste how much tuning one is willing to accept within a theory, but since the very essence of the hierarchy problem is an unnatural cancellation, attempts to solve it should, as a general guideline, aim to minimise tuning as much as possible, which we will attempt to do here.

In this thesis we study the generation of the Higgs potential within CHMs and its relation to the above mentioned problems. A particular focus is placed on the

little hierarchy problem. The thesis consists of three main parts. Firstly, in Chapter 2 the physical basis for the following work is given, which includes reviews on composite Higgs, on GUTs and on the combination of both in the $SU(6)$ GHGUT. Then, in Chapter 3 the scalar potential of the four–dimensional incarnation of the originally five–dimensional GHGUT model is determined analytically via a spurion analysis as well as numerically within the three–site model, and some phenomenological aspects are investigated further, such as the non–custodial nature of the coset $SU(6)/SU(5)$. During the work on Chapter 3 we found a group theoretical mechanism that allows to cancel the quadratic contribution of a fermion to the Higgs potential. The mechanism is generalised and proven mathematically, and furthermore a holographic completion is supplied. Then, it is applied to two exemplary models in Chapter 4 which are analysed both analytically and numerically. The mechanism features a strong decrease in tuning, and in combination with an accidental baryon number symmetry, which is part of both studied cosets and that forbids proton decay, so far unexplored collider signatures of exotic fermions with baryon number $B = 2/3$ are predicted. Lastly, we conclude in Chapter 5 and give a small outlook.

Chapter 2

Basics

While space–time is described by the Poincare group, matter is described with the help of gauge groups. It is apparent that symmetries play a fundamental role in physics. They are an important guiding principle both in the SM and in theories that go beyond it, such as in composite Higgs models (Sec. 2.1), where the Higgs is the pNGB of a spontaneous symmetry breaking, which addresses the hierarchy problem, since shift symmetry[1] forbids a Higgs potential at tree–level, therefore leading to a naturally light Higgs. Additionally, symmetries can hint at fundamental structures hidden in our every–day world. For instance, the SM gauge groups can be unified beautifully into one symmetry group, as is done in Grand Unified Theories (Sec. 2.2). Combining both approaches, i.e. composite Higgs and GUTs, by choosing a subgroup H that contains all three SM gauge groups, and a group G that contains G_{GUT}, leads to Gauge-Higgs Grand Unified Theories (GHGUT) (Sec. 2.3), where in the here–introduced incarnation the Higgs is a pNGB from the coset $SU(6)/SU(5)$, along with a scalar leptoquark and a scalar singlet.

2.1 Composite Higgs

In composite Higgs models, the EW scale is an emergent scale, very much like Λ_{QCD}, and has a strongly coupled origin. As a consequence, the Higgs, like any other scalar particle we have observed in nature so far, is a bound state. Due to dimensional transmutation, its mass is insensitive to new physics above the scale at which the condensation occurs, and therefore stable under quantum corrections. A well–known analogue is the pion, which is the lightest QCD bound state, and arises from chiral symmetry breaking. The following review, as well as most of the methods used in this thesis, follow the extensive lecture notes by G. Panico and A. Wulzer ([11]). See [12] for a more compact review.

In composite Higgs models a global symmetry group G is spontaneously broken to subgroup H, where H contains the EW gauge group G_{EW}. In Sec. 2.3 we will require H to contain the full SM gauge group including colour, but in most composite Higgs incarnations $SU(2)_L \otimes U(1) \subset H$ is sufficient. Previous ideas to solve the hierarchy problem included technicolor models ([13, 14]) where $G_{\text{EW}} \subset G$ is fully broken by condensation, which leads to electroweak symmetry breaking (EWSB) at scale $v \sim f$, but since technicolor models do not predict an elementary–like Higgs, they lost attractiveness in 2012.

If the Higgs was a generic bound state, many bound states would be expected at the same scale, but none have been observed. Therefore, the pNGB nature of the Higgs is essential. Due to it, the Higgs mass is naturally lighter since it is protected by both shift symmetry and compositeness. The Goldstone theorem ([15–18])

[1] In 5D the tree level Higgs potential is forbidden by gauge symmetries.

states that if a continuous global symmetry G is spontaneously broken to subgroup H, massless scalar particles, Nambu–Goldstone bosons (NGB), appear, one per broken generator. If there is additional explicit symmetry breaking of G the NGBs acquire a mass and a potential and become pNGBs. In an exact global symmetry it is always possible to perform a coordinate transformation to set the vev to zero. Instead, after explicit symmetry breaking the vacuum becomes *misaligned*, which is often parametrised by the vacuum misalignment angle ξ defined as

$$\xi \equiv \frac{v^2}{f^2} \,,$$

where v is the Higgs vev and f the scale of SSB[2]. Due to phenomenological constraints $\xi \ll 1$ is required, which will be seen e.g. in Sec. 2.1.2 and throughout the whole thesis. In the case of CHMs one source of the explicit symmetry breaking comes from the gauging of the EW group $G_{\text{EW}} \subset H \subset G$. Additionally, the coupling to SM fermions also breaks G explicitly, as the fermions transform only under the SM gauge groups and not under the full G. In the framework of partial compositeness, where the fermionic mass eigenstates are a mixture of elementary and composite states (which will be explained in detail in Sec. 2.1.1), a CHM consists of three sectors, one composite sector $\mathcal{L}_{\text{composite}}$ in which the Higgs and other composite states live, an elementary sector $\mathcal{L}_{\text{elementary}}$ which contains the SM fields, and mixing $\mathcal{L}_{\text{mixing}}$ between them

$$\mathcal{L} \supset \mathcal{L}_{\text{elementary}} + \mathcal{L}_{\text{composite}} + \mathcal{L}_{\text{mixing}} \,. \tag{2.1}$$

Explicit breaking comes from $\mathcal{L}_{\text{mixing}}$. Through linear interactions between composite operators and SM fields, the Higgs potential is generated. Generally, as in any EFT, every term that is not explicitly forbidden by symmetry arguments should appear. This is immensely useful and it allows us to write down effective theories without the need to know every single detail of the underlying dynamics, since the composite dynamics can be factored out. Such is the case with CHMs, where knowing the global group G and its subgroup H is enough to make relevant predictions, without specifying every detail of the SSB, which here occurs due to the condensation of strongly coupled fields. The fields then form bound states after condensation, to which we will refer generically as composite sector states. It is common to not specify a UV–complete composite sector, although attempts to do so exist, see e.g. [19–28]. The most minimal CHM is $SO(5)/SO(4)$ ([29]), where the coset contains exactly four broken generators, which then furnish the complex Higgs doublet. Non–minimal models often feature additional pNGBs, as will be the case for the $SU(6)/SU(5)$ model analysed in Chapter 3. An overview over some of the studied cosets is given in [30].

Details on the Callan–Coleman–Wess–Zumino (CCWZ) construction ([31, 32]) used to calculate the pNGB potential are delayed until Chapter 3, where they are explained while simultaneously performing the analysis in the GHGUT model.

2.1.1 Partial Compositeness

In this subsection we will give more details on the nature of $\mathcal{L}_{\text{mixing}}$ from Eq. (2.1). In the framework of partial compositeness (PC) ([9, 29, 33]) the SM fields are not

[2] As will become clear in Sec. 3.2.1, the Higgs vev is not in one–on–one correspondence with the vev of the corresponding pNGB field Π. Instead, $v = f \sin(\langle \Pi \rangle / f)$.

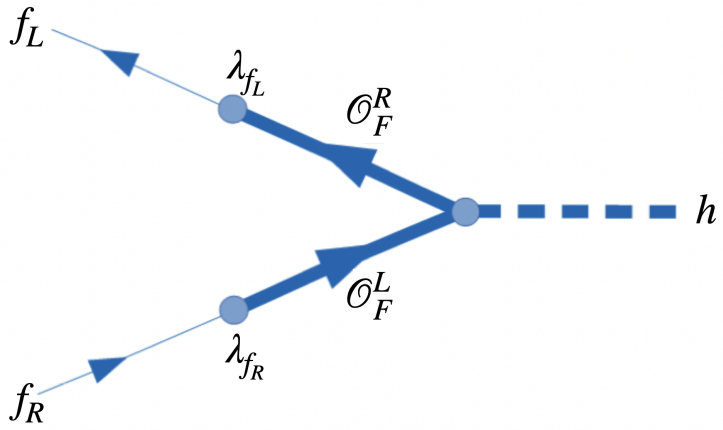

FIGURE 2.1: Linear coupling λ of elementary SM fermions $f_{L/R}$ to composite operators $\mathcal{O}_F^{R/L}$. Adapted from [12].

fully external to the composite sector, in contrast to what had been done before in technicolor ([13, 14, 34, 35]) or within certain composite Higgs models ([8]). The problem with completely external elementary fields is that it becomes difficult to generate large Yukawas while offering a solution to the hierarchy problem, or that they lead to the prediction of flavour–violating interactions which are phenomenologically not viable (see for small review e.g. [11]). Instead, in PC although the SM fields are initially external to the composite sector they couple linearly with strength λ to fermionic composite–sector operators $\mathcal{O}_F$

$$\mathcal{L}_{\text{PC}} = \lambda_{f_L} \bar{f}_L \mathcal{O}_F^L + \lambda_{f_R} \bar{f}_R \mathcal{O}_R^L + \dots , \tag{2.2}$$

where f_L / f_R the left–handed and right–handed fermion respectively. Then, this leads to mass mixing between the elementary and composite states and what we observe as physical SM fields are in fact the lightest mass eigenstates of the mixing.

Since the Higgs is a composite state, the degree to which SM fermions feel the Higgs vev depends on the linear mixing strengths of the left–handed and right–handed components (see Fig. 2.1). Therefore, the Yukawa coupling y_f is proportional to the product of the two mixings

$$y_f \propto \frac{\lambda_{f_L} \lambda_{f_R}}{g_*} \tag{2.3}$$

with g_* the coupling in the strong sector, which is larger than the elementary coupling $g_E \lesssim 1 < g_* \ll 4\pi$, but still small enough to be treated perturbatively. After EWSB, when the Higgs gets a vev, masses for the SM fields are induced. Since the largest Yukawa coupling is the top Yukawa $y_t \sim 1$, the left–handed and right–handed components of the top quark are expected to have the largest mixing with the composite sector. They are also the main source for the explicit symmetry breaking of G, and the leading contributions in the generation of the Higgs potential and mass. After the strong sector condensates, a set of vector–like (VL) resonances is predicted which carry SM quantum numbers, which are called "partners". For instance, there will be coloured fermionic resonances with the quantum numbers of the top, which lead to one of the main problems in generic CHM. The Higgs is the

only SM field that should be fully composite[3], instead of a mixture of elementary and composite states, in order to solve the hierarchy problem.

On an interesting, but in this thesis not relevant, note, PC can also offer a solution to the flavour hierarchy problem, since the IR value of the linear coupling depends on the scaling dimension of the respective composite operator. Then, even without requiring a hierarchy in the UV coupling, due to the exponential enhancement in the renormalisation group running, a realistic V_{CKM} matrix can be reproduced from $\mathcal{O}(1)$ values in the UV (see for details e.g. Chapter 4 in [11]).

2.1.2 Common Problems

Fine Tuning

The Higgs potential can be parameterised as

$$V(h) = -\alpha \sin^2\left(\frac{h}{f}\right) + \beta \sin^4\left(\frac{h}{f}\right) \tag{2.4}$$

where the signs are chosen for convenience and the precise forms of parameters α and β depend on the given model. Since the Higgs potential in CHMs features trigonometric functions, we have chosen the form of Eq. (2.4) to be in agreement. From Eq. (2.4) it is straightforward to determine the SM Higgs vev[4] $\sin\langle h\rangle \equiv v_{\text{SM}}$ as well as the Higgs mass m_H:

$$\left.\frac{dV(h)}{dh}\right|_{\sin\langle h\rangle = v_{\text{SM}}} \stackrel{!}{=} 0 \quad \Rightarrow \quad \xi \equiv \frac{v_{\text{SM}}^2}{f^2} = \frac{\alpha}{2\beta} \tag{2.5}$$

$$\left.\frac{d^2V(h)}{dh^2}\right|_{\sin\langle h\rangle = v_{\text{SM}}} = m_h^2 = 8\frac{\beta}{f^2}\xi \tag{2.6}$$

where $\xi \equiv v_{\text{SM}}^2/f^2$ measures the vacuum misalignment between EW scale v_{SM} and SSB scale f, as explained above. ξ also appears when evaluating the necessary tuning of a model. Naturally, $v_{\text{SM}} \sim f$ would be expected, but the behaviour of the CH has to mimic an elementary Higgs up to a certain degree to be compatible with observations. Phenomenological modifications scale with the ratio v/f, as will be seen extensively in Chapter 3 and Chapter 4, so generally $\xi \ll 1$ is required. This translates to a hierarchy between the parameters α and β, in agreement with Eq. (2.5). The so–called minimal–tuning ([36]), in which both α and β are expected to arise at the same order in couplings[5], i.e. in $\mathcal{O}((\lambda/g_*)^2)$, where λ is the strength of the linear SM field coupling to the composite sector and g_* the strong sector coupling, is given by

$$\Delta_{\text{min}} = \frac{(\alpha/\beta)_{\text{expected}}}{(\alpha/\beta)_{\text{needed}}} \sim \frac{1}{\xi} = \frac{f^2}{v_{\text{SM}}^2}\,, \tag{2.7}$$

where we used Eq. 2.5. In minimal–tuning scenarios the tuning only depends on the desired vacuum misalignment. However, often in generic CHMs the quartic of the Higgs potential arises at sub–leading order in couplings, i.e. $\beta \sim \mathcal{O}((\lambda/g_*)^4)$. Then, the model becomes *double–tuned*, since in addition to the minimal–tuning another cancellation is required to overcome the hierarchy between α and β. With

[3] Also t_R is sometimes assumed to be fully composite, see e.g. [11].

[4] The equivalence $\sin\langle h\rangle \equiv v_{\text{SM}}$ stems from the determination of the gauge boson masses in Sec. 3.2.1.

[5] Details on the expansion in couplings can be found in Sec. 3.2.1.

$(\alpha/\beta)_{\text{expected}} \neq 1$, the tuning is found to be

$$\Delta_{\text{double}} = \frac{(\alpha/\beta)_{\text{expected}}}{(\alpha/\beta)_{\text{needed}}} \sim \frac{\mathcal{O}((\lambda/g_*)^2)}{\mathcal{O}((\lambda/g_*)^4)} \frac{1}{\xi} \sim \left(\frac{g_*}{\lambda}\right)^2 \Delta_{\text{min}} \,. \tag{2.8}$$

In this thesis, where in addition to analytical estimates we perform numerical scans, we will contrast the analytically expected minimal–tuning to the tuning in explicit models by numerically evaluating the Barbieri–Giudice measure ([37])

$$\Delta_{\text{BG}} = \max_i \left| \frac{\partial \log O(x_i)}{\partial \log x_i} \right| \,, \tag{2.9}$$

which measures the maximum sensitivity of observable $\mathcal{O}$ of the theory to the given parameters x_i. The observable will be the Higgs vev, and the parameters will be the ones describing the composite dynamics and the mixings between the two sectors. Previously, tuning in CHMs was addressed e.g. in [38–43].

Light Top Partners

One unambiguous prediction of CHMs is the presence of composite resonances with the same quantum numbers as the SM fields. They decay predominantly into third generation SM fields, due to the larger mixing of heavy SM fields with the composite sector (see Sec. 2.1.1). Therefore, collider searches focus on resonances decaying to top and bottom quarks. However, so far no composite resonances have been observed at the LHC, placing a limit of $\min(m_T) \gtrsim 1.5$ TeV on the lightest top partners ([44–48]). Additionally, light top partner seem essential for correct EWSB ([36, 49–53]) since the mass of the top quark and its resonances are a function of the Higgs vev (see Sec. 3.2.2). The Higgs mass (Eq. (2.6)) can be approximated by m_{top} and $\min(m_T)$:

$$m_h \propto \frac{\min(m_T)}{f} m_{\text{top}} \tag{2.10}$$

Therefore, in addition to the generic prediction of composite resonances, the mass of the lightest top partners is intrinsically linked to the Higgs mass, and the SSB scale f. It becomes clear that the two problems outlined in this section are interconnected. By requiring a light Higgs mass of 125 GeV, and having experimental constraints on $\min(m_T)$, it becomes necessary to push the symmetry breaking scale f to higher and higher values to avoid CHM from being ruled out. Fig. 2.2 shows a graphic depiction of this interplay. Pushing f higher usually reintroduces a *little* hierarchy problem, because the tuning goes quadratically with f (Eq. 2.7). Previous attempts to solve the top partner problem include [36, 40, 41, 53, 54].

2.2 Grand Unified Theories

Unification has been a good guiding principle in the past, as has been proven over and over again, be it A. Einstein with space–time, J. Maxwell with electromagnetism or S. Glashow, A. Salam and S. Weinberg with electroweak interactions. So why should we stop here? Although the ultimate goal might be a theory of everything, which includes gravity in addition to the strong, weak and electromagnetic forces, a first step can be unifying the three fundamental SM interactions which appear

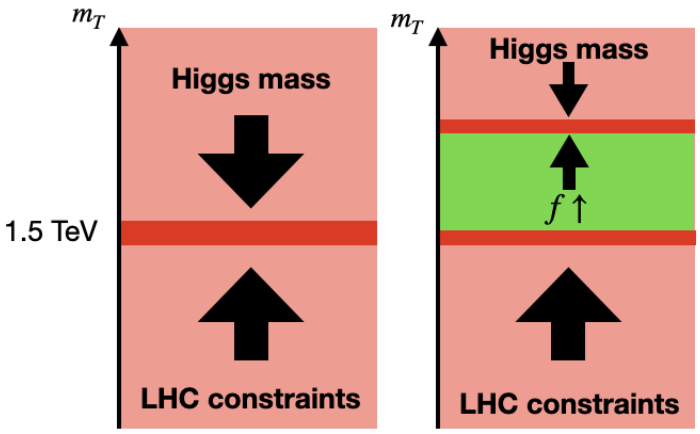

FIGURE 2.2: An illustration of the dilemma in generic CHM: so far, no composite resonances have been observed at colliders, which gives a lower bound for the mass of the lightest top partner. Additionally, at fixed f, the requirement of a light Higgs leads to an upper bound, and no viable parameter space is left, as seen on the left. To still achieve the correct Higgs mass, it becomes necessary to increase the SSB scale f, as seen on the right, which leads to the prediction of experimentally viable top partner masses, but worsens the fine–tuning.

in nature, which was first done by [55][6]. The strong, weak and electromagnetic interactions are all described by nonabelian gauge theories, and can be unified in one single symmetry group. Theories of this type are called Grand Unified Theories (GUTs) ([55, 56]). From a group theoretic point of view, each force is described by a symmetry group where each generator of the Lie algebra of group G corresponds to a gauge boson. We can see this easily with the example of colour: $SU(3)_C$ has $N^2 - 1 = 3^2 - 1 = 8$ generators, which is in line with the eight gluons that exist in nature. This section partly follows the "Group Theory in a nutshell for physicists" book by Anthony Zee ([57]).

2.2.1 Standard Model

The matter content of the universe consists of three generations of quarks and leptons, but for illustration purposes we will focus on the first generation here. It contains the up–quark u, the down–quark d as well as the electron e^- and the electron–neutrino ν_e. In addition, except for the neutrino, they all appear in duplicate, since the fields can be left–handed (LH) or right–handed (RH), and the quarks which are charged under colour appear on top in triplicate. There is no RH neutrino in the SM, one of the several puzzles surrounding it. Then, the first generation of the SM contains 15 fields

$$u_L^r\,,\ u_R^r\,,\ u_L^g\,,\ u_R^g\,,\ u_L^y\,,\ u_R^y\,,\ d_L^r\,,\ d_R^r\,,\ d_L^g\,,\ d_R^g\,,\ d_L^y\,,\ d_R^y\,,\ e^-\,,\ e^+\,,\ \nu_e\,. \tag{2.11}$$

Since RH fields transform like the conjugate of LH fields, it is possible to group the up–/down–quark into a fundamental **3** and $\mathbf{3}^*$ of $SU(3)_C$, whereas the electrons and the neutrino appear as singlets. Gauge bosons transform the fields within a representation into each other. In the weak interaction the LH quarks/leptons transform

[6] J. Pati and A. Salam considered leptons as a fourth colour, and based their unification on $SU(4)_C \otimes SU(2)_L \otimes SU(2)_R$

as a **2** of $SU(2)_L$, i.e. the W^+ and W^- gauge bosons can transform u_L into d_L, and e^- into ν_e. In contrast, the RH fields transform as singlets. $SU(3)_C$ and $SU(2)_L$ are direct product groups which means that they commute, i.e. that $SU(2)$ interactions do not affect colour, and vice versa. To fully describe the SM, one gauge group is still missing: a $U(1)$. In fact, the photon is a linear combination[7] of the $U(1)$ generator $\frac{1}{2}Y$ and the third $SU(2)_L$ generator T^3. Then, the electric charge Q of the fields is given by $Q = T^3 + \frac{1}{2}Y$. It is customary to express SM fields in terms of the three groups, i.e. the RH up–quark as $(\mathbf{3}^*, \mathbf{1})_{-\mathbf{2/3}}$, which describes a field transforming as a triplet under SU(3), a singlet under SU(2) and with a hypercharge $\frac{1}{2}Y = 2/3$. With this in mind, Eq. (2.11) becomes

$$(\mathbf{3}, \mathbf{2})_{\mathbf{1/6}} \oplus (\mathbf{3}^*, \mathbf{1})_{\mathbf{-2/3}} \oplus (\mathbf{3}^*, \mathbf{1})_{\mathbf{1/3}} \oplus (\mathbf{1}, \mathbf{2})_{\mathbf{-1/2}} \oplus (\mathbf{1}, \mathbf{1})_{\mathbf{1}} \,. \tag{2.12}$$

So far, the Higgs has not been mentioned. Once it acquires a vev, it gives a mass to all SM particles by connecting their RH and LH components, with the exception of the neutrino where no RH neutrino has yet been observed, and its mass generation is still a mystery. The Higgs field transforms as $(\mathbf{1}, \mathbf{2})_{\mathbf{1/2}}$ under the SM gauge groups.

Apart from pure mathematical beauty, there are several clues that point in the direction of grand unification. The sum of the hypercharges of the SM matter content is vanishing as can be seen from Eq. (2.12). Since generators of simple groups such as $SU(N)$ or $SO(N)$ are traceless, this fact could be easily explained if Y was a generator of the unified symmetry group. Furthermore, in non-Abelian groups the eigenvalues are discrete, which explains the observed quantised $U(1)$ quantum numbers. Another hint for unification is the running of the SM couplings, seen in Fig. 2.3, since at scales of $M_{\text{GUT}} \sim 10^{15}$ GeV, they come surprisingly close to each other ([58]). Here, only the low–energy running is experimentally measured, while the high–energy behaviour is extrapolated by assuming that the SM is valid until high–energy scales. If the three forces are unified, their coupling originates from a single coupling α_{GUT}, which seems to lie around a value of $\alpha_{\text{GUT}} \sim 1/40$. α_{GUT} is small enough for perturbativity to hold, i.e. leading us to believe that the extrapolation of the running of the couplings is valid. In addition, $M_{\text{GUT}} < M_{\text{Pl}}$ justifies why gravity can be neglected in this description of the three other fundamental forces. One of the most striking hints for unification is however the embedding of the SM matter content into representations of $SU(5)$ or $SO(10)$, which will now be explained in Sec. 2.2.2.

2.2.2 Unifying Symmetry Groups

The most minimal group that contains direct product of the $SU(3)_C$ colour group, the $SU(2)_L$ weak group, and the $U(1)_Y$ hypercharge group is $SU(5)$, the Georgi-Glashow model ([56]). One unambiguous prediction of GUTs is the appearance of additional gauge bosons. Since $SU(5)$ has $5^2 - 1 = 24$ generators, but the SM gauge groups combined only $8 + 3 + 1 = 12$, there will be 12 additional non–SM gauge bosons. These additional gauge bosons do not respect the direct group structure of the SM, which can be easily seen by splitting the $SU(5)$ index μ into an $SU(3)$ index $\alpha = 1, 2, 3$ and an $SU(2)$ index $i = 1, 2$. As $SU(N)$ generators in the adjoint representation are given by the independent components of a traceless $N \times N$ tensor A^{μ}_{ν}, the eight gluons ($(\mathbf{8}, \mathbf{1})_{\mathbf{0}}$) can be described by A^{α}_{β}, the three W bosons ($(\mathbf{1}, \mathbf{3})_{\mathbf{0}}$) by A^{i}_{j}, and the hypercharge B ($(\mathbf{1}, \mathbf{1})_{\mathbf{0}}$) is given by A^{μ}_{μ}, i.e. the trace of the tensor.

[7] The orthogonal combination gives the Z boson.

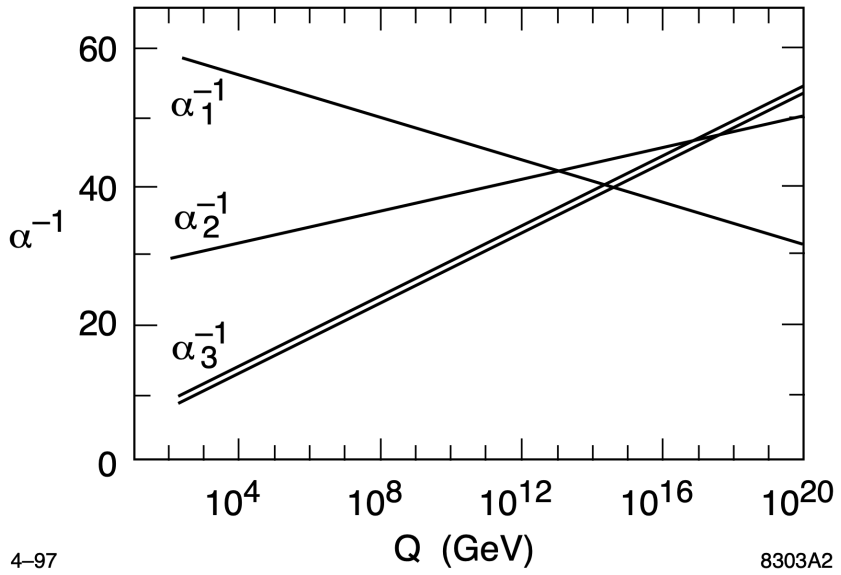

FIGURE 2.3: The running SM couplings α_i against energy scale Q. The couplings almost meet at around 10^{15} GeV which gives hints towards their unification. Figure taken from [59].

Fig. 2.4 shows how the SM gauge fields fit into $SU(5)$. Therefore, additional 12 gauge bosons have to carry an index of both $SU(3)_C$ and $SU(2)_L$, which means that they can transform a quark into a lepton if they are part of the same irreducible representation, see Sec. 2.2.3. They are called leptoquarks (LQ) and decompose under the SM group as $(\mathbf{3},\mathbf{2})$ and $(\bar{\mathbf{3}},\mathbf{2})$. Therefore, the gauge bosons of $SU(5)$ are

$$\mathbf{24} \rightarrow (\mathbf{8},\mathbf{1})_{\mathbf{0}} \oplus (\mathbf{1},\mathbf{3})_{\mathbf{0}} \oplus (\mathbf{1},\mathbf{1})_{\mathbf{0}} \oplus (\mathbf{3},\mathbf{2})_{-\mathbf{5/6}} \oplus (\bar{\mathbf{3}},\mathbf{2})_{\mathbf{5/6}}$$

Next, we have to embed the SM content into representations of $SU(5)$. The defining representation is a 5–vector. It decomposes under the SM gauge group as

$$\mathbf{5} \rightarrow (\mathbf{3},\mathbf{1})_{-\mathbf{1/3}} \oplus (\mathbf{1},\mathbf{2})_{\mathbf{1/2}} \tag{2.13}$$

and its conjugate is

$$\mathbf{5}^* \rightarrow (\mathbf{3}^*,\mathbf{1})_{\mathbf{1/3}} \oplus (\mathbf{1},\mathbf{2})_{-\mathbf{1/2}}\,. \tag{2.14}$$

Additionally, we can inspect the **10** representation. It is an antisymmetric tensor representation, which decomposes as

$$\mathbf{10} \rightarrow (\mathbf{3},\mathbf{2})_{\mathbf{1/6}} \oplus (\mathbf{3}^*,\mathbf{1})_{-\mathbf{2/3}} \oplus (\mathbf{1},\mathbf{1})_{\mathbf{1}}\,. \tag{2.15}$$

Comparing with Eq. 2.12, we see that the SM matter fields fit perfectly into a $\mathbf{5}^*$ and **10** representation of $SU(5)$! It should be noted that the up–quark, the down–quark and the positron are contained in the same multiplet, which becomes relevant when considering the possibility of proton decay in Sec. 2.2.3. To make the Higgs part of an $SU(5)$ multiplet, a $\mathbf{5} \rightarrow (\mathbf{3},\mathbf{1})_{-\mathbf{1/3}} \oplus (\mathbf{1},\mathbf{2})_{\mathbf{1/2}}$ of $SU(5)$ is required, and therefore, an additional scalar triplet is predicted, which can lead to phenomenological challenges, again addressed in Sec. 2.2.3.

Another possible group into which the SM can be unified is $SO(10)$ ([60, 61]). Then, the spinorial **16** representation of $SO(10)$ decomposes under $SU(5)$ as

$$\mathbf{16} \rightarrow \mathbf{10} \oplus \mathbf{5}^* \oplus \mathbf{1}\,, \tag{2.16}$$

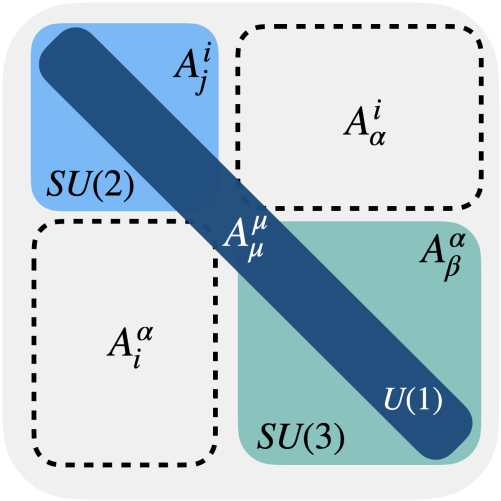

FIGURE 2.4: How the generators of the SM gauge groups fit into a traceless 5×5 tensor of $SU(5)$, and the appearance of leptoquarks which carry indices of both $SU(3)_C$ and $SU(2)_L$.

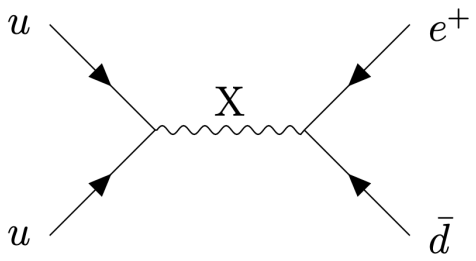

FIGURE 2.5: The appearance of X gauge bosons in GUTs allows two u's to turn into e^+ and $\bar{d}$, therefore enabling proton decay $p \to \pi^0 + e^+$. Diagram from [67].

where an additional singlet with respect to the $SU(5)$–embedding is found, which could be the RH neutrino ν_R. Since it is a singlet, it can be given a Majorana mass term, which makes ν_R heavy, and explains why so far it has not been observed. Furthermore, since the seesaw mechanism ([62–66]) requires a RH neutrino, the puzzle surrounding the neutrino mass generation can be solved in $SO(10)$.

2.2.3 Common Problems

Proton Decay

The appearance of the X and Y gauge bosons, as well as the scalar triplet, can lead to proton decay, because baryon number is not generally conserved. Before, this was not possible, since all quarks have baryon number $B = 1/3$, and without LQs a quark cannot be transformed into something other than a quark. However, as can be seen e.g. by the additional gauge bosons in GUTs which carry both an $SU(3)_C$ and an $SU(2)_L$ index (Fig. 2.4), with LQs it becomes possible to turn quarks and leptons into each other. Fig. 2.5 shows an exemplatory Feynman diagram, where proton decay is mediated by an $SU(5)$ X gauge boson, leading to

$$p \to \pi^0 + e^+ \tag{2.17}$$

The proton lifetime is constrained to be $\gtrsim 10^{34}$ years ([68]), and therefore, to suppress the decay channel masses $> M_{\text{GUT}}$ for the LQs are required. The same problem arises for the scalar LQ, and the consequential mass hierarchy between the Higgs doublet and scalar LQ triplet which are part of the same $SU(5)$-multiplet is called *double–triplet splitting problem*.

Hierarchy Problem

If we assume the SM to be the valid theory until the unification scale, then the leading quantum corrections to the Higgs mass are expected be of the order of $\mathcal{O}\left((10^{15}\text{ GeV})^2\right)$. M_{GUT} is slightly smaller than the Planck mass, but still, the bare mass needs to be tuned incredibly precisely so that the observed Higgs mass is reproduced. In this sense, unless there is some new physics that explains the origin of the EW scale without interfering with the unification, the hierarchy problem manifests even more dominantly, than when the SM is seen as a low energy EFT without specifying any UV completion.

2.3 Gauge-Higgs Grand Unification

Combining the ideas from the previous two sections leads to composite GUTs, in which the Higgs is a composite state, and a pNGB from the spontaneous symmetry breaking $G \to H$, where $H \supset G_{\text{SM}}$ contains the SM gauge group and $G \supset G_{\text{GUT}}$ contains the GUT group. The dual of four–dimensional composite Higgs theories are extra dimensional models, such as the SU(6) Gauge–Higgs Grand Unified Theory (GHGUT) from [10] which features a warped extra dimension, where the Higgs arises as the fifth component of a five-dimensional gauge field of which also the $SU(5)$ gauge group is part of. This unification of gauge interactions and EWSB gives insights into the hierarchy in the EW sector, but the model [10] also addresses flavour hierarchies, see [69]. However, flavour is not a focus of this thesis. Before, $SU(6)$ models were studied in the SUSY context ([70–72]), as well as in the non–SUSY context ([73–75]). Another attractive possibility for GHGUTs are $SO(11)$ models, e.g. in [76, 77].

In this section, we will start by giving an overview over the GHGUT model in Sec. 2.3.1, as well as two important aspects necessary for successful model–building. While Sec. 2.3.2 outlines the emergence of an accidental baryon number symmetry which forbids proton decay, Sec. 2.3.3 details the AdS/CFT correspondence, which explains why strongly–coupled four dimensional theories coincide with weakly–coupled five dimensional theories and vice versa.

2.3.1 5D Incarnation

The hierarchy between EW scale and Planck scale can also be explained by a warped extra dimension, since the exponential warp factor that arises in 5D Anti-de Sitter space can make the size of the Planck scale appear to us as the EW scale, an idea first introduced by L. Randall and R. Sundrum in [78][8]. Keeping in mind that most of the work in this thesis is carried out in 4D, here we will only give a short overview over the topic and refer the interested reader to more elaborate reviews on the Randall–Sundrum model and holographic Higgs, e.g. [81–90]. Holographic Higgs models

[8] Previously, large extra dimensions had also been proposed to explain the hierarchy between the weakness of gravity compared to the other three fundamental forces ([79, 80]).

are attractive as they give a complete description, whereas in effective low energy 4D CHMs the nature of the composite sector does not have to be specified. Additionally, the Higgs potential becomes calculable, since the theory can be treated perturbatively, whereas in purely 4D CH[9] naive dimensional analysis is necessary to estimate observables such as Higgs mass or vev.

The conformal warped metric in the $SU(6)$ GHGUT is ([10])

$$ds^2 = \left(\frac{R}{z}\right)^2 \left(\eta_{\mu\nu} \mathrm{d}x^\mu \mathrm{d}y^\nu - dz^2\right) \tag{2.18}$$

where $z \in [R, R']$ is the coordinate in the extra dimension and $R \sim 1/M_{\mathrm{Pl}}$ and $R' \sim 1/\mathrm{TeV}$ are the positions of UV and IR brane respectively. $SU(6)$ then is the gauge symmetry of the bulk. A five–dimensional gauge field A_M is introduced, with $M = \mu, 5$ spanning additionally the fifth dimension with respect to the commonly known four–dimensional A_μ gauge field. The Higgs will be identified with part of A_5. The global group G is broken by boundary conditions (BC) on the IR and UV branes. The symmetry breaking occurs via gauge BCs and avoiding mixing between A_μ and A_5 and requiring that the variation at the boundaries vanishes, two possible BCs are found, see for details [69],

$$\begin{aligned}
(+): \quad & \partial_5 A_\mu\Big|_{z=R,R'} = 0 \quad \text{(Neumann BCs)}, \; A_5\Big|_{z=R,R'} = 0 \quad \text{(Dirichlet BCs)}, \\
(-): \quad & A_\mu\Big|_{z=R,R'} = 0 \quad \text{(Dirichlet BCs)}, \; \partial_5 A_5\Big|_{z=R,R'} = 0 \quad \text{(Neumann BCs)} \; .
\end{aligned} \tag{2.19}$$

SM fields are described by massless zero modes. See for details on the Kaluza-Klein (KK) decomposition, in which the 5D fields are decomposed into a tower of 4D fields, e.g. [81, 88]. If a tower features a zero–mode the mode can be identified with a massless 4D field, and SM fields are massless before EWSB. As a consequence, to have A_μ zero modes, which describe the SM gauge bosons, Neumann BCs on the (UV,IR) branes $(+,+)$ are required. The A_5 BCs are obtained by flipping the A_μ BCs. Then, in order to have a zero mode for A_5, Dirichlet BCs $(-,-)$ for A_μ are necessary. Mixed BCs do not allow zero–modes, and are given to the remaining dofs. With these conditions in mind, the $SU(6)$ gauge field can be expressed as ([10])

$$A_\mu = \left(\begin{array}{cc|ccc|c}
(++) & (++) & (+-) & (+-) & (+-) & (- -) \\
(++) & (++) & (+-) & (+-) & (+-) & (- -) \\
\hline
(+-) & (+-) & (++) & (++) & (++) & (- -) \\
(+-) & (+-) & (++) & (++) & (++) & (- -) \\
(+-) & (+-) & (++) & (++) & (++) & (- -) \\
\hline
(- -) & (- -) & (- -) & (- -) & (- -) & (- -)
\end{array}\right) . \tag{2.20}$$

The BCs lead to the breaking of the $SU(6)$ symmetry on the branes[10]. Here, the breaking pattern on the UV–brane is $SU(6) \to SU(5)$, whereas on the IR–brane the

[9] Multi–site models, as will be used in Sec. 3.2.2 and Sec. 4.3.2, are an extrapolation between both descriptions. The fifth extra dimension is decomposed into sets of 4D sets of dofs. In these models it is not necessary to rely on naive dimensional analysis, while still keeping the more lightweight aspect of the 4D description.

[10] One can simply read off from Eq. (2.20) which symmetries are respected on the (UV, IR) branes, and finds that the first respect $SU(5)$ whereas the latter breaks $SU(5)$ but still respects the SM gauge groups.

breaking pattern is $SU(6) \to SU(2)_L \otimes SU(3)_C \otimes U(1)_Y$. Later, in [69] the breaking pattern was flipped, and the remaining symmetry on the IR–brane became $SU(5)$, whereas on the UV–brane $SU(2)_L \otimes SU(3)_C \otimes U(1)_Y$ remained. We see that the group that remains unbroken corresponds to the SM gauge group, as can be seen by comparing with Fig. 2.4 for example. The Higgs dofs are contained in the upper right quadrant, and additionally a scalar leptoquark and a scalar singlet are part of the model. A_5 is obtained by flipping the signs of the BCs in Eq. (2.20).

The fermions are embedded in $SU(6)$ representations and modelled by bulk fields that propagate between the branes, which is the equivalent of partial compositeness. The overlap of their profile with the Higgs in the extra dimension corresponds to the linear mixing familiar from Sec. 2.1. The most minimal representation that includes a RH up–type quark ($(\mathbf{3},\mathbf{1})_{\frac{2}{3}}$) which interacts with the A_5 Higgs is a **20** that decomposes as

$$\mathbf{20} \to (\mathbf{3},\mathbf{2})_{\frac{1}{6}} \oplus (\mathbf{3^*},\mathbf{1})_{-\frac{2}{3}} \oplus (\mathbf{1},\mathbf{1})_{\mathbf{1}} \oplus (\mathbf{3^*},\mathbf{2})_{-\frac{1}{6}} \oplus (\mathbf{3},\mathbf{1})_{\frac{2}{3}} \oplus (\mathbf{1},\mathbf{1})_{-\mathbf{1}} \tag{2.21}$$

under the SM gauge group. Additionally, a **15** is needed for the RH down–type quark ($(\mathbf{3},\mathbf{1})_{-\frac{1}{3}}$), which decomposes as

$$\mathbf{15} \to (\mathbf{3},\mathbf{2})_{\frac{1}{6}} \oplus (\mathbf{3^*},\mathbf{1})_{-\frac{2}{3}} \oplus (\mathbf{1},\mathbf{1})_{\mathbf{1}} \oplus (\mathbf{3},\mathbf{1})_{-\frac{1}{3}} \oplus (\mathbf{1},\mathbf{2})_{\frac{1}{2}} \,. \tag{2.22}$$

The LH quark doublet ($(\mathbf{3},\mathbf{2})_{\frac{1}{6}}$) is also embedded in the **15**. In order to connect the quark doublet with both the RH top and the RH bottom, the **20** and **15** must be connected. This is done with the help of IR brane masses[11] which lead to kinetic mixing. Allowed are connections between the $SU(5)$ sub–representations, instead of the full $SU(6)$ multiplets. The reason are the BCs on the IR brane, which leave $SU(5)$ as the remaining symmetry. The representations decompose as

$$\begin{aligned} \mathbf{20} &\to \mathbf{10} \oplus \mathbf{10}^* \,, \\ \mathbf{15} &\to \mathbf{10} \oplus \mathbf{5} \end{aligned} \tag{2.23}$$

under $SU(5)$. Although also the LH lepton doublet ($(\mathbf{1},\mathbf{2})_{\frac{1}{2}}$) and the RH electron–like field ($(\mathbf{1},\mathbf{1})_{\mathbf{1}}$) would fit into the **15**, once mass generation is considered, there is a mass degeneracy between electron and bottom quark.Therefore, a

$$\mathbf{6} \to (\mathbf{3},\mathbf{1})_{-\frac{1}{3}} \oplus (\mathbf{1},\mathbf{2})_{\frac{1}{2}} \oplus (\mathbf{1},\mathbf{1})_{\mathbf{0}} \tag{2.24}$$

is added, into which the RH bottom and lepton doublet are embedded. Then, with the help of boundary terms, the degeneracy can be lifted, see [69]. To allow the connection between RH– and LH–components, an IR brane mass between the **15** and **6** becomes another essential ingredient. The $SU(5)$ decomposition is $\mathbf{6} \to \mathbf{5} \oplus \mathbf{1}$. Finally, to model a full generation of fermion fields, only the neutrino has not been mentioned yet. Although the **6** contains a RH neutrino, adding an additional singlet

$$\mathbf{1} \to (\mathbf{1},\mathbf{1})_{\mathbf{0}} \tag{2.25}$$

allows for naturally light Dirac neutrino masses. This is because if the RH neutrino resided in the **6**, the neutrino mass would be proportional to $\lambda_{\mathbf{6},L}\lambda_{\mathbf{6},R}$, but neither of

[11] The original GHGUT breaking pattern only allows the connection via UV brane masses, i.e. in the elementary sector, which would worsen FCNCs. By changing BCs it is also possible to realise IR brane masses, but those lead to problematically light exotics. See Table 1 in [69] for an overview over the combinations of breaking patterns and brane masses.

those two linear mixings can become tiny without affecting the bottom mass ($m_b \propto \lambda_{\mathbf{6},R}\lambda_{\mathbf{15},L}$) or the electron mass ($m_e \propto \lambda_{\mathbf{6},L}\lambda_{\mathbf{15},R}$). Therefore, by adding the singlet, via kinetic mixing the neutrino mass can become small, where there are no unwanted consequences of choosing the partial compositeness fraction $\lambda_{\mathbf{1},R}$ to be tiny or in the 5D dual of choosing the singlet to be very UV–localised. Of course, a third IR brane mass is required, which connects the **6** and **1**.

Similarly to the gauge fields, the fermion fields BCs have to be specified, in order to ensure zero modes for the SM fields within the bulk. Fields without zero modes will correspond to the composite partners mentioned in Sec. 2.1. Additionally, each 5D bulk field gives rise to a tower of 4D KK modes, which in the 4D dual are also identified with composite resonances. Furthermore, when looking at the representations detailed here, exotic fields appear that do not mix with the SM fermions and are instead part of a different sector. They are

$$(\mathbf{3^*},\mathbf{1})_{-\frac{2}{3}} \quad , \quad (\mathbf{3^*},\mathbf{2})_{-\frac{1}{6}} \quad , \quad (\mathbf{1},\mathbf{1})_{-1} \quad .$$

None are allowed to feature zero modes, as the prediction of non-SM fields that are massless before EWSB and obtain their masses through the Higgs mechanism would be quite problematic. Instead, without zero–mode they are naturally heavy. As mentioned before, the UV BCs have to respect G_{SM}, whereas the IR BCs have to respect $SU(5)$. To permit a non–zero boundary mass between two multiplets, they must have opposite BCs, see for a detailed description Sec. 3.3 in [69]. Then, the (UV, IR) BCs are

$$\begin{aligned}
\mathbf{20} \to & q'(\mathbf{3},\mathbf{2})^{(+,-)}_{1/6} \oplus (\mathbf{3}^*,\mathbf{1})^{(+,-)}_{-2/3} \oplus e^{c\prime}(\mathbf{1},\mathbf{1})^{(+,-)}_{1} \\
& (\mathbf{3}^*,\mathbf{2})^{(+,-)}_{-1/6} \oplus u(\mathbf{3},\mathbf{1})^{(-,-)}_{2/3} \oplus (\mathbf{1},\mathbf{1})^{(+,-)}_{-1}, \\
\mathbf{15} \to & q(\mathbf{3},\mathbf{2})^{(+,+)}_{1/6} \oplus (\mathbf{3}^*,\mathbf{1})^{(-,+)}_{-2/3} \oplus e^{c}(\mathbf{1},\mathbf{1})^{(+,+)}_{1} \\
& d'(\mathbf{3},\mathbf{1})^{(-,+)}_{-1/3} \oplus l^{c\prime}(\mathbf{1},\mathbf{2})^{(-,+)}_{1/2}, \\
\mathbf{6} \to & d(\mathbf{3},\mathbf{1})^{(-,-)}_{-1/3} \oplus l^{c}(\mathbf{1},\mathbf{2})^{(-,-)}_{1/2} \oplus \nu^{c}(\mathbf{1},\mathbf{1})^{(+,+)}_{0}, \\
\mathbf{1} \to & \nu^{c\prime}(\mathbf{1},\mathbf{1})^{(+,-)}_{0}.
\end{aligned} \tag{2.26}$$

In addition to the mentioned IR brane masses, with the given BCs there is the possibility to add one non–vanishing UV brane mass, which connects $(\mathbf{3}^*,\mathbf{1})^{(+,-)}_{-2/3}$ and $(\mathbf{3}^*,\mathbf{1})^{(-,+)}_{-2/3}$. Although not strictly necessary, the UV brane mass between the exotic fields helps generate the desired Higgs potential, and the reason for this will become clear in the spurion analysis in Sec. 3.2.1.

2.3.2 Accidental Baryon Number Conservation

We have seen that the emergence of vector leptoquarks is an artifact of any grand unified theory, and is usually regarded to be problematic. Therefore, the question arises: Does one have to worry the decay of protons, which in turn would require very high leptoquark masses? The answer is no, which is due to the accidental symmetry of the model which conserves baryon number. In 4D GUTs, it is the perfect filling of multiplets that allows proton decay

$$p \to \pi_0 + e^+ \, .$$

However, in the GHGUT the embedding of the right–handed up quark is in the $\mathbf{10}^*$ of the **20** whereas the quark doublet and electron singlet are embedded in the **10** of the **15**. Therefore, the couplings that mediate proton decay do not appear. In fact, the model features a hidden baryon symmetry, since B is conserved at each vertex, which renders the proton stable to all orders in perturbation theory, see [10]. The symmetry is anomalous non–perturbatively but can be gauged after cancelling the anomalies, similarly to [91, 92]. Before, the bounds on the proton lifetime translated to bounds on the LQs masses, to suppress the decay channel. Since proton decay is forbidden, it is no longer a necessity for the X and Y gauge bosons, or for the scalar triplet to be heavy. Therefore, this is a a *GUT without a desert*, a term first coined in [93].

2.3.3 Holographic Dictionary

Most of the analysis in this thesis is done in the four-dimensional dual of the GHGUT. Therefore, it is important to understand how it is possible to switch between describing models as strongly coupled four-dimensional theories and describing them as weakly coupled five-dimensional theories. To do so, the Anti-de Sitter / Conformal Field Theory (AdS/CFT) correspondence ([94–102]) becomes essential. Table 2.1 gives a holographic dictionary, which will be used in the following work to extrapolate between 4D and 5D quantities, and is partly adapted from [103].

4D	5D
elementary sector	UV – localised
composite sector	IR – localised
global symmetry G	bulk symmetry
subgroup H	IR–brane symmetry
gauged symmetry group	UV–brane symmetry
PC elementary field	bulk field
external elementary field	UV–brane localised field
Dirac mass	brane mass
SM fields	zero-modes
composite resonances	KK modes
m_*	m_{KK}
SM Yukawa couplings	overlap of fermion profiles with IR–localised Higgs
fermion mass hierarchy	$\mathcal{O}(1)$ bulk mass parameters and brane masses

TABLE 2.1: Holographic dictionary

Independently of whether a warped fifth dimension exists in nature, this is a powerful tool, since when doing calculations or estimates one can always chose the "basis" that is most convenient. The 5D models are described by the localisation of the bulk fields, as well as the introduced brane BCs and masses, whereas the low energy effective 4D description features many free parameters that stem from the unspecified composite sector. Still, for understanding the interplay of effects the rough analytical estimates possible in 4D give valuable insight while being easier to handle than the full 5D description, which is also why we have chosen to mainly focus on the 4D framework in this work. To do simplified numerical scans, it is furthermore possible to decompose the fifth dimension into sites of 4D dofs, as will be done to support the analytical results derived in this work, see Sec. 3.2.2 and Sec. 4.3.2. Then, focusing on the first one or two sites of composite resonances is

sufficient for collider simulations, since heavier KK modes have no chance of being accessible at current colliders.

Chapter 3

Gauge-Higgs Grand Unification

The analysed model is based on the five–dimensional $SU(6)/SU(5)$ Gauge-Higgs Grand Unified Theory (GHGUT) [10]. The analysis of the four–dimension incarnation is done employing the Callan–Coleman–Wess–Zumino (CCWZ) mechanism ([31, 32]), which is a method to write down effective low–energy Lagrangians for a generic symmetry breaking $G \to H$. Here, we followed the review by Panico and Wulzer ([11]). First, in Sec. 3.1 we will detail how the pNGBs, fermions and gauge bosons appear in this setup, then determine the Higgs potential in Sec. 3.2 both analytically in a spurion analysis and numerically within a deconstructed 3–site model. After a brief study of the phenomenological implications in Sec. 3.3 we discuss the results in Sec. 3.4.

3.1 4D Incarnation

3.1.1 Pseudo Nambu Goldstone Bosons

SU(N) groups have $N^2 - 1$ generators. It is therefore easy to count the number of broken generators in the coset $SU(6)/SU(5)$, each of which corresponds to a massless Nambu-Goldstone-Boson (NGB) degree of freedom (dof), according to the Goldstone theorem. Out of the $35 - 24 = 11$ dofs, four furnish the complex Higgs doublet, whereas the remaining seven dofs belong to a scalar leptoquark, and a scalar singlet. The NGBs are parametrised by the Goldstone matrix

$$U = \exp\left\{ i\frac{2}{f}\Pi_{\hat{a}}\hat{T}^{\hat{a}} \right\} \tag{3.1}$$

where $\Pi_{\hat{a}}$ are the NGB fields, and $\hat{T}^{\hat{a}}$ the 11 broken generators which are part of G but not H with $\hat{a} = \hat{25}, ..., \hat{35}$. We will work with the fundamental representation as is customary although U can be defined for any representation. Since the breaking $G \to H$ is only spontaneous, operators allowed in the Lagrangian have to respect the full G. The U transformation under G

$$U \to g \cdot U \cdot h^{\dagger} \qquad g \in SU(6),\, h \in SU(5) \tag{3.2}$$

ensures that the $SU(6)$ symmetry is respected. Transformations of the unbroken subgroup H act linearly on the Goldstone fields, whereas transformations of the broken generators act non–linearly. Therefore, in the CCWZ mechanism the Goldstone matrix is the fundamental element used to build invariants, because transformations along the broken generators are easily realised. To determine the pNGB potential, we work in unitary gauge and set $\langle \Pi_{\hat{a}} \rangle = h \cdot \delta_{\hat{a}28} + S \cdot \delta_{\hat{a}34} + s \cdot \delta_{\hat{a}35}$ for Higgs h,

leptoquark S and singlet s. Then, U takes the explicit form

$$U = \exp\left\{ i\frac{2}{f}\left(h\hat{T}^{\hat{28}} + S\hat{T}^{\hat{34}} + s\hat{T}^{\hat{35}} \right) \right\} \tag{3.3}$$

with generators

$$\begin{aligned} (T^{\hat{28}})_{IJ} &= -\frac{i}{2}(\delta_{2I}\delta_{6J} - \delta_{6I}\delta_{2J}) \\ (T^{\hat{34}})_{IJ} &= -\frac{i}{2}(\delta_{5I}\delta_{6J} - \delta_{6I}\delta_{5J}) \\ (T^{\hat{35}})_{IJ} &= \frac{1}{2}\left(\sqrt{\frac{1}{15}}\delta_{ij} - \sqrt{\frac{5}{3}}\delta_{I6}\delta_{J6} \right) \end{aligned} \tag{3.4}$$

where i,j $\in [1,5]$ and I,J $\in [1,6]$. Their trace is normalised to $\mathrm{Tr}\{T^a.T^b\} = 1/2\delta^{ab}$. The full set of SU(6) generators is given in Appendix A.1. It is important to note that the vacuum expectation value (vev) of the pNGB Higgs is not in one-to-one correspondence with the SM vev. This can be easily seen by calculating the kinetic Lagrangian with the help of the Maurer–Cartan form, and comparing the gauge boson mass terms to the SM expectation, as will now be done in Sec. 3.1.2.

3.1.2 Gauge Fields

The SM gauge fields can be expressed in terms of unbroken generators of SU(6) (Appendix A.1) as

$$A_\mu = \sqrt{\frac{5}{3}} \cdot g' \cdot B\, T^{24} + \sum_{\alpha=1}^{3} g \cdot W_\alpha\, T^\alpha + \sum_{i=4}^{11} g_S \cdot G_{i-3}\, T^i \tag{3.5}$$

where we used the standard GUT convention for the hypercharge ($g'_{\mathrm{GUT}} = \sqrt{\frac{5}{3}}g'$) [103]. The gauge fields are elementary, but interact with the composite sector by coupling to the global current multiplet $\mathcal{J}$

$$\mathcal{L}_{\mathrm{int}}^{\mathrm{gauge}} = gW_{\mu,\alpha}\mathcal{J}^{\mu,\alpha} + g'B_\mu\mathcal{J}_Y^\mu + g_s G_{\mu,i}\mathcal{J}^{\mu,i} \tag{3.6}$$

Eq. (3.6) explicitly breaks the $SU(6)$ symmetry, since the SM gauge group is only a subgroup of $SU(6)$. However, the explicit breaking in the fermionic sector dominates the generation of the Higgs potential. The kinetic term is formed with the help of the modified Maurer–Cartan form $\bar{A}_\mu$ which includes the covariant derivative of the Goldstone matrix $D_\mu U = \partial_\mu U - iA_\mu U$

$$\bar{A}_\mu = U^{-1}D_\mu U = d_{\mu,\hat{a}}\hat{T}^{\hat{a}} + e_{\mu,a}\hat{T}^a \equiv d_\mu + e_\mu\,. \tag{3.7}$$

$\bar{A}_\mu$ is generally split into two symbols: d_μ and e_μ out of which G–invariants are formed. While under G d_μ transforms linearly with h, e_μ transforms like a gauge field, i.e.

$$\begin{aligned} d_\mu &\to h \cdot d_\mu \cdot h^{-1} \\ e_\mu &\to h \cdot \left(e_\mu + i\partial_\mu\right) \cdot h^{-1}\,. \end{aligned} \tag{3.8}$$

In the CCWZ mechanism, all allowed operators can be formed as combinations of derivatives, e_μ and d_μ, except for the Wess–Zumino–Witten term ([104–106]) which

is however not of interest in this thesis. The simplest G–invariant is formed by contracting d_μ with itself and gives the 2–derivative non–linear σ–model Lagrangian

$$\mathcal{L}_{\text{kin}} = \frac{f^2}{2} d_\mu^{\hat{a}} d_{\hat{a}}^\mu \,. \tag{3.9}$$

It should be noted that the coset structure completely determines Eq. 3.9. The result is general, and independent of the precise cause of the SSB $SU(6) \to SU(5)$. Before giving the explicit form of $\mathcal{L}_{\text{kin}}$, a comment on the relation between SM Higgs vev v_{SM} and physical Higgs vev v is in order. From Eq. 3.9 the W boson mass is given by

$$m_W^2 = \frac{g^2}{4} f^2 \sin^2\left(\frac{v}{f}\right) \tag{3.10}$$

so

$$v_{\text{SM}} \equiv f \sin\left(\frac{v}{f}\right) \tag{3.11}$$

can be easily read off. The full kinetic Lagrangian involving all pNGBs is given in Appendix A.3. Here, setting for better visibility $S \to 0$, $s \to 0$ the kinetic term becomes

$$\begin{aligned}
\mathcal{L}_{\text{kin}}^{\text{Higgs}} = \quad & \frac{1}{2}\partial_\mu h \partial^\mu h + \frac{1}{4} g^2 v_{\text{SM}}^2 |W|^2 + \frac{1}{8\cos^2\theta_w} g^2 v_{\text{SM}}^2 \left(1 - \frac{2}{5}\frac{v_{\text{SM}}^2}{f^2}\right) Z^2 \\
& + \frac{1}{2} g^2 v_{\text{SM}} h \left(\left(1 - \frac{1}{2}\frac{v_{\text{SM}}^2}{f^2}\right)|W|^2 + \frac{1}{2}\left(1 - \frac{13}{10}\frac{v_{\text{SM}}^2}{f^2}\right)\frac{1}{\cos^2\theta_w} Z^2\right) \\
& + \frac{1}{4} g^2 h^2 \left(\left(1 - 2\frac{v_{\text{SM}}^2}{f^2}\right)|W|^2 + \frac{1}{2}\left(1 - \frac{22}{5}\frac{v_{\text{SM}}^2}{f^2}\right)\frac{1}{\cos^2\theta_w} Z^2\right) \\
& + \mathcal{O}\left(\frac{1}{f^4}\right)
\end{aligned} \tag{3.12}$$

The kinetic term features the dim–6 operator $\left(H^\dagger \overleftrightarrow{D_\mu} H\right)\left(H^\dagger \overleftrightarrow{D^\mu} H\right)$ which violates the SM relation between W and Z boson masses, i.e. contributes to the oblique EW precision parameter T at tree–level. Indeed, the Z boson mass is

$$m_Z^2 = \left(1 - \frac{2}{5}\frac{v_{\text{SM}}^2}{f^2}\right)\left(m_Z^{\text{SM}}\right)^2 \,, \tag{3.13}$$

see Sec. 3.3.1 for phenomenological implications. The couplings of the Higgs to the W and Z boson are modified, and can be compared to their SM values. For the W bosons we find

$$c_W \equiv \frac{g_{hWW}^{\text{CH}}}{g_{hWW}^{\text{SM}}} \approx 1 - \frac{1}{2}\frac{v_{\text{SM}}^2}{f^2} \,, \tag{3.14}$$

$$\tilde{c}_W \equiv \frac{g_{hhWW}^{\text{CH}}}{g_{hhWW}^{\text{SM}}} \approx 1 - 2\frac{v_{\text{SM}}^2}{f^2} \,, \tag{3.15}$$

whereas for the Z boson the modification is given by

$$c_Z \equiv \frac{g_{hZZ}^{\text{CH}}}{g_{hZZ}^{\text{SM}}} \approx 1 - \frac{13}{10}\frac{v_{\text{SM}}^2}{f^2} \,, \tag{3.16}$$

$$\tilde{c}_Z \equiv \frac{g^{\mathrm{CH}}_{hhZZ}}{g^{\mathrm{SM}}_{hhZZ}} \approx 1 - \frac{22}{5}\frac{v^2_{\mathrm{SM}}}{f^2} \,. \tag{3.17}$$

In contrast to custodial CHMs, c_W ($\tilde{c}_W$) and c_Z ($\tilde{c}_Z$) are not identical. For $f \to \infty$, composite Higgs and SM Higgs will be indistinguishable, and the hierarchy problem is reintroduced in its totality. To match current observations, a certain scale separation between v_{SM} and f is required. For the here–described GHGUT limits on f are determined in Sec. 3.3.1.

As already mentioned, the gauge bosons explicitly break $SU(6)$, which generates a pNGB potential. However, since the leading contributions to the Higgs potential are fermionic, we will neglect the gauge bosons in the numerical analysis in Sec. 3.2.2. Still, for completeness, the spurion analysis of the gauge bosons is given in Sec. 3.2.1, and we will use is to find a rough estimate for the mass of the scalar leptoquark, for which contributions from the gluons become non–negligible.

3.1.3 Fermion Fields

In contrast to the gauge fields, which are always described by the adjoint representation, i.e. the generators of a Lie group, there is more model–building freedom in the fermion sector, where various representations can be chosen. A minimal embedding of the elementary fermions in $SU(6)$ representations is ([69])

$$\begin{aligned}
\mathbf{20} \to \quad & q'(\mathbf{3},\mathbf{2})_{\frac{1}{6}} \oplus \omega_R(\mathbf{3^*},\mathbf{1})_{-\frac{2}{3}} \oplus e'^c(\mathbf{1},\mathbf{1})_1 \\
& (\mathbf{3^*},\mathbf{2})_{-\frac{1}{6}} \oplus u(\mathbf{3},\mathbf{1})_{\frac{2}{3}} \oplus (\mathbf{1},\mathbf{1})_{-1} \\
\mathbf{15} \to \quad & q(\mathbf{3},\mathbf{2})_{\frac{1}{6}} \oplus \omega_L(\mathbf{3^*},\mathbf{1})_{-\frac{2}{3}} \oplus e^c(\mathbf{1},\mathbf{1})_1 \\
& d'(\mathbf{3},\mathbf{1})_{-\frac{1}{3}} \oplus l'^c(\mathbf{1},\mathbf{2})_{\frac{1}{2}} \\
\mathbf{6} \to \quad & d(\mathbf{3},\mathbf{1})_{-\frac{1}{3}} \oplus l^c(\mathbf{1},\mathbf{2})_{\frac{1}{2}} \\
& \nu^c(\mathbf{1},\mathbf{1})_0 \\
\mathbf{1} \to \quad & \nu'^c(\mathbf{1},\mathbf{1})_0 \ ,
\end{aligned} \tag{3.18}$$

as laid out in Sec. 2.3. Under $SU(5)$ the representations decompose as $\mathbf{20} \to \mathbf{10} \oplus \mathbf{10}^*$, $\mathbf{15} \to \mathbf{10} \oplus \mathbf{5}$ and $\mathbf{6} \to \mathbf{5} \oplus \mathbf{1}$, where the first/second line in the above equation correspond to the first/second $SU(5)$ multiplet named in the decomposition. The singlet of course remains a singlet. The primed fields contain no zero modes, whereas the labelled fields correspond to the SM fermions u, q, e^c, d, l^c, and ν^c. Primed fields carry the same SM quantum numbers as their unprimed counterparts. As explained in Sec. 2.1.1, in partial compositeness the physical mass eigenstates are in fact a mixture of primed and unprimed fermions. The remaining unlabelled fields we call exotics[1]. We chose to consider the RH–component in the $\mathbf{20}$ ($(\mathbf{3^*},\mathbf{1})_{-\frac{2}{3}} \equiv \omega_R$) as well as the LH–component in the $\mathbf{15}$ ($(\mathbf{3^*},\mathbf{1})_{-\frac{2}{3}} \equiv \omega_L$) as they help generating the desired Higgs potential, see Sec. 3.2.1 and Sec. 3.2.2. Additionally, the vector-like mass term between ω_L and ω_R will become important in the generation of the quartic of the Higgs potential, see also Sec. 3.2. Since all exotics feature a Dirac mass, they can be easily made heavy and then decouple from all observables of phenomenological interest, which is what we assume for the unlabelled exotics.

[1] In the $\mathbf{20}$ there is an electron–like exotic ($(\mathbf{1},\mathbf{1})_{-1}$), and quark–doublet–like exotic ($(\mathbf{3^*},\mathbf{2})_{-\frac{1}{6}}$) which features an up–type and a down–type exotic. Additionally there are the two up–type exotics ($(\mathbf{3^*},\mathbf{1})_{-\frac{2}{3}}$), one in the $\mathbf{20}$ and one in the $\mathbf{15}$, which will be included in the analysis.

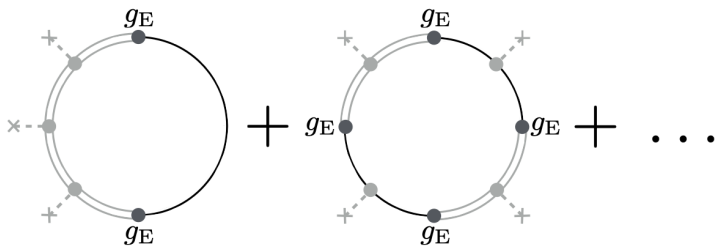

FIGURE 3.1: Leading contributions to the Higgs potential, where g_E is the coupling in the elementary sector, double lines correspond to composite sector fields and dashed insertions are the Higgs field. Fig. taken from [11].

The masses of the SM fields are generated once the Higgs acquires a vev. In the holographic dual IR brane masses allowed to connect the RH– and LH–components of fields that reside in different multiplets. In the 4D description, we introduce masses between the resonances, as will become very clear in the multi–site model in Sec. 3.2.2. Still, an analytical estimate of masses and Yukawa couplings of the SM fermions is also possible without defining the dynamics of the composite sector further. This will be addressed in the next section, Sec. 3.2.1, where we will also show how both gauge fields and fermions explicitly break G, and by doing so generate the Higgs potential.

3.2 Scalar Potential

In the following section, the scalar potential in the GHGUT model will be analysed, first analytically via a spurion analysis (Sec.3.2.1), and the numerically within a multi–side model (Sec. 3.2.2). While former gives a more straightforward understanding of the interplay between the contributions of the elementary fields to the explicit symmetry breaking, the latter allows for more quantitative results.

3.2.1 Spurion Analysis

In the framework of PC (Sec. 2.1.1) the composite operators couple linearly to the elementary fields leading to a mass mixing between them. The SM particles are identified as the lightest mass eigenstates, and the other mass eigenstates as composite resonances with the same SM quantum numbers. The Lagrangian containing the fermions has the following form

$$\mathcal{L}_{\text{PC}} = \lambda_R \bar{f}_R \mathcal{O}_{\text{CS}} + \lambda_L \bar{f}_L \mathcal{O}_{\text{CS}} + \text{ h.c. }, \tag{3.19}$$

where O_{CS} are composite operators that transform under $SU(6)$, $f_{L/R}$ are the elementary fermions and $\lambda_{L/R}$ parametrise the mixing between the fields. The bigger the mixing the more influential the elementary field is for the explicit breaking and therefore the generation of the Higgs potential. This allows us to focus on the top quark, due to its large Yukawa $y_t \sim 1 \propto \lambda_{t_R}\lambda_{q_L}$ (Eq. 2.3). Contributions from other SM fields will be subleading. However, in addition to the well known SM particles, this set-up also contains exotic vector–like (VL) fermions, whose linear mixings can be comparable in size to the ones of the top quark. It turns out that their VL nature is crucial in generating the desired Higgs potential, as we will motivate now and confirm with numerical results from the three-site model in Sec. 3.2.2.

To investigate the generation of the scalar potential we use the CCWZ mechanism ([31, 32]), which allows to write effective low–energy Lagrangians without specifying how the symmetry breaking occurs. The elementary fields are lifted by objects Δ, called spurions, that formally respect $SU(6)$, but are not filled completely. We will use these to build $SU(6)$ invariant structures for the scalar potential. Then, setting the spurions to their vev reflects that the SM fields in fact do not transform under $SU(6)$, which explicitly breaks the symmetry. Specifically, in our model the top and exotic are contained in the **20** and **15**, so the partial compositeness Lagrangian for these fields can be expressed as

$$\begin{aligned}\mathcal{L}_{\text{PC}} = \quad & \left(f\lambda_{t_R}\bar{t}_R\Delta_{t_R} + f\lambda_{\omega_R}\bar{\omega}_R\Delta_{\omega_R}\right)\mathcal{O}_L^{\mathbf{20}} + \text{ h.c.} \\ & + \left(f\lambda_{q_L}\bar{q}_L^i\Delta_{q_L,i} + f\lambda_{\omega_L}\bar{\omega}_L\Delta_{\omega_L}\right)\mathcal{O}_R^{\mathbf{15}} + \text{ h.c. .}\end{aligned} \tag{3.20}$$

The spurions are dressed with the Goldstone matrix (Eq. 3.3). As a result, an index that before transformed with G now transforms with H, and we split the dressed spurions into H representations, e.g. for a t_R spurion

$$U^{-1}\Delta_{t_R}^{\mathbf{20}} \to \begin{pmatrix}\Delta_{t_R,D}^{\mathbf{10}} \\ \Delta_{t_R,D}^{\mathbf{10}^*}\end{pmatrix} , \tag{3.21}$$

where the subscript D highlights that the spurions are dressed. Now, they carry a Goldstone dependence. While Eq. (3.21) has to be understood symbolically, since the Goldstone matrix is a 5×5 matrix, which can expressed in unitary gauge (and setting scalar LQ and scalar singlet to zero) as

$$U = \begin{pmatrix} 1 & 0 & 0 & 0 & 0 & 0 \\ 0 & \cos\frac{h}{f} & 0 & 0 & 0 & \sin\frac{h}{f} \\ 0 & 0 & 1 & 0 & 0 & 0 \\ 0 & 0 & 0 & 1 & 0 & 0 \\ 0 & 0 & 0 & 0 & 1 & 0 \\ 0 & -\sin\frac{h}{f} & 0 & 0 & 0 & \cos\frac{h}{f} \end{pmatrix} , \tag{3.22}$$

but $\Delta^{\mathbf{20}}$ a $6 \times 6 \times 6$ tensor, Appendix A.2 gives the explicit dressings for all spurions. Since G–invariance[2] is built into the Goldstone matrix, it is sufficient to form H–invariant objects out of the dressed spurions, which will then give us the Higgs potential. The lowest order (LO) term possible is formed via the contraction of two spurions. The corresponding loop diagram can be seen as the left–most diagram in Fig. 3.1, which shows the spurion expansion in terms of Feynman diagrams. Keeping t_R as example, there are two possible terms in the Higgs potential

$$\begin{aligned}\text{Tr}\left\{\left(\Delta_{t_R,D}^{\mathbf{10}}\right)^\dagger . \left(\Delta_{t_R,D}^{\mathbf{10}}\right)\right\} &\propto \sin^2\frac{h}{f} , \\ \text{Tr}\left\{\left(\Delta_{t_R,D}^{\mathbf{10}^*}\right)^\dagger . \left(\Delta_{t_R,D}^{\mathbf{10}^*}\right)\right\} &\propto \cos^2\frac{h}{f} ,\end{aligned} \tag{3.23}$$

where, evaluating the contraction of the dressed spurions, one finds trigonometric functions of the Higgs field that stem from the Goldstone matrix in Eq. (3.22). The composite dynamics factor out, and are parametrised by unknown parameters c,

[2] Since in SSB the symmetry is not truly broken, but instead realised non–linearly, all terms have to formally respect G.

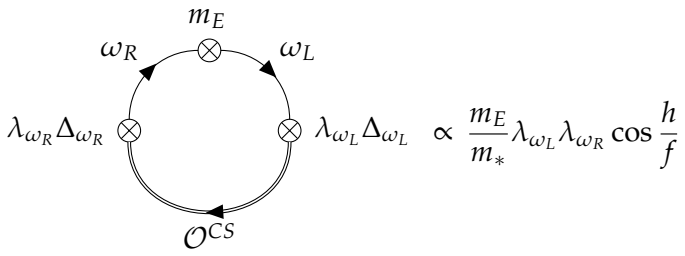

$$\propto \frac{m_E}{m_*}\lambda_{\omega_L}\lambda_{\omega_R}\cos\frac{h}{f}$$

FIGURE 3.2: Feynman diagram that is the source of the $\cos\left(\frac{h}{f}\right)$–term at LO in the Higgs potential.

expected to be $\mathcal{O}(1)$. The Higgs potential stemming from the t_R is then

$$V(h) \propto c_{\mathbf{10}}\sin^2\frac{h}{f} + c_{\mathbf{10}^*}\cos^2\frac{h}{f} = c_{\mathbf{20},\text{aux}}\sin^2\frac{h}{f} + \text{const}\,, \tag{3.24}$$

where rewriting $\cos^2(x) = 1 - \sin^2(x)$ and introducing $c_{\mathbf{20},\text{aux}} \equiv c_{\mathbf{10}} - c_{\mathbf{10}^*}$ leaves us with only one functional dependency, and a contribution to the vacuum energy. Each spurion insertion comes with a factor of λ_i/g_*, which means that at lowest order we expand up to second order in couplings $(\lambda_i/g_*)^2$. The spurion analysis relies on the hierarchy between the strong coupling in the composite sector and the weak SM couplings $\lambda_i \ll g_*$. Otherwise, the validity of the spurion expansion (Fig. 3.1) would be questionable[3]. Although this is not the case, one should keep in mind that, due to the large top Yukawa, the next–to–leading order contribution from the top quark can be easily more dominant than the leading order stemming from e.g. the lepton sector, if $\lambda_{t_R}^4/g_*^4 > \lambda_l^2/g_*^2$. When analysing the invariants stemming from all elementary fermion fields, two distinct functional forms are found

$$V(h)^{\text{LO}}_{\text{SM}} \propto \sin^2\frac{h}{f} \tag{3.25}$$

$$V(h)^{\text{LO}}_{\text{exotic}} \propto \frac{m_E}{m_*}\cos\frac{h}{f}\,. \tag{3.26}$$

The second term stems from a contraction of the right-handed exotic spurion with the left-handed exotic spurion which we can only write down due to the vector-like nature of the exotic fermions

$$\text{Tr}\left\{\left(\Delta^{\mathbf{10}}_{\omega_R,D}\right)^\dagger.\left(\Delta^{\mathbf{10}}_{\omega_L,D}\right)\right\} \propto \cos\frac{h}{f}\,. \tag{3.27}$$

In contrast to the LO top loop ($\mathcal{O}_{CS} \to t_R \to \mathcal{O}_{CS}$), the presence of a Dirac mass m_E between ω_L and ω_R allows a loop, which is still second order in elementary couplings, but closes as $\mathcal{O}_{CS} \to \omega_L \to \omega_R \to \mathcal{O}_{CS}$, where an insertion of m_E allows $\omega_L \to \omega_R$. The reason why the contribution goes as $\cos(h/f)$ and not as $\sin^2(h/f)$ is the nature of ω_L. It does not talk directly to the Higgs, only to the scalar triplet. Therefore, it is exactly the combination of ω_R and ω_L that allows us to find a term like Eq. (3.26). Fig. 3.2 shows the corresponding Feynman diagram, where $\mathcal{O}^{CS}$

[3]The 3–site model in Sec. 3.2.2 does not rely on an expansion in λ_i/g_*.

contains the composite sector dynamics, which we do not specify here[4]. If these exotic fermions were not part of the model, as is the case in most generic CHMs, it would become necessary to include higher orders of SM fermions, or the subleading gauge contributions, in order to find a contribution to the Higgs quartic, i.e. generate the well-known mexican hat shape for the Higgs potential. However, the next–to–leading order is suppressed by an additional $\frac{y_t^2}{g_*^2}$ and therefore the necessary fine-tuning would become worse. One way to alleviate that will be shown in Chapter 4, where the leading order contributions to α are suppressed. Interestingly, the VL nature of the exotics is also what generates the singlet potential, since the singlet generator corresponds to a global $U(1)_X$, which otherwise remains unbroken, see Appendix A.4.

So far, we have only talked about functional dependencies, but to make more precise predictions for the scalar potential, it becomes important to estimate the size of the contribution. To do so, we use the power counting formula[5] determined by dimensional analysis which is given by ([11])

$$\mathcal{L}_{\text{EFT}} = \frac{m_*^4}{g_*^2}\hat{\mathcal{L}}_{\text{tree}} + \frac{g_*^2}{16\pi^2}\frac{m_*^4}{g_*^2}\hat{\mathcal{L}}_{\text{1-loop}} \,. \tag{3.28}$$

where

$$\hat{\mathcal{L}} = \hat{\mathcal{L}}\left[\frac{\partial}{m_*}, \frac{g_*\Pi}{m_*}, \frac{gA_\mu}{m_*}, \frac{\lambda\psi}{m_*^{3/2}}, \frac{g_*\sigma}{m_*}, \frac{g_*\Psi}{m_*^{3/2}}\right] \tag{3.29}$$

is dimensionless. σ are the bosonic resonances, and Ψ the fermionic resonances. Since the pNGBs do not have a tree–level potential, we can set $\hat{\mathcal{L}}_{\text{tree}} = 0$ here. The LO Higgs potential is

$$V(h) = \alpha \sin^2\left(\frac{h}{f}\right) + \beta\frac{m_E}{m_*}\cos\frac{h}{f} \tag{3.30}$$

with

$$\begin{aligned}\alpha \quad &= \frac{m_*^2 f^2}{16\pi^2}\left(c_{\mathbf{6},\text{aux}}\cdot(\lambda_{l_L}^2) + c_{\mathbf{15},\text{aux}}\cdot(3\lambda_{q_L}^2 + \lambda_{e_R}^2) + 3\cdot c_{\mathbf{20},\text{aux}}\cdot(\lambda_{t_R}^2 - \lambda_{\omega_R}^2)\right)\\ &\approx 3\frac{m_*^2 f^2}{16\pi^2}\left(c_{\mathbf{15},\text{aux}}\,\lambda_{q_L}^2 + c_{\mathbf{20},\text{aux}}\,(\lambda_{t_R}^2 - \lambda_{\omega_R}^2)\right)\,,\end{aligned} \tag{3.31}$$

where in the second line only the dominating contributions were kept, and

$$\beta = 3\frac{m_*^2 f^2}{16\pi^2}c_{VL}\lambda_{\omega_R}\lambda_{\omega_L}\,. \tag{3.32}$$

It should be noted that α, β here are not identical to α, β from the parametrised Higgs potential in Eq. (2.4) of the fine–tuning introduction. The latter instead should be compared to the prefactors in the following Eq. (3.33). Including the contribution from the exotic, both quadratic and quartic of the Higgs potential arise at the same order in couplings (λ^2). Without exotic the model would feature the well-known problem of double–tuning. Still, although quadratic and quartic are expected to be of similar size, an additional factor m_E/m_* appears between them, as can be clearly

[4] As will be seen in the 3–site model in Sec. 3.2.2, connecting two multiplets on the composite side, analogous to the Dirac mass between the elementary fields, is necessary to close the loop.

[5] The following was determined assuming a one–scale–one–coupling framework, i.e. one single coupling g_* as well as a single resonance mass m_*, instead of allowing for a more diverse composite sector.

fermion	f_R-$SU(6)$	f_R-$SU(5)$	f_L-$SU(6)$	f_L-$SU(5)$	invariant term
top	**20**	$\mathbf{10}^*$	**15**	**10**	$\frac{1}{2}\,\mathrm{Tr}\left\{\left(\Delta^{\mathbf{10}}_{q_L,D}\right)^\dagger_\alpha \Delta^{\mathbf{10}}_{t_R,D}\right\}$ + h.c.
bottom	**6**	**5**	**15**	**10**	$\left(\Delta^{\mathbf{5}}_{q_L,D}\right)^\dagger_\alpha \Delta^{\mathbf{5}}_{b_R,D}$ + h.c.
electron	**15**	**10**	**6**	**5**	$\left(\Delta^{\mathbf{5}}_{l_L,D}\right)^\dagger_\alpha \Delta^{\mathbf{5}}_{e_R,D}$ + h.c.
neutrino	**6**	**1**	**6**	**5**	$\left(\Delta^{\mathbf{1}}_{l_L,D}\right)^\dagger_\alpha \Delta^{\mathbf{1}}_{\nu_R,D}$ + h.c.
exotic	**20**	**10**	**15**	**10**	$\frac{1}{2}\,\mathrm{Tr}\left\{\left(\Delta^{\mathbf{10}}_{\omega_L,D}\right)^\dagger \Delta^{\mathbf{10}}_{\omega_R,D}\right\}$ + h.c.

TABLE 3.1: Fermion mass generation. The second and third column show the embedding of the RH–component first under $SU(6)$, then under $SU(5)$, and the fourth and fifth column show the respective embeddings of the LH–component. The last column gives the invariant term formed by contracting two spurions that appears in $\mathcal{L}_{\text{Yuk}}$.

seen when expressing Eq. 3.30 in powers of $\sin(h/f)$

$$V(h) = \left(\alpha + \frac{m_E}{2m_*}\beta\right)\sin^2\left(\frac{h}{f}\right) + \frac{m_E}{8m_*}\beta\sin^4\left(\frac{h}{f}\right) + \mathcal{O}\left(\sin^6\left(\frac{h}{f}\right)\right). \tag{3.33}$$

A mild tuning persists, which is related to m_E/m_*. If $m_E > m_*$ the exotics would decouple phenomenologically. As a matter of fact, instead we expect m_E/m_* to act as a suppression, which will be explained in detail in Sec. 4.2, and is furthermore desirable in order to obtain a light Higgs, which is related to having a small quartic. From Eq. (3.31) for $\lambda_{t_R} = \lambda_{\omega_R}$ the quadratic t_R contribution to the scalar potential can be cancelled, but we are still left with the contribution stemming from q_L. In fact, $\lambda_{t_R} = \lambda_{\omega_R}$ can be motivated very well in 5D since t_R and ω_R are part of the same bulk field and therefore have the same localisation with respect to the Higgs. In Chapter 4 we investigate why the cancellation between t_R and ω_R occurs, and extend the mechanism to include the $\lambda^2_{q_L}$ contribution, but in this chapter we keep the fermion embeddings from [10], even though the required tuning is non–minimal. The full scalar potential, i.e. including all three pNGBs, is given in Appendix A.4.

Yukawas and Mass Generation

The embedding of the fermion fields (Eq. 3.18) determines their mass generation. Table 3.1 gives an overview over the embedding of the RH– and LH–fields under $SU(6)$ and $SU(5)$. Although the exotic, due to its Dirac mass, is not massless before EWSB, its mass changes once the Higgs acquires a vev, which is why we include it in Table 3.1. The last column gives the invariant which, once the spurions are set to their vevs, and after EWSB, gives rise to masses for the elementary fields. Taking as example the top quark, we find

$$\begin{aligned}\mathcal{L}^t_{\text{Yuk}} &= -c^t\frac{m_*}{g_*}\lambda_{q_L}\lambda_{t_R}\bar{q}^\alpha_L\frac{1}{2}\,\mathrm{Tr}\left\{\left(\Delta^{\mathbf{10}}_{q_L,D}\right)^\dagger_\alpha \Delta^{\mathbf{10}}_{t_R,D}\right\}t_R + \text{h.c.}\\ &= -c^t\frac{m_*}{g_*}\lambda_{q_L}\lambda_{t_R}\bar{q}_L\sin\left(\frac{H}{f}\right)t_R + \text{h.c.}\,,\end{aligned} \tag{3.34}$$

where $c^t \sim \mathcal{O}(1)$ incorporates the composite dynamics and α sums over the two entries of the LH quark doublet. However, since $\mathrm{Tr}\left\{ \left(\Delta^{\mathbf{10}}_{q_L,D}\right)^\dagger_{b_L} \Delta^{\mathbf{10}}_{t_R,D} \right\} = 0$, as expected, we can set $\alpha \to t_L$ and neglect the doublet nature of q_L. Next, the deviation of the top Higgs coupling from the SM can be found by expanding $\mathcal{L}^t_{\text{Yuk}}$ around $H = h + v$ for small h

$$\mathcal{L}^t_{\text{Yuk}} = -m_t \cdot \bar{t}t - k_t \frac{m_t}{v_{\text{SM}}} h\bar{t}t - c_t \frac{m_t}{v^2_{\text{SM}}} h^2\bar{t}t + ... \tag{3.35}$$

where the top mass is given by $m_t = c^t \frac{\lambda_{q_L}\lambda_{t_R}}{g_*} v_{\text{SM}}$. The trilinear $h\bar{t}t$ coupling modification is found to be

$$k_t \equiv \frac{g^{\text{comp}}_{htt}}{g^{\text{SM}}_{htt}} = \sqrt{1 - \frac{v^2_{\text{SM}}}{f^2}} \tag{3.36}$$

and the $h^2\bar{t}t$ coefficient is

$$c_t = -\frac{v^2_{SM}}{2f^2}\,, \tag{3.37}$$

where we used Eq. (3.11) to express the modifications in terms of the SM Higgs vev. As before in Sec. 3.1.2, the coefficients approach their SM values in the limit $f \to \infty$ for which the Higgs becomes elementary. The modifications for the other SM fermions are identical to Eq. (3.36) and Eq. (3.37). The exotic mass term instead takes the form

$$\begin{aligned} \mathcal{L}^\omega_{\text{Yuk}} &= -c^\omega \frac{m_*}{g_*} \lambda_{\omega_L}\lambda_{\omega_R} \bar{\omega}_L \frac{1}{2} \mathrm{Tr}\left\{ \left(\Delta^{\mathbf{10}}_{\omega_L,D}\right)^\dagger \Delta^{\mathbf{10}}_{\omega_R,D} \right\} \omega_R + \text{h.c.} \\ &= -c^\omega \frac{m_*}{g_*} \lambda_{\omega_L}\lambda_{\omega_R} \bar{\omega}_L \cos\left(\frac{H}{f}\right) \omega_R + \text{h.c.}\,, \end{aligned} \tag{3.38}$$

which we recognise from Eq. (3.27). In contrast to the Yukawa terms of the SM fields, which do not give a contribution to the SM field mass for vanishing Higgs vev, the exotics get a mass contribution even for $v = 0$. This can be motivated by looking at their quantum numbers. Since ω_L and ω_R have the same quantum numbers and both couple to the composite sector, they can form a mass even without the Higgs, which is not possible for SM fields. In fact, when expanding the cosine appearing in Eq. (3.38), the first term including the Higgs will be of the order h^2, since $\bar{\omega}_L H^\dagger H \omega_R$ is necessary to form a singlet. In turn, the SM fields can form a singlet with a single Higgs insertion, e.g. $\bar{q}_L H t_R$, as is reflected when expanding the sine.

Gauge Contributions

In contrast to the fermion sector, where there is model–building freedom, in the gauge sector the fields are necessarily described by the adjoint representation which in turn is fixed by the coset structure. Although we give the spurion analysis for the gauge fields in Appendix A.4.1, since the top and exotic sectors dominate the Higgs potential, the loops including gauge fields and their composite resonances are negligible.

However, the gluons do constitute the leading contribution in the generation of the scalar leptoquark potential. To estimate the mass of the leptoquark, it is a good approximation to set the Higgs and singlet to zero, and by applying the same

spurion method as above, the leptoquark potential is found to be

$$V(S) = \frac{m_*^2 f^2}{16\pi^2}\frac{g_s^2}{3}\left(8\, c_{\text{aux}}^{\mathbf{24}} \sin^2\left(\frac{S}{f}\right) + (c_{\text{aux}}^{\mathbf{1}} - c_{\text{aux}}^{\mathbf{24}}) \sin^4\left(\frac{S}{f}\right)\right) \tag{3.39}$$

where $c_{\text{aux}}^{\mathbf{24}} > 0$ and $c_{\text{aux}}^{\mathbf{1}} > 0$ incorporate the dynamics of the composite sector vector resonances. In contrast to the zero–temperature Higgs potential, which should have a non–zero vev, the leptoquark potential has to remain unbroken to be phenomenologically viable. There are several difficulties otherwise, e.g. a mass term for the photon stemming from the kinetic Lagrangian in Eq. (A.12). Additionally, we require $c_{\text{aux}}^{\mathbf{1}} > c_{\text{aux}}^{\mathbf{24}}$ which ensures a stable potential. Now, the leptoquark mass is given by

$$m_S^2 = \left.\frac{d^2V(S)}{dS^2}\right|_{S=0} = \frac{m_*^2 g_s^2}{3\pi^2} c_{\text{aux}}^{\mathbf{24}}\,. \tag{3.40}$$

Although this is just an estimate, it can give us a rough idea of the order of magnitude of the leptoquark mass. For $\alpha_S = \frac{g_s}{4\pi} \approx 0.11$ and $m_* = g_* f \approx 3.5\, f$ we find a leptoquark mass of $m_S \approx 0.9\, c_{\text{aux}}^{\mathbf{24}} f$. Of course, there are further contributions e.g. from the fermions, but as these contributions also affect the Higgs potential, and the zero–temperature Higgs mass is tachyonic, we expect them to give an overall negative contribution to the quadratic term of the potential. This would results in lowering m_S, and therefore the above estimate can be seen as a rough upper bound. On the other hand, the coupling in the composite sector could be stronger, as long as it remains perturbative ($g_* < 4\pi$), but a more precise numerical calculation of the gauge boson contributions is out of the scope of this thesis. Since the focus lies on the generation of the Higgs potential, we have decided to include only fermionic resonances when implementing the three site model in Sec. 3.2.2.

3.2.2 Three-Site Model

The spurion approach works very well as a qualitative estimate. It is based on the symmetry breaking dynamics, but does not contain any information about the strong sector. To make predictions for the LHC, there is a need for more quantitative results and often, this is done by going to holographic 5d models and using the AdS/CFT correspondence. However, most Kaluza-Klein modes are not accessible at colliders and can therefore be neglected, so 5d models are unnecessarily precise. [107] propose a framework in which dimensional deconstruction is used to discretise the fifth coordinate into sites, where each site has a set of 4d degrees of freedom.

Although the lowest site–model in which the Higgs potential is finite is the three–site model, for illustration purposes we start in the two–site model, where, in addition to the mixing terms, we write Dirac mass terms for the composite resonances, which come in both chiralities. On the composite side, necessarily the G-multiplets are filled completely. Explicit breaking stems only from the elementary sector. By looking at Eq. (3.18) the fermionic resonances with top quantum numbers can be easily read off: Q is a doublet resonance with quantum numbers of q_L, whereas U is a singlet with t_R quantum numbers. Since the embedding contains $(\mathbf{3},\mathbf{2})_{\mathbf{1/6}}$ twice, although only one features a zero–mode which corresponds to q_L, there will be two Q resonances. For better readability, the composite Yukawas are reabsorbed into the mass terms, as is done in [53]. Then, the mass mixing Lagrangian in the top sector is

given by

$$\begin{aligned}\mathcal{L}_{\text{mass}} = \quad & -\lambda_{t_R} f\, \bar{t}_R \Delta_{t_R} \mathcal{O}^{\mathbf{20}}_{CS,L} + \text{h.c.} \\ & -\lambda_{q_L} f\, \bar{q}_L\, \Delta_{q_L} \mathcal{O}^{\mathbf{15}}_{CS,L} + \text{h.c.} \\ & -m_{\mathbf{10}} \bar{Q}^{\mathbf{15}} Q^{\mathbf{20}} - m'_{\mathbf{10}} \bar{Q}^{\mathbf{20}} Q^{\mathbf{15}} \\ & -m^{\mathbf{20}}_{\mathbf{10}^*} \bar{U}^{\mathbf{20}} U^{\mathbf{20}} - m^{\mathbf{20}}_{\mathbf{10}} \bar{Q}^{\mathbf{20}} Q^{\mathbf{20}} - m^{\mathbf{15}}_{\mathbf{10}} \bar{Q}^{\mathbf{15}} Q^{\mathbf{15}}\,, \end{aligned} \tag{3.41}$$

where the composite operators decompose as

$$\begin{aligned} \mathcal{O}^{\mathbf{20}}_{CS,L} \to \; & U^{\mathbf{20}}_L \oplus ... \\ & Q^{\mathbf{20}}_L \oplus ... \\ \mathcal{O}^{\mathbf{20}}_{CS,R} \to \; & U^{\mathbf{20}}_R \oplus ... \\ & Q^{\mathbf{20}}_R \oplus ... \\ \mathcal{O}^{\mathbf{15}}_{CS,L} \to \; & Q^{\mathbf{15}}_L \oplus ... \\ & .. \\ \mathcal{O}^{\mathbf{15}}_{CS,R} \to \; & Q^{\mathbf{15}}_R \oplus ... \\ & .. \end{aligned} \tag{3.42}$$

under H, and resonances that do not talk to the top are not listed. Before diagonalisation, the mass matrix has the form

$$\begin{pmatrix} \bar{t}_L \\ \bar{Q}^{\mathbf{15}}_L \\ \bar{Q}^{\mathbf{20}}_L \\ \bar{U}^{\mathbf{20}}_L \end{pmatrix}^T \begin{pmatrix} 0 & f\lambda_{q_L} c_R & 0 & 0 \\ 0 & m^{\mathbf{15}}_{\mathbf{10}} & m_{\mathbf{10}} & 0 \\ -f\lambda_{t_R} b_L \sin\frac{h}{f} & m'_{\mathbf{10}} & m^{\mathbf{20}}_{\mathbf{10}} & 0 \\ f\lambda_{t_R} a_L \cos\frac{h}{f} & 0 & 0 & m^{\mathbf{20}}_{\mathbf{10}^*} \end{pmatrix} \begin{pmatrix} t_R \\ Q^{\mathbf{15}}_R \\ Q^{\mathbf{20}}_R \\ U^{\mathbf{20}}_R \end{pmatrix},$$

where a_L, b_L and c_R are dimensionless parameters. As opposed to the spurion analysis, where there was one parameter per composite multiplet, here we allow for $a_L \neq b_L \neq c_L$, since we start distinguishing between individual resonances. Still, all three parameters are expected to be $\mathcal{O}(1)$. Expanding in zeroth order of the Goldstone matrix ($U \sim \mathbb{1}_{6\times 6}$) the mass eigenstates of the heavy resonances, denoted by subscript "phys", are

$$m^2_{U,\text{phys}} = \quad \left(m^{\mathbf{20}}_{\mathbf{10}^*}\right)^2 + (a_L \lambda_{t_R} f)^2 \tag{3.43}$$

$$\begin{aligned}\left(m_{Q_+,\text{phys}}\, m_{Q_-,\text{phys}}\right)^2 = \quad & \left(m_{\mathbf{10}} m'_{\mathbf{10}} - m^{\mathbf{20}}_{\mathbf{10}} m^{\mathbf{15}}_{\mathbf{10}}\right)^2 \\ & + \left(f\lambda_{q_L} c_R\right)^2 \left((m_{\mathbf{10}})^2 + (m^{\mathbf{20}}_{\mathbf{10}})^2\right)\,. \end{aligned} \tag{3.44}$$

After EWSB, the top mass at leading order is, for $a_L \sim b_L \sim c_R \sim 1$,

$$\begin{aligned} m_t^2 \approx \quad & \frac{f^4 (m^{\mathbf{20}}_{\mathbf{10}^*})^2 m^2_{\mathbf{10}}}{\left(m_{Q_+,\text{phys}}\, m_{Q_-,\text{phys}}\right)^2 m^2_{U,\text{phys}}} \lambda^2_{t_R} \lambda^2_{q_L} \sin^2\frac{v}{f} \\ \approx \quad & \frac{f^2 (m^{\mathbf{20}}_{\mathbf{10}^*})^2 m^2_{\mathbf{10}}}{\left(m_{Q_+,\text{phys}}\, m_{Q_-,\text{phys}}\right)^2 m^2_{U,\text{phys}}} \lambda^2_{t_R} \lambda^2_{q_L} v^2_{\text{SM}} \end{aligned} \tag{3.45}$$

where in the second line we expressed the top mass in terms of the SM vev (Eq. 3.11). From the determination of the Higgs mass from the parametrised Higgs potential (2.4) we can combine Eq.(3.45) and Eq. (2.6) to find a relation between the mass of

the top, the top partners and m_h

$$\begin{aligned} m_h^2 = \quad & 8\frac{\beta}{f^4}\frac{\left(m_{Q_+,\text{phys}}\, m_{Q_-,\text{phys}}\right)^2 m_{U,\text{phys}}^2}{f^2\lambda_{t_R}^2\lambda_{q_L}^2(m_{\mathbf{10}^*}^{\mathbf{20}})^2 m_{\mathbf{10}}^2} m_t^2 \\ \approx \quad & 8\frac{\beta}{f^4}\frac{1}{\lambda_{t_R}^2\lambda_{q_L}^2}\frac{\min(m_{\text{res, top}}^2)}{f^2} m_t^2 \\ \propto \quad & \frac{\min(m_{\text{res, top}}^2)}{f^2} m_t^2\,, \end{aligned} \tag{3.46}$$

where in the last line we recognise the problematic relation between lightest top partner and Higgs mass that was mentioned in Sec. 2.1.2 already. However, while in generic CHMs $\beta(\lambda_{t_R}, \lambda_{q_L}, ...)$ is predominantly driven by the top quark, here, due to the appearance of the exotic fermions, $\beta(\lambda_{t_R}, \lambda_{q_L}, \lambda_{\omega_R}, \lambda_{\omega_L}, ...)$ is more complicated. If a convenient cancellation occurs within β, $\min(m_{\text{res, top}})$ can become larger while still reproducing a Higgs mass around 125 GeV. We believe this to be the reason why in the following numerical scan we find a few heavy top partners.

Going from the two–site model to the three–site model is straight–forward, since one only has to add another set of resonances. Now, the first site still respects $SU(6)$, and the breaking occurs in the second site, where the respected symmetry is $SU(5)$. The explicit mass matrices for top, bottom and exotic sector are given in Appendix A.5.1. The Higgs potential is calculated with the Coleman–Weinberg formula ([108])

$$V_i(h) = -\frac{2N_c}{8\pi^2}\int \mathrm{d}p\, p^3 \log\left(\det\left(M_i^\dagger(h)M_i(h) + p^2\mathbb{1}\right)\right) \tag{3.47}$$

where we include into $M_i(h)$ the mass matrices of the top, exotic and bottom sector. N_C is the number of QCD colours. The numerical scan is performed by randomly choosing values from a uniform distribution over a range of $[-5f, 5f]$ for the three–site model parameters, with the exception of the linear mixings λ_{t_R} and λ_{b_R}, which are fixed by top mass $m_t(f) \sim 150$ GeV and bottom mass $m_b(f) \sim 3$ GeV at scale $f = 1600$ GeV respectively. Since $V(0)$ is divergent and Higgs–independent it can be removed and from now on we refer to $V(h) - V(0)$ when mentioning the Higgs potential. As can be seen in Eq. (3.31), there is a perfect cancellation of $\lambda_{t_R}^2$, when $\lambda_{\omega_R} = \lambda_{t_R}$ are identical. To decrease tuning, in the following we set the two linear mixings equal. Still, a quadratic contribution remains ($\lambda_{q_L}^2$), which will be addressed in Chapter 4.

The results are filtered first for $v_{\text{SM}} \in 246 \pm 40$ GeV, and in a second step for $m_h \in (125 \pm 15)$ GeV. The range is chosen so broadly because of the nature of the three–site model scan. By changing individual parameters slightly it is very easily possible to produce small shifts in the Higgs potential, but to scan over a fine grid of all possible parameter combinations would take a disproportionate amount of computing power and time. Therefore, any potential that leads to $v_{\text{SM}} \in 246 \pm 40$ GeV is accepted while keeping in mind that in the near neighbourhood of the parameter space there will be a combination that leads to $v_{\text{SM}} = 246$ GeV (see Appendix A.5.1 for details). The shaded red region shows the current experimental bounds $m_T \gtrsim 1500$ GeV ([44–48]) on the lightest top partner.

While in Fig. 3.3 we are interested in the range of Higgs masses produced in relation to the mass of the lightest top partner, we later constrain $m_h \in (125 \pm 15)$ GeV when evaluating the Barbieri–Giudice measure (Eq. 2.9). Several top partners with $m_T > 1.5$ TeV are found that give $m_h \in (125 \pm 15)$ GeV and evade current

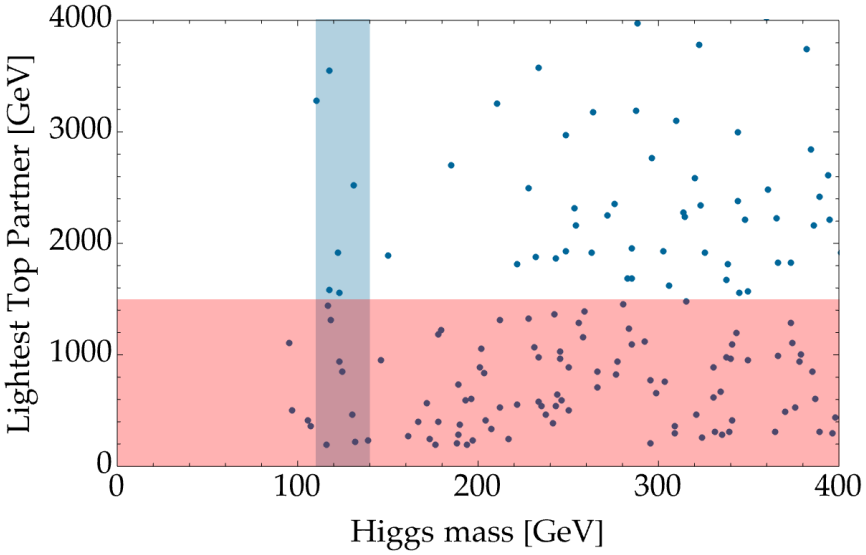

FIGURE 3.3: Mass of the lightest top partner m_T vs Higgs mass m_h for results of the 3–site model scan and SSB scale $f = 1600$ GeV. The blue band shows $m_h \in (125 \pm 15)$ GeV, whereas the experimentally excluded mass range $m_T \lesssim 1.5$ TeV ([44–48]) is shown in red.

experimental constraints, which are shown as the shaded red area in Fig. 3.3. This is an improvement with respect to generic CHMs which often do not allow for any heavy top partners. Still, the other common problem of CHMs has to be examined too, which is fine–tuning. In Fig. 3.4, where fine–tuning is plotted against mass of the lightest top partner, the dashed vertical black line shows the expected minimal tuning $\Delta_{\text{min}}(1600\text{ GeV}) = \frac{1}{v_{\text{SM}}{}^2/f^2} \approx 42$. The overall tuning varies up to ~ 420 which corresponds to tuning at the 0.1% level, and very few points are assigned tuning values that correspond to to minimal tuning or less[6]. It becomes clear that heavy top partners require tuning $\gtrsim 100$, which is around 1%. So although selected top partners decouple, their increase in mass comes at the cost of tuning. In Chapter 4 this will no longer be the case. Additionally, in Fig. 3.5 the mass range of lightest exotics is shown versus Higgs mass. Comparing with Fig. 3.3 the mass range lies lower than the one of the top partner. The exotic seems to have replaced the lightest top partner as lightest new expected state. This is supported by Fig. 3.6 which plots lightest top partner versus lightest exotic, and there is a trend: Heavy top partners come at the cost of very light exotics. Still, not all points lie above the dotted $(m_T = m_{\text{ex}})$–line, but the ones of phenomenological interest do, i.e. all points with $m_T \gtrsim 1.5$ TeV. In Sec. 4.4.1 we address the phenomenology of the exotic fermions, but as will be explained in the next section, the GHGUT model requires $f \gg 1600$ GeV due to its non–custodial nature, and this automatically pushes the average masses of the exotics and top partners higher which makes it more difficult to find collider bounds that can restrict the model. Therefore, the precise phenomenology of their decays and the question about possible bounds is not of interest in this chapter.

[6] In Appendix A.5.1 a plot can be found which shows the improvement in tuning when $\lambda_{t_R} = \lambda_{\omega_R}$ versus $\lambda_{t_R} \neq \lambda_{\omega_R}$.

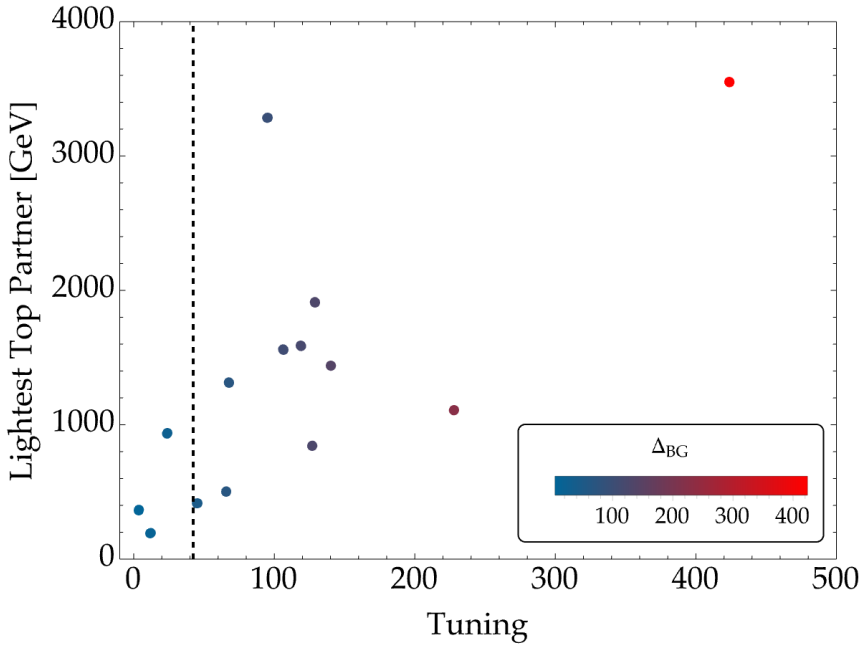

FIGURE 3.4: Barbieri–Giudice measure for lightest top partner masses found in numerical scans which reproduce $v_{SM} \in 246 \pm 40$ GeV and $m_h \in (125 \pm 15)$ GeV for $f = 1600$ GeV. The minimal tuning $\Delta_{min} \sim 42$ is shown as the dashed vertical black line, and the colour–coding and x-axis coincide.

3.3 Phenomenology

Although there are several interesting phenomenological predictions stemming from CHM, such as deviations of the couplings between SM particles and the Higgs, these tend to be suppressed by the SSB scale f, see e.g. Appendix A.6 for modifications to the Higgs–gluon coupling. As will now be explained, f has to be chosen to be at least several TeV, which renders these effects negligible, and therefore we will not further investigate them here.

3.3.1 Custodial Symmetry

$SU(6)/SU(5)$ is non–custodial, since the relation

$$\rho = \frac{m_W^2}{(\cos\theta_w\, m_Z)^2} \tag{3.48}$$

between the masses of the W and Z gauge bosons, which at tree–level in the SM is $\rho_0 = 1$, is not preserved. θ_w is the weak mixing angle. After EWSB a residual global $SU(2)$ symmetry is expected, which would ensure Eq. (3.48), and is supported by experimental data. However, the relation is not necessarily respected in BSM physics, such as in our model, where there is no underlying $SO(4) \simeq SU(2)_L \times SU(2)_R$ symmetry in the unbroken group. Specifically, the dimension–6 operator that violates custodial symmetry in our model is of the following form:

$$\mathcal{L} \supset \frac{1}{2f^2}\frac{2}{5}\left(H^\dagger \overleftrightarrow{D_\mu} H\right)\left(H^\dagger \overleftrightarrow{D^\mu} H\right) \equiv \frac{c_T}{2f^2}\left(H^\dagger \overleftrightarrow{D_\mu} H\right)\left(H^\dagger \overleftrightarrow{D^\mu} H\right) , \tag{3.49}$$

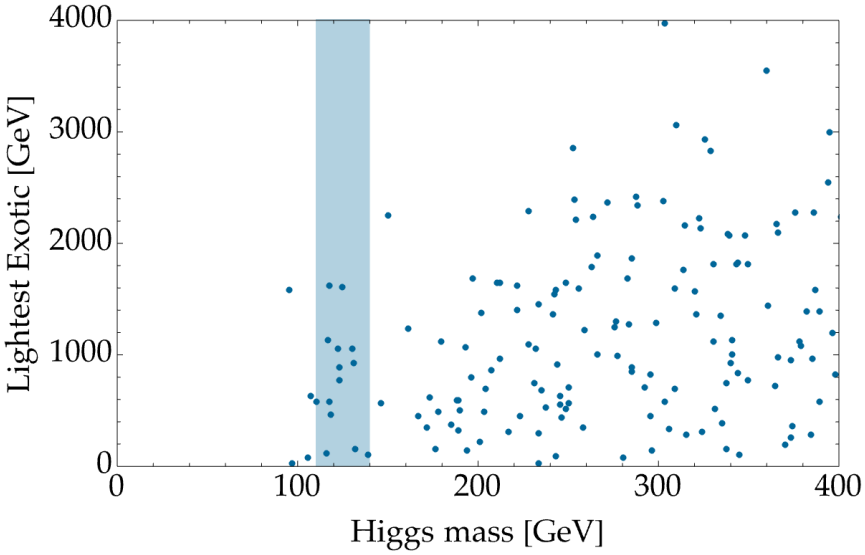

FIGURE 3.5: Mass of the lightest exotic vs Higgs mass m_h for results of the 3–site model scan with $f = 1600$ GeV. The blue band shows $m_h \in (125 \pm 15)$ GeV.

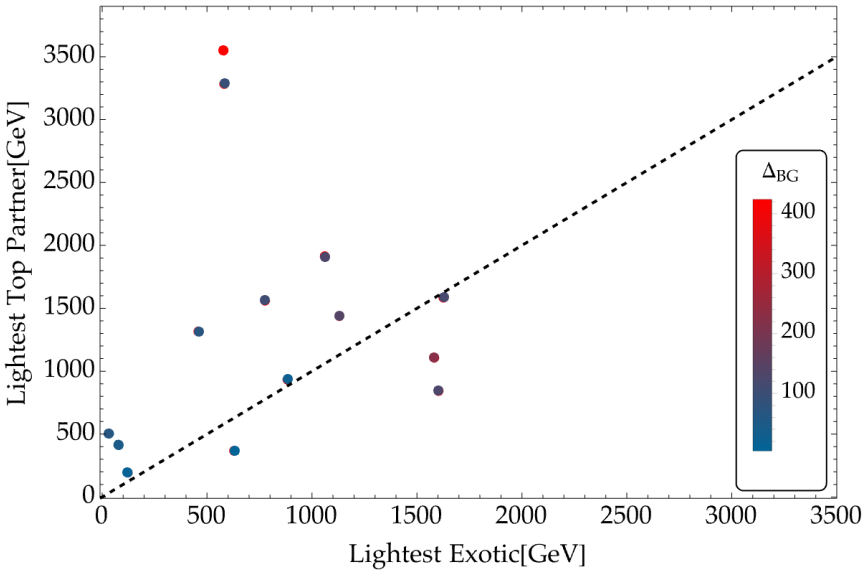

FIGURE 3.6: Lightest exotic m_{ex} versus lightest top partner m_T for $f = 1600$ GeV, where the dashed black line gives $m_T = m_{\text{ex}}$. The Barbieri–Giudice measure is encoded through colour.

where $\left(H^\dagger \overleftrightarrow{D_\mu} H\right) \equiv H^\dagger D_\mu H - (D_\mu H)^\dagger H$. The contribution to the oblique Peskin-Takeuchi parameter T is given by ([109])

$$\Delta\rho = \hat{T} = c_T \frac{v_{SM}^2}{f^2} = \frac{2}{5}\frac{v_{SM}^2}{f^2} \qquad \text{where} \quad \hat{T} \equiv \alpha T \tag{3.50}$$

with $v_{SM} = 246$ GeV the EW Higgs vev and $\alpha = 1/137$ the fine–structure constant. The recent CDF II measurement [110] found that large positive values of T are preferred. They define the T parameter in terms of the Warsaw basis

$$\mathcal{L} \supset T \left(\frac{2\alpha}{v_{SM}^2}\right) \left|\Pi^\dagger D_\mu \Pi\right|^2 \tag{3.51}$$

which can be related to the here–used SILH basis operator via Eq. (2.5) of [111] as

$$\mathcal{O}_T = \frac{1}{2}\left(\Pi^\dagger \overleftrightarrow{D_\mu} \Pi\right)\left(\Pi^\dagger \overleftrightarrow{D^\mu} \Pi\right) \quad \longleftrightarrow \quad Q_{HD} = -2\left|\Pi^\dagger D_\mu \Pi\right|^2 \tag{3.52}$$

when higher order operators are neglected. From the CDF II measurements best fit [110] ($T = 0.27$) the lower bound on f is set to

$$f \gtrsim 3.5 \text{ TeV}. \tag{3.53}$$

in line with the PDG 2022 2σ upper bound $T = 0.27$ ([112]). However, if the EW precision parameter U is set to zero, then the 2σ upper bound becomes $T = 0.16$ ([112]) which gives a constraint of

$$f \gtrsim 4.5 \text{ TeV} \tag{3.54}$$

and the best fit value ($T = 0.04$) gives an even stronger constraint of

$$f \gtrsim 9.1 \text{ TeV}. \tag{3.55}$$

With a SSB scale of, optimistically speaking, 3.5 TeV, the model becomes less attractive. At this scale, the composite resonances are not expected to be within reach of the LHC, and significant tuning has to be reintroduced to achieve a light Higgs. Therefore, although the appearance of the VL mass term would lead to heavy top partners for a SSB scale of $f = 1600$ GeV with little tuning, f is pushed upwards once the non–custodial nature of the coset is taken into account.

3.4 Overview

In this chapter we have performed an analytical spurion analysis of the scalar potential in the GHGUT model by [10], specifically of the potential of the Higgs, which appears as a pNGB of the coset $SU(6)/SU(5)$, and have examined the two commonly found problems in composite Higgs theories, which are the prediction of very light top partners, and the necessity of strong tuning to achieve correct EWSB. We have seen a convenient cancellation of the contribution of the right–handed top quark at leading order in couplings, due to the emergence of exotic fermions, which decreases fine-tuning, as well as a vector-like mass term for the exotics that allows the top partners to decouple. Still, we are plagued by the quadratic contribution of the left-handed quark doublet, which pushes the tuning to higher values than minimally

expected. So naturally, the question arises: What mechanism leads to the cancellation between exotic and right-handed quark, and, most importantly: Is it possible to reproduce it? The short answer is yes, but a more detailed answer will be given in the next part of this thesis, where we show how the current model can be improved with respect to fine-tuning, and how the cancellation mechanism can be applied to other cosets, which furthermore do not suffer from being non–custodial. In turn, in the current GHGUT model the SSB scale f has to be several TeV due to a dimension–6 operator featured in the model which contributes to the oblique T parameter, which renders improvements with regards to the top partner problem negligible. There are many advantages of the $SU(6)$ GHGUT that are not directly concerned with minimising the tuning necessary to achieve correct EWSB, such as in the flavour sector, where it is possible to reproduce a realistic CKM matrix (see [69] for details) or how the additional scalar singlet might be able to help with baryogenesis, but they are not focus of this thesis.

Chapter 4

Mirror Fermions

After noticing that the cancellation mechanism found in Chapter 3 is generalisable, in the following chapter we establish the precise conditions under which the quadratic contribution to the scalar potential can be cancelled in Sec. 4.1, proof our claim in Sec. 4.2, then analyse a concrete model incarnation in Sec. 4.3, discuss the resulting phenomenology in Sec. 4.4 and finally compare to other mechanisms in Sec. 4.5, which also includes a small outlook. The chapter is partly published in [113] and was worked on in collaboration with Andrei Angelescu, Andreas Bally and Florian Goertz.

4.1 Theorem

> *The quadratic contribution of a chiral fermion ψ to the pNGB potential of a coset G/H is cancelled when a new chiral fermion ψ' with conjugated gauge quantum numbers is added, called mirror fermion, if the fermions talk to the same composite operator in a pseudoreal representation* $\mathbf{R}$ *of the group G which decomposes as* $\mathbf{R} \to \mathbf{C} \oplus \bar{\mathbf{C}}$ *under H, with* $\mathbf{C}$ *a complex representation and* $\bar{\mathbf{C}}$ *its complex conjugate.*
>
> (in [113])

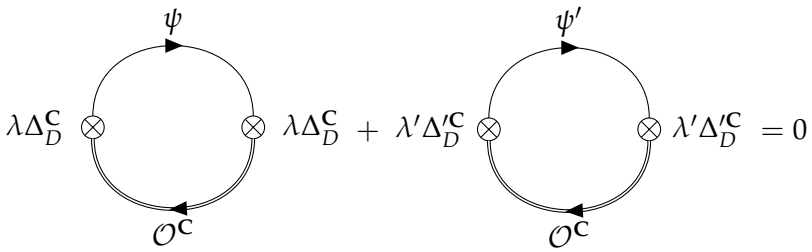

FIGURE 4.1: Cancellation mechanism of the quadratic contribution in terms of Feynman diagrams when $\lambda = \lambda'$. Figure adapted from [113].

4.2 Proof

We prove the theorem via a spurion analysis, similarly to how the scalar potential was characterised in Chapter 3. The spontaneous symmetry breaking (SSB) of group G to subgroup H is considered, with pNGBs arising from the broken generators. They obtain their mass through explicit breaking of G, which stems from the partial compositeness (PC) of fermionic fields. Specifically, the contribution of a

chiral fermion ψ, embedded in the complex H–subrepresentation $\mathbf{C}$ of a pseudoreal G–representation $\mathbf{R}$ is analysed, where $\mathbf{R}$ decomposes under H such that $\mathbf{R} \to \mathbf{C} \oplus \bar{\mathbf{C}}$, where $\bar{\mathbf{C}}$ is the complex conjugate of $\mathbf{C}$. Then, a new chiral fermion ψ' that carries conjugated quantum numbers with respect to ψ can be embedded in $\bar{\mathbf{C}}$. The PC Lagrangian, which parametrises the linear mixing between the elementary fermions and the composite operators, is given by

$$\mathcal{L}_{\text{PC}} = \lambda\, \bar{\psi} \Delta\, \mathcal{O}^{\mathbf{R}} + \lambda'\, \bar{\psi}' \Delta'\, \mathcal{O}^{\mathbf{R}} + \text{ h.c.}, \tag{4.1}$$

with spurions that can chosen to take the form

$$\Delta = \begin{pmatrix} \delta & 0 \\ 0 & 0 \end{pmatrix}, \quad \Delta' = \begin{pmatrix} 0 & 0 \\ 0 & \delta \end{pmatrix}, \tag{4.2}$$

where δ is a diagonal $C \times C$ matrix. The fact that the same matrix δ appears in Δ and Δ' is a consequence of the decomposition $\mathbf{R} \to \mathbf{C} \oplus \bar{\mathbf{C}}$. In a generic embedding of ψ and ψ', the upper left entry of Δ and the lower right entry Δ' would be distinct. Eq. 4.1 can be expressed in matrix form via

$$\mathcal{L}_{\text{PC}} = \begin{pmatrix} \lambda\bar{\psi} & \lambda'\bar{\psi}' \end{pmatrix} \begin{pmatrix} \delta & 0 \\ 0 & \delta \end{pmatrix} \mathcal{O}^{\mathbf{R}} + \text{ h.c.}\,. \tag{4.3}$$

As in Chapter 3, the spurions are incompletely filled G multiplets. When set to their vev, they automatically select the entries of ψ and ψ' that correspond to the SM fermion and its conjugate. Therefore, with slight misuse of notation we give the same name to ψ (ψ') in Eq. (4.1) and Eq. (4.3), although the dimensions of the vectors differ. To calculate the scalar potential, it is necessary to define the Goldstone matrix

$$U = \exp\{i\Pi_{\hat{a}} T^{\hat{a}}\}, \tag{4.4}$$

where $\Pi_{\hat{a}}$ are the Goldstone bosons, and $T^{\hat{a}}$ the broken generators of G/H. Numerical factors are absorbed into the definition of $\Pi_{\hat{a}}$, so that they are canonically normalised.

As is done in [53], we will use the CCWZ mechanism to express the PC Lagrangian in terms that are H–symmetric. By employing the Goldstone matrix to make sure the full G is still respected, we can split the composite operator into its representations under H

$$\mathcal{O}^{\mathbf{R}} = U \left(\mathcal{O}^{\mathbf{C}}, \mathcal{O}^{\bar{\mathbf{C}}}\right)^T, \tag{4.5}$$

and find

$$\mathcal{L}_{\text{PC}} = \begin{pmatrix} \lambda\bar{\psi} & \lambda'\bar{\psi}' \end{pmatrix} \begin{pmatrix} \delta & 0 \\ 0 & \delta \end{pmatrix} \begin{pmatrix} U_{11} & U_{12} \\ U_{21} & U_{22} \end{pmatrix} \begin{pmatrix} \mathcal{O}^{\mathbf{C}} \\ \mathcal{O}^{\bar{\mathbf{C}}} \end{pmatrix} + \text{ h.c. }. \tag{4.6}$$

By expressing the Goldstone matrix U, which is an element of G, in the $\mathbf{R}$ representation, we can make use of the properties of group elements in pseudoreal representations. That is, one can always find an antisymmetric matrix S so that $SgS^{-1} = g^*$. S is unique, and therefore we chose to derive its form for a transformation along the unbroken generators ($T^a_{\mathbf{R}}$), where S immediately becomes clear, since

$$g = \exp\left(i\, x_a T^a_{\mathbf{R}}\right) = \exp\left[i\, x_a \begin{pmatrix} T^a_{\mathbf{C}} & 0 \\ 0 & -\left(T^a_{\mathbf{C}}\right)^* \end{pmatrix}\right]. \tag{4.7}$$

Then, S can be chosen to be

$$S = \begin{pmatrix} 0 & 1 \\ -1 & 0 \end{pmatrix}, \tag{4.8}$$

without loss of generality, from which we deduce

$$\begin{aligned} & SUS^{-1} = U^* \\ \Rightarrow \quad & U_{22} = U_{11}^*, \quad U_{21} = -U_{12}^*. \end{aligned} \tag{4.9}$$

Next, we calculate the contributions to the scalar potential, equivalently to how it is done in Sec. 3.2.1. To do so, the spurions are dressed with the Goldstone matrix as

$$\begin{pmatrix} U_{11} & U_{12} \\ U_{21} & U_{22} \end{pmatrix}^\dagger \begin{pmatrix} \delta & 0 \\ 0 & \delta \end{pmatrix} = \begin{pmatrix} U_{11}^\dagger \delta & U_{21}^\dagger \delta \\ U_{12}^\dagger \delta & U_{22}^\dagger \delta \end{pmatrix} \equiv \begin{pmatrix} \Delta_D^{\mathbf{C}} & \Delta_D'^{\mathbf{C}} \\ \Delta_D^{\bar{\mathbf{C}}} & \Delta_D'^{\bar{\mathbf{C}}} \end{pmatrix}. \tag{4.10}$$

The lowest order[1] $\mathbf{C}$–contribution to the potential is

$$V^{\mathbf{C}} \propto \lambda^2 \mathrm{Tr}\left[(\Delta_D^{\mathbf{C}})^\dagger \Delta_D^{\mathbf{C}}\right] + \lambda'^2 \mathrm{Tr}\left[(\Delta_D'^{\mathbf{C}})^\dagger \Delta_D'^{\mathbf{C}}\right], \tag{4.11}$$

where we neglect power counting. Fig. 4.1 shows the corresponding Feynman loop diagrams. The above equation does not carry any Goldstone dependence, as we will show now by proving the following identity

$$\mathrm{Tr}\left[(\Delta_D'^{\mathbf{C}})^\dagger \Delta_D'^{\mathbf{C}}\right] = \mathrm{Tr}\left[(\Delta_D^{\bar{\mathbf{C}}})^\dagger \Delta_D^{\bar{\mathbf{C}}}\right], \tag{4.12}$$

i.e. that the ψ' contribution running in a loop with $\mathcal{O}^{\mathbf{C}}$ is identical to the ψ contribution running in a loop with $\mathcal{O}^{\bar{\mathbf{C}}}$. In the following we will use that the trace is unchanged if a matrix is transposed

$$\mathrm{Tr}\left[M\right] = \mathrm{Tr}\left[M^T\right] \tag{4.13}$$

and start by explicitly writing

$$\begin{aligned} \mathrm{Tr}\left[(\Delta_D^{\bar{\mathbf{C}}})^\dagger \Delta_D^{\bar{\mathbf{C}}}\right] \quad &= \mathrm{Tr}\left[(U_{12}^\dagger \delta)^\dagger U_{12}^\dagger \delta\right] \\ &= \mathrm{Tr}\left[\delta^\dagger U_{12} U_{12}^\dagger \delta\right] \\ &\overset{(4.9)}{=} \mathrm{Tr}\left[\delta^\dagger (-U_{21}^*)(-U_{21}^T)\delta\right] \\ &\overset{(4.13)}{=} \mathrm{Tr}\left[\delta^T U_{21} (U_{21}^\dagger) \delta^*\right]. \end{aligned} \tag{4.14}$$

Since in the chosen basis δ is a diagonal matrix with entries that are real (either 0 or 1), $\delta^* = \delta = \delta^\dagger = \delta^T$, and

$$\begin{aligned} \mathrm{Tr}\left[\delta^T U_{21} (U_{21}^\dagger) \delta^*\right] \quad &= \mathrm{Tr}\left[\delta^\dagger U_{21} (U_{21}^\dagger) \delta\right] \\ &= \mathrm{Tr}\left[(U_{21}^\dagger \delta)^\dagger (U_{21}^\dagger \delta)\right] \\ &= \mathrm{Tr}\left[(\Delta_D'^{\mathbf{C}})^\dagger \Delta_D'^{\mathbf{C}}\right], \end{aligned} \tag{4.15}$$

[1] As before, lowest order corresponds to second order in couplings, i.e. $\mathcal{O}(\lambda/g_*)^2$.

which concludes the proof of Eq. (4.12). Then, Eq. (4.11) can be expressed as

$$V^{\mathbf{C}} \propto \lambda^2 \mathrm{Tr}\left[(\Delta_D^{\mathbf{C}})^\dagger \Delta_D^{\mathbf{C}}\right] + \lambda'^2 \mathrm{Tr}\left[(\Delta_D^{\bar{\mathbf{C}}})^\dagger \Delta_D^{\bar{\mathbf{C}}}\right]. \tag{4.16}$$

If additionally $\lambda = \lambda'$, this simplifies to

$$V^{\mathbf{C}} \propto \lambda^2 \mathrm{Tr}\left[\Delta^\dagger U U^\dagger \Delta\right] = \lambda^2 N\,, \tag{4.17}$$

where, due to the unitary of the Goldstone matrix ($U^\dagger U = \mathbb{1}$), all Goldstone dependence drops out. At quadratic order, there is no contribution to the scalar potential left, although a pNGB–independent contribution to the vacuum energy remains that is proportional to $\mathrm{Tr}\left[\Delta^\dagger \Delta\right] \equiv N$, the fermionic degrees of freedom. For instance, when $\psi = t_R$, then $N = 3$. The cancellation for the $\bar{\mathbf{C}}$–contribution to the scalar potential proceeds analogously, but we will not explicitly give it here.

Additional Conditions for Cancellation

Apart from the decomposition of pseudoreal representation $\mathbf{R} \to \mathbf{C} \oplus \bar{\mathbf{C}}$ under H, there are two additional conditions that have to hold for the cancellation to work and to be effective. In the following, we will motivate why $\lambda = \lambda'$ can be assumed, and, since ψ' will be given a Dirac mass, which is another source of explicit symmetry breaking, why the resulting contribution to the potential is $\frac{m_E^2}{m_*^2}\lambda'^2$ suppressed, i.e. why $m_E < m_*$ is expected.

Composite Sector Dynamics

One essential ingredients to achieve the cancellation of the quadratic contribution to the pNGB potential is that the linear mixings of SM field and mirror fermion are identical, so $\lambda = \lambda'$. In the general PC framework the motivation is based on the fact that both fields are coupled to the same operator which has scaling dimension $d_{L/R}$. Therefore, if the linear mixing strength is identical in the UV, they will scale identically in the IR [9, 11, 29, 89, 114]

$$(\lambda_{\mathrm{IR}})_{R/L} \sim (\lambda_{\mathrm{UV}})_{R/L} \left(\frac{\Lambda_{\mathrm{IR}}}{\Lambda_{\mathrm{UV}}}\right)^{d_{L/R}-5/2}. \tag{4.18}$$

Without specifying a UV–completion, setting $\lambda_{\mathrm{UV}} = \lambda'_{\mathrm{UV}}$ is an assumption. However, in the holographic dual $\lambda_{\mathrm{UV}} = \lambda'_{\mathrm{UV}}$ is immediately clear as the SM fermion and its mirror fermion are part of the same bulk field, and therefore have the same localisation in the bulk. See section 2.3.3 for details.

Dirac Mass for Mirror Fermions

So far, the mirror fermions have the same linear mixings as the SM fermions, and couple to the Higgs in the same manner. Therefore, without additional ingredients the mirror fermions would behave similarily to the SM fields, i.e. be massless until the Higgs acquires a vev after EWSB, and then gain similar masses as the SM fields[2]. As a consequence, it becomes necessary to introduce opposite–chirality partners $\tilde{\psi}'$ and a Dirac mass m_E for the mirror fermions. For simplicity it is assumed that the

[2]It should be noted that – in the 5D dual – the BCs of the exotics have changed with respect to the mixed BCs in the original embedding from [10] (see Sec. 2.3.1) to allow for zero modes.

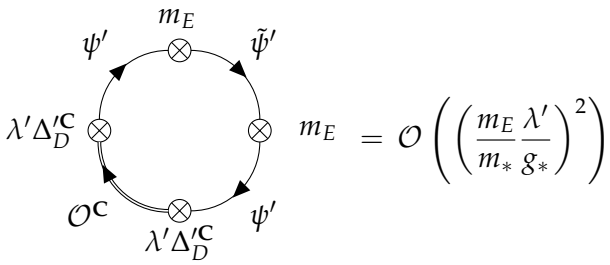

FIGURE 4.2: Remaining quadratic contribution in the presence of a Dirac mass m_E for the mirror fermion.

$\tilde{\psi}'$ are purely elementary and do not couple to the composite sector. Otherwise, the opposite–chirality partner could contribute at leading order to the pNGB potential, reintroducing the double–tuning problem[3]. Still, they do lead to new contributions at $\mathcal{O}(\frac{m_E^{2n}}{m_*^{2n}}\lambda'^2)$, with an even number of m_E insertions, where the lowest order can be seen in Fig. 4.2, and is calculated in Sec. 4.3.1. For the cancellation of the quadratic contribution to the Higgs potential to be effective, the new contribution has to be suppressed, i.e. $m_E < m_*$ is required. As explained in Sec. 2.3.3, the partially composite elementary fermions stem from 5D bulk fields, whereas fields external to the composite sector are described by UV brane–localised fields. Then, the mirror fermion itself is part of a bulk field, whereas its opposite–chirality partner lives on the UV brane, and UV brane–localised mass mixing gives their 4D Dirac mass

$$\int \mathrm{d}^4x \frac{M_{UV}}{\sqrt{R}} \bar{\tilde{\psi}}'(x)\psi'(x, z = R) + \text{ h.c.}, \tag{4.19}$$

where $M_{UV} \sim \mathcal{O}(1)$. Inserting the bulk profiles for the 5D fermions ([69]), we find two regimes for m_E

$$m_E \sim \frac{M_{\mathrm{UV}}}{R} \times \begin{cases} 1 & (c > 0.5) \\ (R'/R)^{c-1/2}\,(1-c) & (c < 0.5) \end{cases}, \tag{4.20}$$

where $c < 0.5$ ($c > 0.5$) corresponds to IR (UV) localisation of the mirror fermion bulk field. The Higgs, as a composite state, is IR–localised itself, and since large partial compositeness fractions correspond to a large overlap between bulk field and Higgs field, both the t_R and the q_L bulk field will have $c < 0.5$, due to the large top Yukawa. Since also these two fields are the biggest source of explicit symmetry breaking, and mirror fermion and its SM counterpart are part of the same bulk field, we expect that m_E will become suppressed, and that $m_E < m_*$ is justified, instead of an imposed coincidence.

4.3 Analysis of concrete Model

Since the top Yukawa y_t is a combination of the linear mixings of t_R and t_L, the contributions of both the right–handed top quark, and the left–handed quark doublet should be cancelled by respective mirror fermions ω_R and θ_L. Then, the PC

[3] In Chapter 3 $\omega_L \in \mathbf{15}$ does not talk to the Higgs, and therefore does not contribute at leading order to the Higgs potential

Lagrangian is given by

$$\begin{aligned}\mathcal{L}_{\text{PC}} = \quad & (f\,\lambda_{t_R}\bar{t}_R\Delta_{t_R} + f\,\lambda_{\omega_R}\bar{\omega}_R\Delta_{\omega_R})\,O_L^{\mathbf{R}} + \text{ h.c.} \\ & + (f\,\lambda_{q_L}\bar{q}_L^i\Delta_{q_L,i} + f\,\lambda_{\theta_L}\bar{\theta}_L\Delta_{\theta_L})\,O_R^{\mathbf{R}} + \text{ h.c.} \\ & + m_\omega\bar{\omega}\omega + m_\theta\bar{\theta}\theta \end{aligned} \tag{4.21}$$

with Dirac masses m_ω and m_θ for the mirror fermions. One possible coset in which the mirror fermion mechanism can be applied is $SU(6)/SU(5)$ since it prompted its discovery in Chapter 3. When the embedding of q_L is shifted from the **15** to the **20** of $SU(6)$, and the additional mirror fermion θ_L is introduced, so that the pseudoreal **20**–representation decomposes as

$$\begin{aligned}\mathbf{20} \to \quad & q_L(\mathbf{3},\mathbf{2})_{\frac{1}{6}} \oplus \omega_R(\mathbf{3^*},\mathbf{1})_{-\frac{2}{3}} \oplus e'^c(\mathbf{1},\mathbf{1})_1 \\ & \theta_L(\mathbf{3^*},\mathbf{2})_{-\frac{1}{6}} \oplus u_R(\mathbf{3},\mathbf{1})_{\frac{2}{3}} \oplus (\mathbf{1},\mathbf{1})_{-1}\,, \end{aligned}$$

then neither t_R nor q_L will contribute to the pNGB potential at quadratic order.

However, $SU(6)/SU(5)$ is non-custodial, and due to the bounds on the EW precision parameter T having a SSB scale of $f \gtrsim 3.6$ TeV is required (see Sec. 3.3.1). Since even minimal tuning goes with f^2, there is no huge advantage in trying to eliminate double–tuning. Another coset in which the mirror fermion mechanism can be applied is $SO(11)/SO(10)$. Previously, $SO(11)$ models in warped dimensions were worked on e.g. in [76] or [77]. In $SO(11)$, the choice for pseudoreal representation **R** is a **32** which decomposes into **16** and $\bar{\mathbf{16}}$ of $SO(10)$. Since the **16** of $SO(10)$ contains a **10** of $SU(5)$,

$$\mathbf{16} \to \mathbf{10} \oplus \mathbf{5}^* \oplus \mathbf{1}\,, \tag{4.22}$$

the numerical analysis in the fermion sector proceeds identically for both cosets and a dedicated analysis including the gauge sector is out of the scope of this thesis. It should also be noted that all model–building freedom lies within the fermionic sector, where representations can be chosen at will (while attempting to stay as minimal as possible), whereas gauge fields are fixed by the adjoint representation, i.e. the generators of the group G.

Our goal is to give a rounded description, so we will model the full third generation of quarks, i.e. include the bottom sector into the analysis. Since q_L is already part of the set–up, the only field missing is b_R, which transforms as $(\mathbf{3},\mathbf{1})_{-1/3} \subset \mathbf{5}$ of $SU(5)$. For $SU(6)/SU(5)$ the situation is known from Chapter 3 and an additional **15** multiplet has to be introduced, which then is connected to the **20** multiplet. For $SO(11)/SO(10)$ one might think that it is sufficient to embed b_R into the $SU(5)$ **5** which is contained in the $\bar{\mathbf{16}}$

$$\bar{\mathbf{16}} \to \mathbf{10}^* \oplus \mathbf{5} \oplus \mathbf{1}\,,$$

but that would lead to a mass degeneracy between top and bottom quark. Therefore, it becomes necessary to introduce and additional $SO(11)$ multiplet $\mathbf{R}'$ that contains b_R and decomposes as

$$\mathbf{R}' \to \bar{\mathbf{16}} \oplus \ldots\,.$$

For simplicitly, we have chosen another **32**. In general terms, the additional G multiplet has to allow for the RH bottom to be part of it and decompose into at least the H multiplet into which the LH quark doublet is embedded.

4.3.1 Spurion Analysis

The spurion analysis proceeds analogously to Sec. 4.2, i.e. the elementary fields are lifted to full G–multiplets, and spurions Δ are incompletely filled to restore their true transformation behaviour. Then, the spurions are dressed with the Goldstone matrix, and the lowest order contribution to the scalar potential is found by contracting two spurions with each other. The leading contributions to the Higgs potential are

$$V(h) \propto \sin^2\left(\frac{h}{f}\right)\left(c_{\mathbf{20},L}\left(\lambda_{t_R}^2-\lambda_{\omega_R}^2\right)+c_{\mathbf{20},R}\left(\lambda_{\theta_L}^2-\lambda_{q_L}^2\right)\right)\,, \tag{4.23}$$

where $c_{\mathbf{20},L}$ and $c_{\mathbf{20},R}$ are the auxiliary parameters that incorporate the composite sector dynamics. They are not identical to each other, since t_R and ω_R couple to the LH composite operator, whereas q_L and ω_L couple to the RH composite operator. For $\lambda_{t_R}=\lambda_{\omega_R}$ and $\lambda_{\theta_L}=\lambda_{q_L}$ the above expression vanishes, as was expected from our theorem, and is now confirmed in an explicit model. The equivalence between the linear mixings with the composite sector can be motivated from the 5D dual due to the localisation of the bulk fields as is described in Sec. 4.2, and from now on we refer to $\lambda_{t_R}=\lambda_{\omega_R}\equiv\lambda_R$ and $\lambda_{q_L}=\lambda_{\theta_L}\equiv\lambda_L$. With this in mind, the quadratic and quartic in the Higgs potential both seem to arise at fourth order in couplings, when no further SM fields are considered. Therefore, one would expect the fine-tuning to be minimal (Eq. 2.7).

However, it is also necessary to take the VL nature of the exotic fermions into account. Following [40], the external opposite-chirality fields ($\theta_R(\mathbf{3^*},\mathbf{2})_{-\frac{1}{6}}$ and $\omega_L(\mathbf{3^*},\mathbf{1})_{-\frac{2}{3}}$) that give a VL mass to the exotics ($\theta_L(\mathbf{3^*},\mathbf{2})_{-\frac{1}{6}}$ and $\omega_R(\mathbf{3^*},\mathbf{1})_{-\frac{2}{3}}$) can be incorporated in the analysis by rewriting the mass term with the help of undressed spurions $\Delta^{\theta/\omega}$

$$\begin{aligned}\mathcal{L}\supset\quad & m_\omega\left(\bar\omega_L\omega_R+\bar\omega_R\omega_L\right)+m_\theta\left(\bar\theta_R\theta_L+\bar\theta_L\theta_R\right)\\ & \propto m_\omega\,\bar\omega_L\Delta_L^\omega\left(\Delta_L^\omega\right)^\dagger\omega_R+m_\theta\,\bar\theta_R\Delta_R^\theta\left(\Delta_R^\theta\right)^\dagger\theta_L\,.\end{aligned} \tag{4.24}$$

It can be easily calculated that $\mathrm{Tr}\left\{\Delta_L^\omega\left(\Delta_L^\omega\right)^\dagger\right\}=\mathrm{Tr}\left\{\Delta_R^\theta\left(\Delta_R^\theta\right)^\dagger\right\}=1$. There is explicit breaking stemming from the VL masses, but the Goldstone dependence resides in the PCs of the mirror fermions, not in their opposite–chirality partners or the mass terms[4]. To form a loop involving both chirality fields and the composite sector it is necessary to have an even number of m_E insertions, since the opposite–chirality partners do not couple directly to the composite sector. The lowest–order contribution then is of the order

$$\begin{aligned}V(h)\quad & \propto\lambda_{\omega_R}^2\,\mathrm{Tr}\left\{(\Delta^{\mathbf{10}}_{\omega_R,D})^\dagger.\Delta^{\mathbf{10}}_{\omega_R,D}\right\}m_\theta^2\,\mathrm{Tr}\left\{\Delta_L^\omega\left(\Delta_L^\omega\right)^\dagger\right\}\\ & \propto(m_\theta/m_*)^2\frac{\lambda_{\omega_R}^2}{g_*^2}\sin^2\left(\frac{h}{f}\right)\\ & \sim\mathcal{O}\left((m_\omega/m_*)^2(\lambda_{\omega_R}/g_*)^2\right)\,,\end{aligned} \tag{4.25}$$

where in the last two lines we inserted power counting factors to clearly show how the term compares to the usual contributions (Sec. 3.2.1). The corresponding Feynman diagram can be seen in Fig. 4.2.

[4] In Chapter 3 the VL mass term did contribute to the scalar potential, but only because ω_L was also partially composite.

4.3.2 Three–site Model

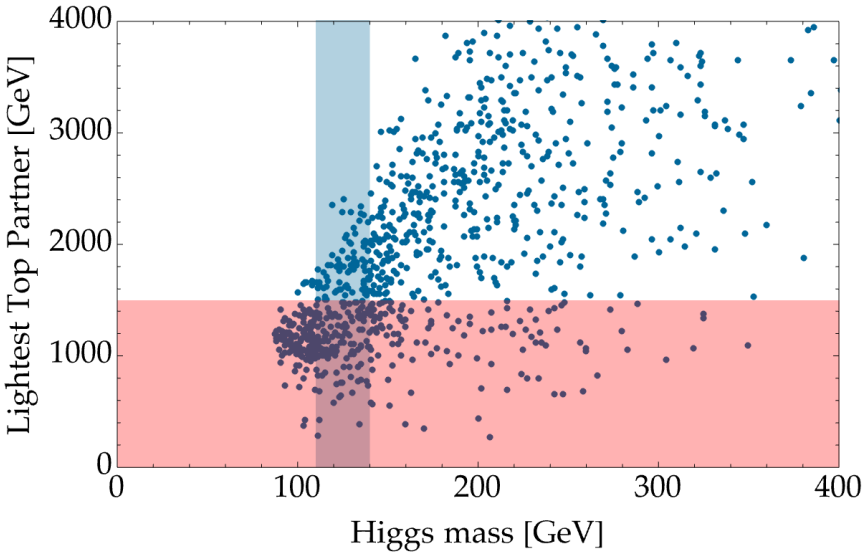

FIGURE 4.3: Lightest top partner m_T versus Higgs mass for $f = 1600$ GeV. The shaded blue region highlights $m_H \in 125 \pm 15$ GeV, whereas the red region shows $m_T \gtrsim 1.5$ TeV experimental bounds (([44–48])).

Like in Sec. 3.2.2 we employ dimensional deconstruction ([107]) and numerically determine the Higgs potential in a three–site model to support the spurion results. In order to do so, two sites of resonances are introduced, which carry the quantum numbers of their elementary partners. In the composite sector, the first site of resonances respects the G symmetry, whereas the second site of resonances is only H–symmetric. IR brane masses connect the two representations $\mathbf{R}$ and $\mathbf{R}'$, where $\mathbf{R}$ contains q_L and $\mathbf{R}'$ contains b_R, to enable the Higgs to generate a mass for the bottom quark after EWSB. Then, with the help of the Coleman–Weinberg formula (Eq. (3.47)) a parameter scan is performed, analogously to Sec. 3.2.2, and top, exotic and bottom sector are included. Their explicit mass matrices in the three–site model are given in Appendix A.5.2. For simplicity, we set $\lambda_L = \lambda_R$, which is fixed by the top mass $m_t(f) \sim 150$ GeV for $f = 1600$ GeV, while the other three–site model parameters are randomly chosen from a uniform distribution ranging from $[-5f, 5f]$. Next, the Higgs potential is evaluated and from it the Higgs mass and vev are determined. Fig. 4.3 shows the lightest top partner versus the Higgs mass for parameter combinations that lead to a Higgs vev of $v_{\text{SM}} \in 246 \pm 40$ GeV, where the broadness of the vev range is motivated by the coarseness of the parameter scan, see Sec. 3.2.2. It is immediately visible that the model contains many viable parameter combinations that lead to heavy top partners $m_T > 1.5$ TeV (([44–48])). The fine–tuning of the points that lie within the blue band which indicates $m_h \in (125 \pm 15)$ GeV is evaluated in Fig. 4.4 via the Barbieri–Giudice measure (Eq. 2.9). The measure assesses the maximum sensitivity of the Higgs vev to small deviations in individual parameters. For a SSB scale $f = 1600$ GeV, the expected minimal tuning would be $\Delta_{\text{min}} = f^2/v^2 \sim 42$ (Eq. 2.7), seen as the vertical black dashed line in the plot. Yet, the majority of points cluster at significantly lower tuning around $\Delta_{BG} \sim 10 - 20$, and tuning even as low as ~ 5 can be found. Expressed as a percentage, the tuning

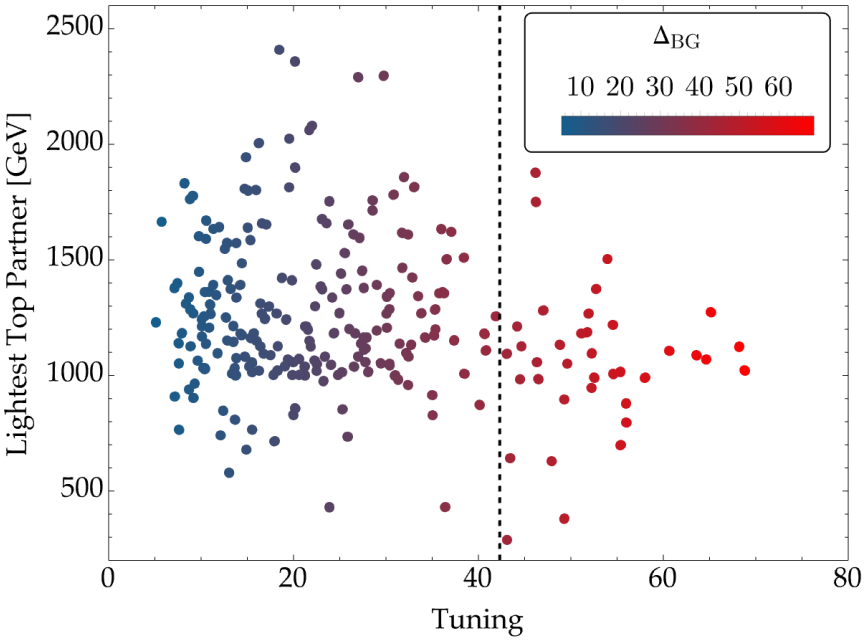

FIGURE 4.4: Lightest top partner versus fine–tuning, which is determined by the Barbieri–Giudice measure (Eq. 2.9), for $f = 1600$ GeV. See text for details.

can be better than 10 %, even for such a high SSB scale. This is remarkable compared to generic CHMs with $f = 800$ GeV where minimal tuning lies around 10 %, but which are plagued by phenomenological issues.

Fig. 4.5 shows the masses for the lightest exotic versus Higgs mass for the same parameter points. No experimental limits are indicated, but see Sec. 4.4.1 for a discussion on the exotic decays. The average mass that leads to correct EWSB is lower than for the lightest top partner, as can be seen by comparing with Fig. 4.3. Since in Chapter 3 the appearance of heavy top partners came at the cost of very light exotics, we plot the two lightest states against each other in Fig. 4.6. All viable top partners are heavier than the lightest exotic, where the equality in masses is shown by the diagonal dashed black line. Additionally, no strong correlation between heavy top partners and exotic masses are found. Instead, top partners $\gtrsim 1.5$ TeV are fairly evenly spread over exotic masses. This contrasts the GHGUT case where heavy top partners were centered in an area $m_{\text{exotic}} \lesssim 500$ GeV, see Fig. 3.6. Although one reason could be the sparseness of the heavy top partners in Fig. 3.6, a more educated guess is related to the requirement of a light Higgs mass. Since $m_h \propto \beta$ (Eq. (2.6)), which in the GHGUT embedding receives its leading contribution from the VL exotic mass invariant, constraints for the lightest exotic appear, similar to the usual relation to the lightest top partner (Eq. 2.10). Instead, here we have chosen $f = 1600$ GeV and exotic and top contributions have the same functional form, since the opposite–chirality partners of the exotics are external, so the shift from top sector dependence to exotic sector dependence of the Higgs mass is not as strong.

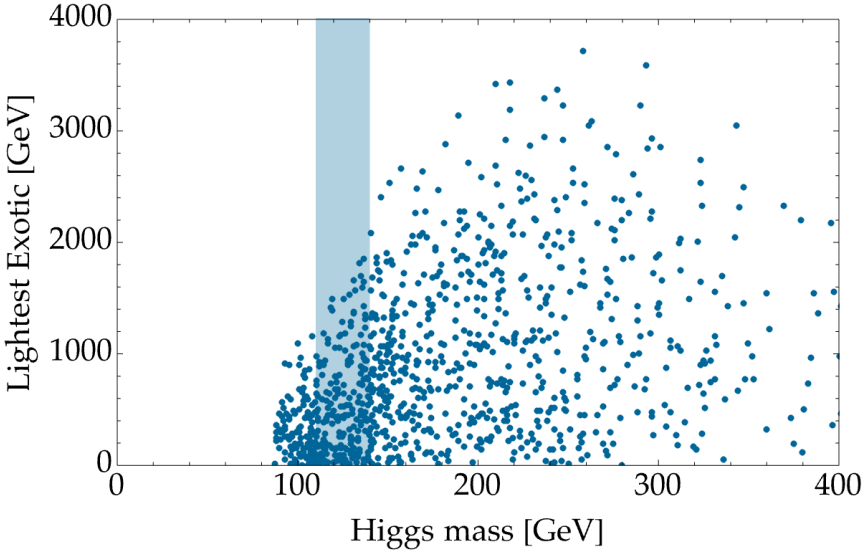

FIGURE 4.5: Lightest exotic versus Higgs mass for $f = 1600$ GeV. The shaded blue region highlights $m_H \in 125 \pm 15$ GeV.

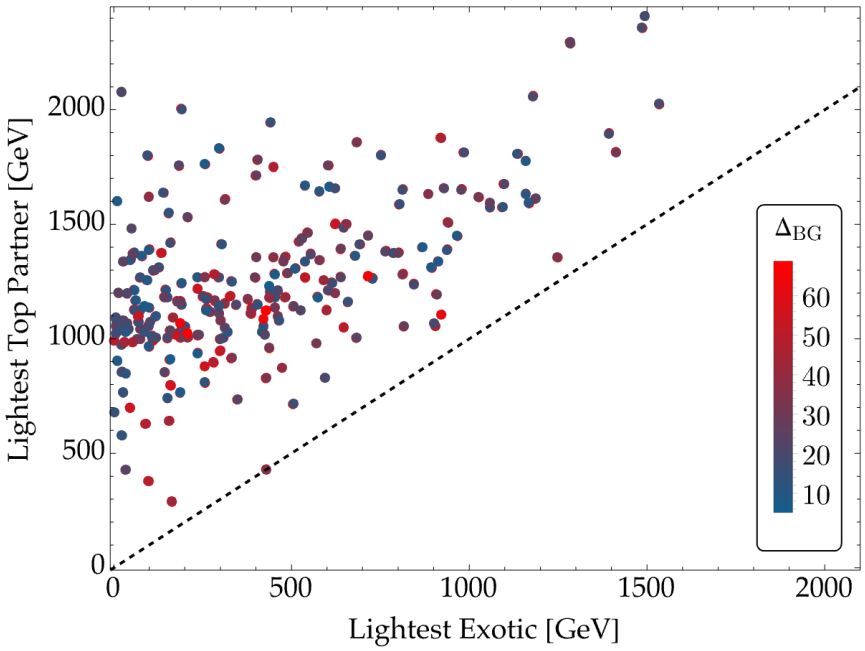

FIGURE 4.6: Lightest top partner versus lightest exotic for $f = 1600$ GeV. The colour–coding corresponds to the tuning of the given points, which is determined by the Barbieri–Giudice measure (Eq. 2.9). The dashed line shows where lightest top partner and lightest exotic would have the same mass.

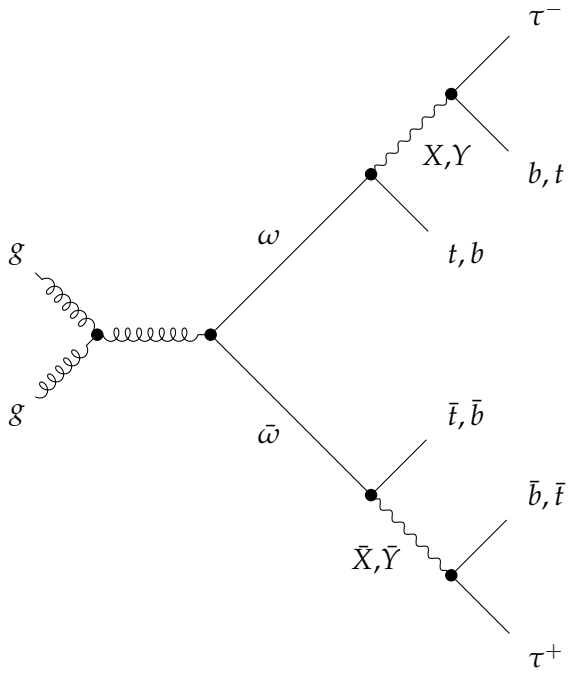

FIGURE 4.7: Exotic decay.

4.4 Phenomenology

4.4.1 Exotic Decay

Before considering possible decay channels for the exotic fermions, their electromagnetic charge and baryon number have to be determined. The electromagnetic charge can simply be read off from e.g. Eq. (3.18). The baryon number is slightly less straightforward, but as explained in the Appendix of [10], the baryon symmetry can be expressed in form of a generator T_B[5]. Then, acting with T_B on the fermion representations reproduces their baryon number, and we find $B(\omega) = B(\theta) = 2/3$.

In this section we call any exotic ω although we will mostly refer to the lightest exotic mass eigenstate, since it is the easiest to detect. Then, respecting baryon number and electromagnetic charge conservation, we expect the exotic to predominantly decay in the following two ways with equal branching ratio:

$$\begin{aligned} \omega_{-2/3} &\to Y_{-1/3} + b_{-1/3} \\ \omega_{-2/3} &\to X_{-4/3} + t_{2/3}, \end{aligned} \tag{4.26}$$

and the off–shell X, Y vector LQs decay to SM fields as

$$\begin{aligned} X_{-4/3} &\to \tau_{-1} + b_{-1/3} \\ Y_{-1/3} &\to \tau_{-1} + t_{2/3} \\ Y_{-1/3} &\to \nu_0 + b_{-1/3}, \end{aligned} \tag{4.27}$$

where we except that all the decays proceed through third generation fermions as they couple most strongly to the composite sector resonances. The decay $\omega_{-2/3} \to$

[5] In $SU(6)$ for instance $T_B = \mathrm{diag}(0, 0, 1, 1, 1, 0)$.

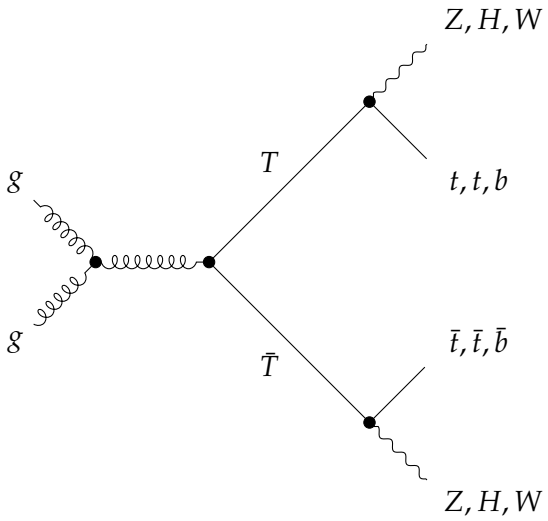

FIGURE 4.8: Top Partner Decay.

$Y_{-1/3} + b_{-1/3} \to \nu_0 + b_{-1/3} + b_{-1/3}$ will be suppressed because of the embeddings of the respective fields. Taking as an example the $SU(6)$ model, but keeping in mind that any phenomenologically viable model has to have the same hierarchy in couplings, both top and tau mostly reside in the **20** and **15**, and have a higher compositeness fraction, whereas bottom and neutrino mostly reside in the **6**, which is more elementary. Roughly speaking, the linear mixings of **15** and **20** are fixed by the top mass, whereas the linear mixing of the **6** is fixed by the mass of the τ. Then, the ratio of couplings is $\sim m_\tau/m_t$, and the decay width of $Y_{-1/3} \to \nu_0 + b_{-1/3}$ suppressed by $(m_\tau/m_t)^2$ with respect to $Y_{-1/3} \to \tau_{-1} + t_{2/3}$. Therefore, we assume that the exotic will decay with $\mathrm{BR}(\omega \to t\,b\,\tau^-) \sim 1$, leading to the six–particle final state seen in Fig. 4.7.

Top Partner Searches

In this subsection we will give a brief overview over top partner searches, including reasons why they cannot be applied to constrain the lightest exotic. An example for the decay of pair-produced top partner T is given in Fig. 4.8. The decay can proceed as $T \to tH$, $T \to tZ$, or $T \to bW$. Therefore, once the gauge bosons or the Higgs decay the same six–particle final state can be reproduced that we predict for the exotics in Sec. 4.4.1. However, the top partner searches often use tagging to identify which parent particle the final states originated from. In addition, the number and charges of leptons are often constrained, which can be reproduced if the taus predicted for the exotic decay only hadronically, or in a specific combination of leptonically and hadronically. The branching ratio of a τ decaying leptonically into an electron or muon is $\sim 35\%$ ([112]). So it could be possible to have a single electron or muon in the final state, but generally, in the cases in which a very specific combination of decays of both taus and tops is required to match the final state of the top partner search we expect that a dedicated analysis would lead to a significantly lower bound on the lightest exotic mass than is set on the lightest top partner. In cases in which neural networks are used to analyse the collider data the comparison is not straight–forward. We list these cases, but refrain from judgement on how

Top Partner Search	Experiment	Details
[115]	CMS (2017)	W boson tagging
[116]	CMS (2017)	H or W boson tagging and exactly one lepton
[117]	CMS (2018)	jet originating from W, and either single electron / muon, or two leptons with same sign of electric charge, or at least three leptons
[118]	CMS (2018)	Z boson tagging
[47]	CMS (2019)	cut–based analysis: W boson tagging; neural–network analysis: exactly four jets and tagging
[44]	CMS (2022)	algorithm (DEEPAK8) to identify parent particle, and either single electron / muon, or two leptons with same sign of electric charge, or at least three leptons
[119]	ATLAS (2017)	W boson tagging
[120]	ATLAS (2017)	large missing momentum from Z boson decaying into neutrinos
[121]	ATLAS (2018)	two same charge leptons or three leptons
[122]	ATLAS (2018)	W boson tagging
[123]	ATLAS (2018)	at least two jets tagged as Higgs or vector boson and exactly zero leptons
[124]	ATLAS (2018)	either single electron / muon, or missing energy with zero leptons
[45]	ATLAS (2018)	combination of a selection of the above analyses
[125]	ATLAS (2018)	Z boson tagging
[46]	ATLAS (2022)	Z boson tagging
[48]	ATLAS (2022)	single production top partner, fully hadronic decay

TABLE 4.1: Overview over top partner searches and details of the analyses.

applicable the constraints are, stressing that there can be heavy exotics with little tuning, as seen in Fig. 4.6. Table 4.1 shows an overview over top partner searches and reasons why the constraints cannot be directly translated to give bounds on the mass of the lightest exotic.

Leptoquark Searches

A comment should be made about leptoquark searches. Since the main decay of the exotic proceeds through X and Y gauge bosons (Fig. 4.7), which are leptoquarks, the constraints placed on pair-produced leptoquarks automatically cover four out of the six final states. However, our expected LQs are produced off–shell so the resonance searches do not fit. Additionally, there would be two more jets which would need to be missed in order to match the final state of the leptoquark searches. Therefore, it is questionable whether it is possible to apply any current leptoquark bounds to the exotics and we do not attempt to do it here. Furthermore, we expect that current leptoquark bounds would lead to significantly lower if not negligible constraints for the exotic.

4.4.2 Higgs Gluon Coupling Modification

Additional fermions can lead to new loop contributions to the Higgs coupling to gluons. The modification of the Higgs production cross section through gluon fusion was first calculated in [126]. [127] give an approximation for the contribution of new heavy fermion with $M_i > m_H$

$$\delta g_{Hgg} \propto \sum_{M_i > m_H} \frac{Y_{ii}}{M_i} = \frac{\partial \log(\det M)}{\partial v} - \sum_{M_i < m_H} \frac{Y_{ii}}{M_i} \tag{4.28}$$

For the exotic fermions the first part of the expression is sufficient, and we can calculate, using the mass matrix determined in Sec. 3.2.2, that the modification from the exotics is found to be vanishing

$$\delta g_{hgg}^{\text{exotic}} \sim \frac{\partial \log(\det M_{\text{exotic}})}{\partial v} = 0. \tag{4.29}$$

The vanishing of the contributions can be compared to the GHGUT embedding which is sketched in Appendix A.6. There, the exotics do contribute to a modification of the Higgs gluon coupling. The difference is the nature of the opposite–chirality fermions. Here, we have chosen them to be completely elementary, and not directly coupled to the composite sector. Therefore, they do not lead to loop contributions. Still, there are modifications stemming from the top and bottom partners. For the top partners we find, expressing the results in terms of the SM Higgs vev (Eq. 3.11)

$$\frac{\partial \log(\det M_{\text{top}})}{\partial v} = \frac{1}{v_{\text{SM}}} \left(\frac{1 - 2\frac{v_{\text{SM}}^2}{f^2}}{\sqrt{1 - \frac{v_{\text{SM}}^2}{f^2}}} \right) \approx \frac{1}{v_{\text{SM}}} \left(1 - \frac{3\, v_{\text{SM}^2}}{2 f^2} + \mathcal{O}\left(\frac{1}{f^4}\right) \right) \tag{4.30}$$

which does not carry a dependence on the strong sector dynamics. For the bottom quark, the lightest mode is lighter than the Higgs, so using the approximation $M_i \gg m_H$ becomes inaccurate. Instead, the modification due to bottom partners is given by

$$\delta g_{Hgg}^{\text{bottom}} \propto \frac{\partial \log(\det M_{\text{bottom}})}{\partial v} - \frac{y_b}{m_b} \tag{4.31}$$

and we can calculate

$$\frac{\partial \log(\det M_{\text{bottom}})}{\partial v} = \frac{1}{v_{\text{SM}}} \sqrt{1 - \frac{v_{\text{SM}}^2}{f^2}} \approx \frac{1}{v_{\text{SM}}} \left(1 - \frac{v_{\text{SM}^2}}{2 f^2} + \mathcal{O}\left(\frac{1}{f^4}\right) \right) \tag{4.32}$$

but have to deduct the lightest mode, as per Eq. 4.31

$$\begin{aligned} \frac{y_b}{m_b} = \quad & \frac{1}{m_b} \frac{\partial m_b}{\partial v} \approx \frac{1}{v_{\text{SM}}} \sqrt{1 - \frac{v_{\text{SM}}^2}{f^2}} \\ & + \frac{c_b}{v_{\text{SM}}} \left(\frac{v_{\text{SM}}^2}{f^2} \right) + \mathcal{O}\left(\frac{1}{f^4}\right) \end{aligned} \tag{4.33}$$

where c_b is a function of the composite resonance parameters that has to be evaluated numerically, and can become significant for low SSB scales (see [127]), since the modification of the Higgs Gluon coupling due to the top and bottom partners

goes as $\mathcal{O}(\frac{v_{SM}^2}{f^2}) \sim \mathcal{O}(2\%)$. For the here–assumed symmetry breaking scale of 1600 GeV the effects are not relevant yet, as the current experimental level of precision is $\delta g_{hgg} \sim \pm 7\%$ ([112]).

4.5 Overview

In conclusion, the mirror fermion mechanism significantly reduces tuning without leading to phenomenologically problematic consequence. Instead, an exciting new signature, the six–particle final state stemming from the decay of the exotic fermion, is proposed which can be looked for at the LHC. The mechanism is reminiscent of twin Higgs ([128]), which was also done in a composite Higgs context ([129–131]), but instead of introducing a full copy of the SM gauge group, which cancels both fermionic and gauge contributions at quadratic order, ideally two mirror fermions are introduced[6] which transform under the SM group, which means they also carry colour. Then, only the quadratic top quark contribution is cancelled. The mechanism can also be contrasted to softened Goldstone symmetry breaking ([40]) where additional exotic fields are introduced to completely fill G–multiplets, which prevents explicit breaking through partial compositeness. Instead, the symmetry is explicitly broken by Dirac masses between the exotic fermions and external opposite–chirality partners. Although then top partners decouple, additional ingredients have to be imposed to alleviate the tuning, as is addressed in [41, 54].

Here, the cancellation stems from intrinsically group theoretic properties. The pseudoreal $SU(6)$ representation **20** and the $SO(11)$ representation **32** naturally give rise to the appearance of exotic fermions. Additionally, their unusual baryon number is not imposed to avoid collider limits, but a consequence of the accidental baryon number symmetry, which in turn also prevents proton decay. It is exactly the interplay of both properties that allows to solve the common problems; heavy top partner with little tuning are found, there is no EW hierarchy problem and, in the composite GUT scenarios the proton is stable. One could argue that the two additional requirements for the cancellation, which are identical linear mixing parameters, and a small elementary mass for the exotics, are not as clear, but as shown in Sec. 4.2 both assumptions can be motivated very well in the 5D dual.

A next step would be to see how including the gauge sector into the 3–site model affects the findings. Furthermore, additional cosets in which the mechanism can be effectively applied should be identified.

[6] That is, when the objective is to cancel $\lambda_{q_L}^2$ and $\lambda_{t_R}^2$, which are the driving forces for tuning in CHMs. Cancelling additional SM fermion contributions is not advantageous, because the next–to–leading order in top quark couplings can easily be bigger in size than the leading order contributions from leptons, or second generation quarks.

Chapter 5

Conclusion & Outlook

We started the thesis by stating common problems in composite Higgs models and of grand unified theories, which include the prediction of light top partners, fine–tuning and proton decay. Fascinatingly, it is the interplay of mechanisms in both theories that solves all of them at once. Due to the incomplete filling of multiplets in the composite GUT, baryon number becomes an accidental symmetry of the model. Therefore, the proton is stable to all orders in perturbation theory. Furthermore, the incomplete filling of multiplets naturally leads to the emergence of exotic fields, which then cancel the quadratic contribution of the top quark to the pNGB Higgs potential, thereby reducing the fine–tuning. Additionally, in Chapter 3 the vector–like nature of the exotics allows to decouple the lightest top partners from the Higgs mass. In Chapter 4 the complete cancellation of the quadratic top contribution to the Higgs potential by the exotics allows to double the symmetry breaking scale from the usual (but phenomenologically problematic) $f = 800$ GeV to $f = 1600$ GeV, thus raising the mass of the lightest top partners while keeping the tuning comparable to minimal tuning predictions for $f = 800$ GeV. Also due to the accidental baryon number symmetry, the exotics feature baryon number $B = 2/3$, which leads to an expected decay to a 6–particle final state that has not yet been searched for at colliders.

Beyond the further exploration of the aforementioned features, there are even more aspects of the model to delve into, in order to address additional BSM questions. The following list gives a small outlook of directions that would be interesting to investigate in the future:

- So far, to the best of our knowledge, there have not been dedicated collider searches for particles that carry a different baryon number than the known SM fields. It would be very exciting to see if there are other theories that predict particles with such peculiar baryon numbers, and, more importantly, to actually perform a designated analysis of collider data.

- We have shown that the model–building mechanism is generalisable to other cosets, as long as the top quark and its mirror fermion are embedded in a pseudoreal G–representation $\mathbf{R} \to \bar{\mathbf{C}} \oplus \mathbf{C}$ that decomposes into a complex representation $\mathbf{C}$ and its complex conjugate $\bar{\mathbf{C}}$ under H. In this work, the mechanism has only been applied to two cosets: the non–custodial $SU(6)/SU(5)$ and the custodial $SO(11)/SO(10)$. It would be interesting to find further cosets to which the mirror fermion mechanism is applicable.

- The cosets taken into account in the present work feature more scalar pNGB fields than just the Higgs, as both include a scalar LQ and, in $SU(6)/SU(5)$, an additional scalar singlet can be found. A non–standard phase transition history, where either the singlet or the LQ (or both) obtains a non–zero vev in the

early Universe, could lead to baryogenesis via the fulfillment of the Sakharov criteria [132] to generate a primordial matter–antimatter asymmetry. Moreover, the singlet could potentially play the role of an axion and be a candidate for particle dark matter.

To conclude, we can say that applying the mirror fermion mechanism to composite GUT models leads to intriguing new signatures that can be probed at the LHC while at the same time solving several previous phenomenological problems and restoring naturalness to composite Higgs models.

Appendix A

Additional Calculations and Mathematical Details

A.1 Generators $SU(6)$

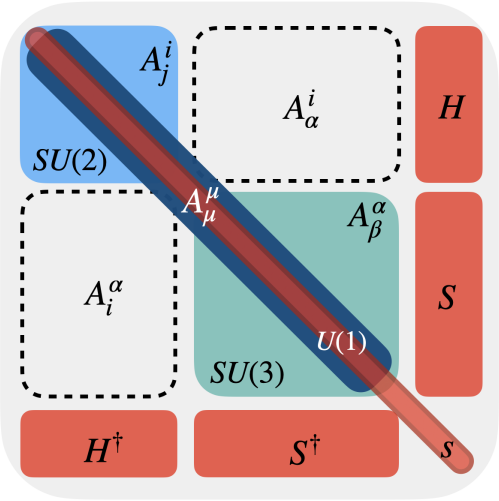

FIGURE A.1: $SU(6)$ generators

The $SU(6)$ generators are traceless 6×6 matrices normalised to $\mathrm{Tr}\{T^a.T^b\} = 1/2\delta^{ab}$. Table A.1 describes what each of the $6^2 - 1 = 35$ generators corresponds to, while Fig. A.1 can be contrasted with Fig. 2.4 to see exactly how the broken generators lead to the emergence of the pNGBs, once $SU(6)$ is spontaneously broken to $SU(5)$.

generators	form	dofs	physical fields
$T^{1,\ldots,3}$	(2×2) Pauli matrices in upper left	3	$SU(2)_L$ gauge bosons
$T^{4,\ldots,11}$	(3×3) Gell–Mann matrices in middle	8	$SU(3)_C$ gauge bosons
$T^{12,\ldots,23}$	complex triplets	12	X & Y $SU(5)$ gauge bosons
T^{24}	diagonal (5×5) matrix	1	$U(1)$ gauge boson
$T^{25,\ldots,28}$	complex doublet	4	pNGB Higgs doublet
$T^{29,\ldots,34}$	complex triplet	6	scalar pNGB triplet
T^{35}	singlet	1	scalar pNGB singlet

TABLE A.1: $SU(6)$ generators

A.2 Dressing of $SU(6)$ Spurions

In the following, greek letters denote an $SU(5)$–index, i.e. $\alpha = 1, ..., 5$, whereas roman letters correspond to an $SU(6)$ index, i.e. $i = 1, ..., 6$. Then, the dressing of the **20** spurion of $SU(6)$ is

$$\left(U^{-1}\right)_i^6 \left(U^{-1}\right)_j^\alpha \left(U^{-1}\right)_k^\beta \left(\Delta^{\mathbf{20}}\right)^{ijk} \equiv \Delta_D^{\mathbf{20,10}} \,, \tag{A.1}$$

$$\frac{1}{3!}\epsilon_{\alpha\beta\gamma\delta\zeta} \left(U^{-1}\right)_i^\gamma \left(U^{-1}\right)_j^\delta \left(U^{-1}\right)_k^\zeta \left(\Delta^{\mathbf{20}}\right)^{ijk} \equiv \Delta_D^{\mathbf{20,10^*}} \,, \tag{A.2}$$

where ϵ is the Levi-Civita tensor. Dressing of the **15** spurion of $SU(6)$ goes as

$$\left(U^{-1}\right)_i^\alpha \left(U^{-1}\right)_j^\beta \left(\Delta^{\mathbf{15}}\right)^{ij} \equiv \Delta_D^{\mathbf{15,10}} \,, \tag{A.3}$$

$$\left(U^{-1}\right)_i^\alpha \left(U^{-1}\right)_j^6 \left(\Delta^{\mathbf{15}}\right)^{ij} \equiv \Delta_D^{\mathbf{15,5}} \,, \tag{A.4}$$

and dressing of **6** spurion of $SU(6)$ as

$$\left(U^{-1}\right)_i^\alpha \left(\Delta^{\mathbf{6}}\right)^{i} \equiv \Delta_D^{\mathbf{6,5}} \,, \tag{A.5}$$

$$\left(U^{-1}\right)_i^6 \left(\Delta^{\mathbf{6}}\right)^{i} \equiv \Delta_D^{\mathbf{6,1}} \,. \tag{A.6}$$

The singlet of $SU(6)$ does not carry any Goldstone dependence.

A.3 Full Kinetic Term – GHGUT

It is useful to redefine the fields in the following way

$$\frac{H}{f}\frac{\sin\sqrt{\left(\frac{H}{f}\right)^2+\left(\frac{S}{f}\right)^2+\left(\frac{s}{f}\right)^2}}{\sqrt{\left(\frac{H}{f}\right)^2+\left(\frac{S}{f}\right)^2+\left(\frac{s}{f}\right)^2}} \to \frac{H}{f} \,, \tag{A.7}$$

$$\frac{S}{f}\frac{\sin\sqrt{\left(\frac{H}{f}\right)^2+\left(\frac{S}{f}\right)^2+\left(\frac{s}{f}\right)^2}}{\sqrt{\left(\frac{H}{f}\right)^2+\left(\frac{S}{f}\right)^2+\left(\frac{s}{f}\right)^2}} \to \frac{S}{f} \,, \tag{A.8}$$

$$\frac{s}{f}\frac{\sin\sqrt{\left(\frac{H}{f}\right)^2+\left(\frac{S}{f}\right)^2+\left(\frac{s}{f}\right)^2}}{\sqrt{\left(\frac{H}{f}\right)^2+\left(\frac{S}{f}\right)^2+\left(\frac{s}{f}\right)^2}} \to \frac{s}{f} \,. \tag{A.9}$$

Then, the kinetic term can be expressed with the help of the covariant derivative

$$D_\mu \Pi = \left(\partial_\mu - iA_\mu\right)\Pi \tag{A.10}$$

$$\text{with } \Pi \equiv (H, S)^T \tag{A.11}$$

where Π is a fundamental of $SU(5)$, and A_μ the gauge fields (Eq. 3.5). Explicitly, we find, involving all scalar fields

$$\begin{aligned}\mathcal{L}_{\text{kin}} &= \left(D_\mu \Pi\right)^\dagger \left(D^\mu \Pi\right) + \frac{1}{2}\partial_\mu s \partial^\mu s \\ &+ \frac{1}{5f^2}\left(\Pi^\dagger \overleftrightarrow{D_\mu} \Pi\right)\left(\Pi^\dagger \overleftrightarrow{D^\mu} \Pi\right) \\ &+ \frac{2}{9}\frac{1}{f^2}\Pi^\dagger\Pi\left(\partial_\mu s\right)^2 + \frac{11}{15f^2}\left(s\partial_\mu s\right)\partial^\mu\left(\Pi^\dagger\Pi\right) \\ &+ \frac{1}{2f^2}\left(\partial_\mu\left(\Pi^\dagger\Pi\right)\right)^2 + \frac{3}{10f^2}\left(s\,\partial_\mu s\right)^2 + \mathcal{O}\left(\frac{1}{f}\right)^4 \end{aligned} \tag{A.12}$$

A.4 Full Spurion Analysis – Scalar potential

Following the same procedure as in Sec. 3.2.1, but employing the notation of Eq. (A.7,A.8,A.9) to improve readability, the scalar potential without including the VL–term becomes

$$V(h,S)^{\text{no VL}} = \alpha^h \frac{H^2}{f^2} + \alpha^S \frac{S^2}{f^2} \tag{A.13}$$

with

$$\alpha^h = \frac{m_*^2 f^2}{16\pi^2}\left(c_{\mathbf{6},\text{aux}}(\lambda_{l_L}^2) + c_{\mathbf{15},\text{aux}}(3\lambda_{q_L}^2 + \lambda_{e_R}^2) + 3c_{\mathbf{20},\text{aux}}(\lambda_{t_R}^2 - \lambda_{\omega_R}^2)\right) \tag{A.14}$$

$$\alpha^s = \frac{m_*^2 f^2}{16\pi^2}\left(c_{\mathbf{15},\text{aux}}(2\lambda_{q_L}^2 + \lambda_{\omega_L}^2) + c_{\mathbf{20},\text{aux}}(\lambda_{t_R}^2 - \lambda_{\omega_R}^2)\right) \tag{A.15}$$

where we recognise α^h as Eq. (3.31). In Eq. (A.13) the scalar triplet potential, like the Higgs potential, only receives contributions to its quadratic at second order in couplings. The invariant stemming from the contraction of ω_L and ω_R instead mixes the fields and contributes to the quartic

$$\begin{aligned}V(h,S,s)^{\text{VL}} = \quad & \beta^{\text{mix}}\left(1 - \frac{1}{2}\left(\frac{H^2}{f^2} + \frac{S^2}{f^2}\right) - \frac{1}{8}\left(\frac{H^4}{f^4} + \frac{S^4}{f^4}\right) - \frac{1}{4}\frac{H^2S^2}{f^4}\right) \\ & + \beta^{\text{mix}}\left(-\frac{25}{18}\frac{s^2}{f^2} - \frac{275}{1944}\frac{s^4}{f^4} - \frac{35}{108}\frac{s^2}{f^2}\left(\frac{H^2}{f^2} + \frac{S^2}{f^2}\right)\right) \\ & + \mathcal{O}\left(\frac{1}{f^6}\right)\end{aligned} \tag{A.16}$$

with

$$\beta^{\text{mix}} = 3\frac{m_*^2 f^2}{16\pi^2} c_{VL}\lambda_{\omega_R}\lambda_{\omega_L}\,, \tag{A.17}$$

where c_{VL} incorporates the dynamics of the composite sector, analgously to the c's introduced in Eq. (A.14) and Eq. (A.15). Additionally, since ω_R and ω_L carry different $U(1)_X$ charges, the term

$$V \propto \text{Tr}\left\{\left(\Delta^{\mathbf{10}}_{\omega_L,D}\right)^\dagger \Delta^{\mathbf{10}}_{\omega_R,D}\right\} + \text{ h.c.}$$

explicitly breaks the global $U(1)_X$ symmetry and therefore generates the singlet potential. Another possibility to give a mass to the singlet comes from the neutrino

sector, because an elementary Majorana mass term between the two $(1,1)_0$ in the **6** and **1** of $SU(6)$ would also carry a singlet dependence.

A.4.1 Gauge Fields

The spurion can be defined as an adjoint matrix of couplings

$$\mathcal{G} \equiv \sqrt{\frac{5}{3}} \cdot g' T_{24} + \sum_{\alpha=1}^{3} g T_\alpha + \sum_{i=4}^{11} g_s T_i \tag{A.18}$$

which is dressed with the Goldstone matrix in the following way ([11])

$$\mathcal{G}_D \equiv U^\dagger \cdot \mathcal{G} \cdot U \tag{A.19}$$

and decomposes as

$$\mathbf{35} \to \mathbf{24} \oplus \mathbf{5} \oplus \mathbf{5}^* \oplus \mathbf{1} \tag{A.20}$$

under $SU(5)$. Therefore, naively four invariants can be formed, which are

$$\begin{aligned}
&\mathrm{Tr}\Big\{ \left(\Delta_D^{\mathbf{24}}\right)^\dagger \left(\Delta_D^{\mathbf{24}}\right) \Big\} + \text{ h.c.}\,, \\
&\left(\Delta_D^{\mathbf{5}}\right)^\dagger \left(\Delta_D^{\mathbf{5}}\right) + \text{ h.c.}\,, \\
&\left(\Delta_D^{\mathbf{5}^*}\right)^\dagger \left(\Delta_D^{\mathbf{5}^*}\right) + \text{ h.c.}\,, \\
&\left(\Delta_D^{\mathbf{1}}\right)^\dagger \left(\Delta_D^{\mathbf{1}}\right) + \text{ h.c.}\,.
\end{aligned}$$

However, since here $\left(\Delta_D^{\mathbf{5}}\right)^\dagger \left(\Delta_D^{\mathbf{5}}\right) = \left(\Delta_D^{\mathbf{5}^*}\right)^\dagger \left(\Delta_D^{\mathbf{5}^*}\right)$, and the sum of the invariants is Goldstone–independent, we are left with only two independent terms. Since all gauge fields couple to the same global multiplet, see Eq.(3.6), the c–parameters that describe the unknown composite dynamics are not independent, as is the case for the fermions where the composite resonances reside in different multiplets, but instead identical for gluons, W and B gauge bosons. Without loss of generality we choose $c_{\text{aux}}^{\mathbf{24}}$ and $c_{\text{aux}}^{\mathbf{1}}$ for parametrisation. Employing the notation from Eq. (A.7), (A.8) and (A.9), we find that the following functional dependencies appear in the scalar

potential

$$\begin{aligned}
\frac{H^2}{f^2}\times &\begin{cases} c^{\mathbf{24}}_{\text{aux}}\left(-\frac{3}{2}g^2-\frac{g'^2}{2}\right) \\ c^{\mathbf{1}}_{\text{aux}}\left(\frac{g'^2}{4}\right)\end{cases}, \\
\frac{H^4}{f^4}\times &\begin{cases} c^{\mathbf{24}}_{\text{aux}}\left(\frac{g^2}{4}+\frac{g'^2}{4}\right) \\ c^{\mathbf{1}}_{\text{aux}}\left(\frac{g^2}{4}\right)\end{cases}, \\
\frac{S^2}{f^2}\times &\begin{cases} c^{\mathbf{24}}_{\text{aux}}\left(-\frac{2g'^2}{9}-\frac{8g_s^2}{3}\right) \\ c^{\mathbf{1}}_{\text{aux}}\left(\frac{g'^2}{9}\right)\end{cases}, \\
\frac{S^4}{f^4}\times &\begin{cases} c^{\mathbf{24}}_{\text{aux}}\left(\frac{g'^2}{9}+\frac{g_s^2}{3}\right) \\ c^{\mathbf{1}}_{\text{aux}}\left(\frac{g_s^2}{3}\right)\end{cases}, \\
\frac{H^2S^2}{f^4}\times &\begin{cases} c^{\mathbf{24}}_{\text{aux}}\left(-\frac{g'^2}{9}\right) \\ c^{\mathbf{1}}_{\text{aux}}\left(-\frac{g'^2}{9}\right)\end{cases}.
\end{aligned} \tag{A.21}$$

No singlet potential is generated in the gauge sector[1].

A.5 Explicit Form of Mass Matrices in 3-Site Model

A.5.1 GHGUT

The explicit mass matrices in the GHGUT embedding are

$$M^{\text{top}} = \begin{pmatrix}
0 & f\lambda_{u_R}\sin(\xi) & f\lambda_{u_R}\cos(\xi) & 0 & 0 & 0 & 0 \\
0 & m_{20} & 0 & 0 & d_{20} & 0 & 0 \\
0 & 0 & m_{20} & 0 & 0 & d_{20} & 0 \\
-f\lambda_Q & 0 & 0 & m_{15} & 0 & 0 & d_{15} \\
0 & d_{20} & 0 & 0 & m_{20,10} & 0 & d10_{1520} \\
0 & 0 & d_{20} & 0 & 0 & m_{20,10*} & 0 \\
0 & 0 & 0 & d_{15} & d10_{2015} & 0 & m_{15,10}
\end{pmatrix}, \tag{A.22}$$

$$M^{\text{exotic}} = \begin{pmatrix}
m_\omega & 0 & -f\lambda_{\omega_R}\cos(\xi) & -f\lambda_{\omega_R}\sin(\xi) & 0 & 0 & 0 \\
0 & 0 & m_{20} & 0 & 0 & d_{20} & 0 \\
-f\lambda_{\omega_L} & m_{15} & 0 & 0 & d_{15} & 0 & 0 \\
0 & 0 & 0 & m_{20} & 0 & 0 & d_{20} \\
0 & 0 & d_{20} & 0 & d10_{1520} & m_{20,10} & 0 \\
0 & d_{15} & 0 & 0 & m_{15,10} & d10_{2015} & 0 \\
0 & 0 & 0 & d_{20} & 0 & 0 & m_{20,10*}
\end{pmatrix}, \tag{A.23}$$

[1] If the only source of explicit breaking was the gauging of G_{SM}, the breaking pattern would be $SU(6) \to G_{SM} \otimes U(1)_X$.

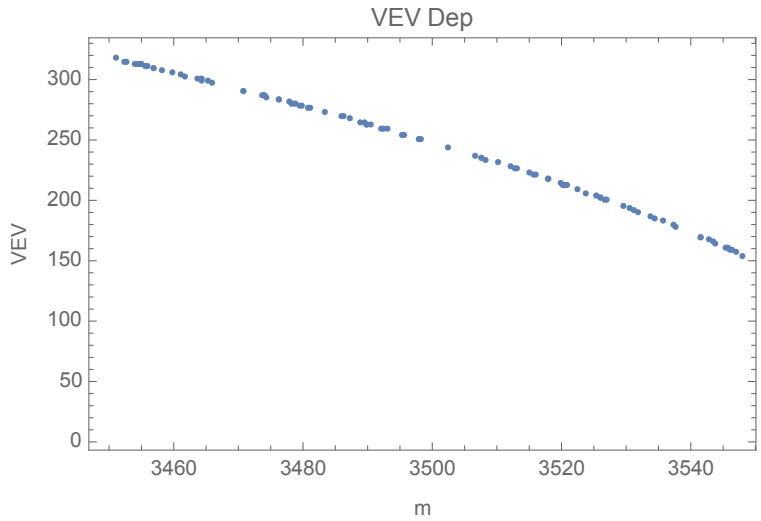

FIGURE A.2: How a small shift in one of the parameters slightly shifts the Higgs vev (in GeV). Here, m (in GeV) is the brane mass connecting the two composite **10**s on the second site of composite resonances. All other parameters are kept unchanged.

$$M^{\text{bottom}} = \begin{pmatrix} 0 & f\lambda_{b_R} & 0 & 0 & 0 & 0 & 0 & 0 & 0 \\ 0 & m_6 & 0 & 0 & 0 & d_6 & 0 & 0 & 0 \\ -f\lambda_Q \sin(\xi) & 0 & m_{15} & 0 & 0 & 0 & d_{15} & 0 & 0 \\ -f\lambda_Q \cos(\xi) & 0 & 0 & m_{15} & 0 & 0 & 0 & d_{15} & 0 \\ 0 & 0 & 0 & 0 & m_{20} & 0 & 0 & 0 & d_{20} \\ 0 & d_6 & 0 & 0 & 0 & m_{6,5} & d5_{156} & 0 & 0 \\ 0 & 0 & d_{15} & 0 & 0 & d5_{615} & m_{15,5} & 0 & 0 \\ 0 & 0 & 0 & d_{15} & 0 & 0 & 0 & m_{15,10} & d10_{2015} \\ 0 & 0 & 0 & 0 & d_{20} & 0 & 0 & d10_{1520} & m_{20,10} \end{pmatrix}. \tag{A.24}$$

Motivation for choice of broad $v \in (246 \pm 40)$ GeV range

For an example point of the numerical scan in Sec. 3.2.2, we varied one parameter, here the brane mass m between the $SU(5)$ **10** of the $SU(6)$ **20** resonance, and the the $SU(5)$ **10** of the $SU(6)$ **15** resonance, while keeping all other parameters fixed. Fig. A.2 shows how sensitive the Higgs vev is to m. We made similar plots for other parameters of the three–site model, but do not show them here for space reasons. It suffices to say that, in the absence of a very finely–grained parameter scan, which, with the amount of parameters in the three–site model, would be incredibly time intensive, choosing to filter for $v \in (246 \pm 40)$ GeV seems absolutely justified. The vev–sensitivity is of course related to the Barbieri–Giudice measure which measure the maximum sensitivity of Higgs vev to parameters,

$$\Delta_{BG} = \max_i \left| \frac{\partial \log O(x_i)}{\partial \log x_i} \right| = \max_i \left| \frac{x_i}{O(x_i)} \frac{\partial O(x_i)}{\partial x_i} \right| , \tag{A.25}$$

where $\frac{\partial O(x_i)}{\partial x_i}$ for $O(x_i) = v$ and $x_i = m$ corresponds to the slope seen in Fig. A.2, which is then scaled by the ratio $\frac{x_i}{O(x_i)}$ to determine the fine–tuning.

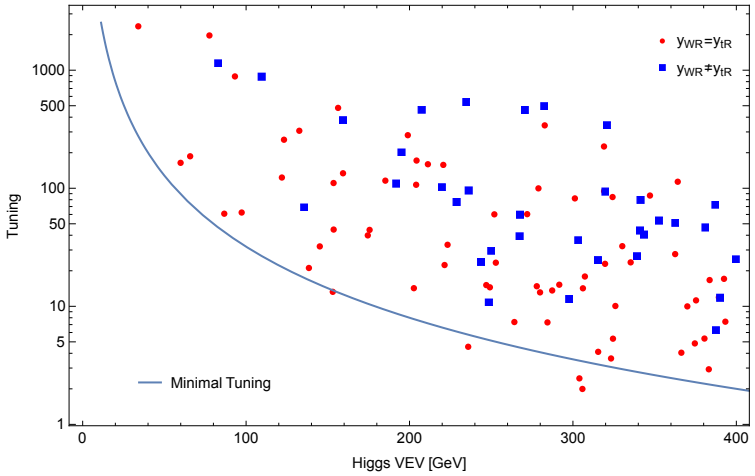

FIGURE A.3: Numerical tuning versus Higgs vev of 3–site model scans for GHGUT model in comparison to minimal tuning. See text for details.

Cancellation of $\lambda_{t_R}^2$ versus no cancellation

Fig. A.3 compares two numerical scans in the 3–site model of the GHGUT embedding. For the red points we set $\lambda_{t_R} = \lambda_{\omega_R}$, whereas the blue squares correspond to $\lambda_{t_R} \neq \lambda_{\omega_R}$. On average, there is less tuning when the two linear mixings are fixed to be equal, although neither model incarnation is comparable to minimal tuning, which is shown by the blue line. The reason is λ_{q_L} which still contributes at quadratic order to the quadratic of the Higgs potential. In contrast to other fields, such as b_R or the leptonic contributions, q_L cannot be neglected with respect to t_R because the top Yukawa is proportional to the product of the two (Eq. (2.3)), and therefore both λ_{t_R} and λ_{q_L} can be expected to be large.

A.5.2 Mirror Fermions

The explicit mass matrices in the mirror fermion embedding are

$$M^{\text{top}} = \begin{pmatrix} 0 & f\lambda_{u_R}\cos(\xi) & f\lambda_{u_R}\sin(\xi) & 0 & 0 & 0 & 0 \\ f\lambda_Q \sin(\xi) & m_{20} & 0 & 0 & d_{20} & 0 & 0 \\ -f\lambda_Q\cos(\xi) & 0 & m_{20} & 0 & 0 & d_{20} & 0 \\ 0 & 0 & 0 & m_{15} & 0 & 0 & d_{15} \\ 0 & d_{20} & 0 & 0 & m_{2010s} & 0 & 0 \\ 0 & 0 & d_{20} & 0 & 0 & m_{2010} & d10_{1520} \\ 0 & 0 & 0 & d_{15} & 0 & d10_{2015} & m_{15,10} \end{pmatrix}, \tag{A.26}$$

$$M^{\text{exotic}} = \begin{pmatrix} m_\omega & 0 & -f\lambda_{\omega_R}\sin(\xi) & -f\lambda_{\omega_R}\cos(\xi) & 0 & 0 & 0 & 0 \\ 0 & m_\theta & 0 & 0 & 0 & 0 & 0 & 0 \\ 0 & f\lambda_{\theta_L}\cos(\xi) & m_{20} & 0 & 0 & d_{20} & 0 & 0 \\ 0 & -f\lambda_{\theta_L}\sin(\xi) & 0 & m_{20} & 0 & 0 & d_{20} & 0 \\ 0 & 0 & 0 & 0 & m_{15} & 0 & 0 & d_{15} \\ 0 & 0 & d_{20} & 0 & 0 & m_{2010s} & 0 & 0 \\ 0 & 0 & 0 & d_{20} & 0 & 0 & m_{2010} & d10_{1520} \\ 0 & 0 & 0 & 0 & d_{15} & 0 & d10_{2015} & m_{15,10} \end{pmatrix}, \tag{A.27}$$

$$M^{\text{bottom}} = \begin{pmatrix} 0 & 0 & f\lambda_{b_R}\cos(\xi) & -f\lambda_{b_R}\sin(\xi) & 0 & 0 & 0 & 0 & 0 \\ 0 & m_6 & 0 & 0 & 0 & d_6 & 0 & 0 & 0 \\ 0 & 0 & m_{15} & 0 & 0 & 0 & d_{15} & 0 & 0 \\ 0 & 0 & 0 & m_{15} & 0 & 0 & 0 & d_{15} & 0 \\ -f\lambda_Q & 0 & 0 & 0 & m_{20} & 0 & 0 & 0 & d_{20} \\ 0 & d_6 & 0 & 0 & 0 & m_{6,5} & d5_{156} & 0 & 0 \\ 0 & 0 & d_{15} & 0 & 0 & d5_{615} & m_{15,5} & 0 & 0 \\ 0 & 0 & 0 & d_{15} & 0 & 0 & 0 & m_{15,10} & d10_{2015} \\ 0 & 0 & 0 & 0 & d_{20} & 0 & 0 & d10_{1520} & m_{2010} \end{pmatrix}. \tag{A.28}$$

A.6 Higgs–Gluon Coupling Modification – GHGUT

Analogously to Sec. 4.4.2, we are interested in possible changes to the Higgs gluon coupling that arise from the additional states for the GHGUT setup in Chapter 3. After having determined the mass matrix in the 3-site model (Sec. 4.3.2) the modification from the exotics is found to be

$$\frac{\partial \log(\det M_{\text{exotic}})}{\partial v} = -\frac{v_{\text{SM}}}{f^2}\left(\frac{1}{\sqrt{1-\frac{v_{\text{SM}}^2}{f^2}}+\frac{m_\omega}{f}c_\omega^{\text{GHGUT}}}\right) \tag{A.29}$$

where c_ω^{GHGUT} is given below and incorporates the dependence on the three–site model parameters. It should be noted that for a vanishing VL mass $m_\omega \to 0$ the prediction becomes independent of the specific parameters.

$$c_\omega^{\text{GHGUT}} = \frac{d_{15}^2\left(d_{20}^2 - m_{20}m_{20,10}\right) - m_{15}\left(m_{20}\left(d10_{1520}d10_{2015} - m_{15,10}m_{20,10}\right) + d_{20}^2 m_{15,10}\right)}{d10_{1520}d_{15}d_{20}f\lambda_{\omega_L}\lambda_{\omega_R}} \tag{A.30}$$

This is the case for the contributions coming from the top quark sector, where

$$\frac{\partial \log\left(\det M_{\text{top}}\right)}{\partial v} = \frac{1}{v_{\text{SM}}}\sqrt{1-\frac{v_{\text{SM}}^2}{f^2}}\,. \tag{A.31}$$

The situation is different for the bottom partners, where the lightest mode is $m_b < m_h$, then

$$\delta g_{Hgg}^{\text{bottom}} \propto \frac{\partial \log(\det M_{\text{bottom}})}{\partial v} - \frac{y_b}{m_b}\,. \tag{A.32}$$

Here, y_b/m_b carries a parameter dependence

$$\frac{y_b}{m_b} = \frac{1}{m_b}\frac{\partial m_b}{\partial v} = \frac{1}{v_{\mathrm{SM}}}\sqrt{1-\frac{v_{\mathrm{SM}}^2}{f^2}} + c_b^{\mathrm{GHGUT}}\left(\frac{v_{\mathrm{SM}}}{f^2}+\mathcal{O}\left(\frac{c^{\mathrm{GHGUT}}}{f^4}\right)\right). \tag{A.33}$$

The first part of the expression is identical to $(\partial \log(\det M_{\mathrm{bottom}})/\partial v)$, so only the parameter–dependent part is left and we find

$$\delta g_{Hgg}^{\mathrm{bottom}} \approxeq c_b^{\mathrm{GHGUT}}\frac{v_{\mathrm{SM}}}{f^2} \tag{A.34}$$

where c_b^{GHGUT} is a complicated expression of the composite sector parameters. By evaluating $c_\omega^{\mathrm{GHGUT}}$ and c_b^{GHGUT} numerically it is possible to set bounds on the SSB scale f. However, as detailed in the Sec. 3.3.1, strong phenomenological constraints for f come from the violation of custodial symmetry, and compared to them the modifications of the Higgs–gluon coupling are negligible, which are currently measured with a precision of $\delta g_{hgg} \sim \pm 7\%$ ([112]).

List of Figures

List of Tables

Bibliography

[1] Serguei Chatrchyan et al. "Observation of a New Boson at a Mass of 125 GeV with the CMS Experiment at the LHC". In: *Phys. Lett. B* 716 (2012), pp. 30–61. DOI: 10.1016/j.physletb.2012.08.021. arXiv: 1207.7235 [hep-ex].

[2] Georges Aad et al. "Observation of a new particle in the search for the Standard Model Higgs boson with the ATLAS detector at the LHC". In: *Phys. Lett. B* 716 (2012), pp. 1–29. DOI: 10.1016/j.physletb.2012.08.020. arXiv: 1207.7214 [hep-ex].

[3] A. Masiero, S. K. Vempati, and O. Vives. "Flavour physics and grand unification". In: *Les Houches Summer School on Theoretical Physics: Session 84: Particle Physics Beyond the Standard Model*. Aug. 2005, pp. 1–78. arXiv: 0711.2903 [hep-ph].

[4] David B. Kaplan and Howard Georgi. "SU(2) x U(1) Breaking by Vacuum Misalignment". In: *Phys. Lett. B* 136 (1984), pp. 183–186. DOI: 10.1016/0370-2693(84)91177-8.

[5] Howard Georgi and David B. Kaplan. "Composite Higgs and Custodial SU(2)". In: *Phys. Lett. B* 145 (1984), pp. 216–220. DOI: 10.1016/0370-2693(84)90341-1.

[6] David B. Kaplan, Howard Georgi, and Savas Dimopoulos. "Composite Higgs Scalars". In: *Phys. Lett. B* 136 (1984), pp. 187–190. DOI: 10.1016/0370-2693(84)91178-X.

[7] Howard Georgi, David B. Kaplan, and Peter Galison. "Calculation of the Composite Higgs Mass". In: *Phys. Lett. B* 143 (1984), pp. 152–154. DOI: 10.1016/0370-2693(84)90823-2.

[8] Michael J. Dugan, Howard Georgi, and David B. Kaplan. "Anatomy of a Composite Higgs Model". In: *Nucl. Phys. B* 254 (1985), pp. 299–326. DOI: 10.1016/0550-3213(85)90221-4.

[9] Roberto Contino, Yasunori Nomura, and Alex Pomarol. "Higgs as a holographic pseudoGoldstone boson". In: *Nucl. Phys. B* 671 (2003), pp. 148–174. DOI: 10.1016/j.nuclphysb.2003.08.027. arXiv: hep-ph/0306259.

[10] Andrei Angelescu et al. "Minimal SU(6) gauge-Higgs grand unification". In: *Phys. Rev. D* 105.3 (2022), p. 035026. DOI: 10.1103/PhysRevD.105.035026. arXiv: 2104.07366 [hep-ph].

[11] Giuliano Panico and Andrea Wulzer. *The Composite Nambu-Goldstone Higgs*. Vol. 913. Springer, 2016. DOI: 10.1007/978-3-319-22617-0. arXiv: 1506.01961 [hep-ph].

[12] Florian Goertz. "Composite Higgs theory". In: *PoS* ALPS2018 (2018), p. 012. DOI: 10.22323/1.330.0012. arXiv: 1812.07362 [hep-ph].

[13] Steven Weinberg. "Implications of Dynamical Symmetry Breaking". In: *Phys. Rev. D* 13 (1976). [Addendum: Phys.Rev.D 19, 1277–1280 (1979)], pp. 974–996. DOI: 10.1103/PhysRevD.19.1277.

[14] Leonard Susskind. "Dynamics of Spontaneous Symmetry Breaking in the Weinberg-Salam Theory". In: *Phys. Rev. D* 20 (1979), pp. 2619–2625. DOI: 10.1103/PhysRevD.20.2619.

[15] Yoichiro Nambu. "Quasiparticles and Gauge Invariance in the Theory of Superconductivity". In: *Phys. Rev.* 117 (1960). Ed. by J. C. Taylor, pp. 648–663. DOI: 10.1103/PhysRev.117.648.

[16] Yoichiro Nambu and G. Jona-Lasinio. "Dynamical Model of Elementary Particles Based on an Analogy with Superconductivity. 1." In: *Phys. Rev.* 122 (1961). Ed. by T. Eguchi, pp. 345–358. DOI: 10.1103/PhysRev.122.345.

[17] J. Goldstone. "Field Theories with Superconductor Solutions". In: *Nuovo Cim.* 19 (1961), pp. 154–164. DOI: 10.1007/BF02812722.

[18] Jeffrey Goldstone, Abdus Salam, and Steven Weinberg. "Broken Symmetries". In: *Phys. Rev.* 127 (1962), pp. 965–970. DOI: 10.1103/PhysRev.127.965.

[19] James Barnard, Tony Gherghetta, and Tirtha Sankar Ray. "UV descriptions of composite Higgs models without elementary scalars". In: *JHEP* 02 (2014), p. 002. DOI: 10.1007/JHEP02(2014)002. arXiv: 1311.6562 [hep-ph].

[20] Gabriele Ferretti and Denis Karateev. "Fermionic UV completions of Composite Higgs models". In: *JHEP* 03 (2014), p. 077. DOI: 10.1007/JHEP03(2014)077. arXiv: 1312.5330 [hep-ph].

[21] Gabriele Ferretti. "UV Completions of Partial Compositeness: The Case for a SU(4) Gauge Group". In: *JHEP* 06 (2014), p. 142. DOI: 10.1007/JHEP06(2014)142. arXiv: 1404.7137 [hep-ph].

[22] Giacomo Cacciapaglia and Francesco Sannino. "Fundamental Composite (Goldstone) Higgs Dynamics". In: *JHEP* 04 (2014), p. 111. DOI: 10.1007/JHEP04(2014)111. arXiv: 1402.0233 [hep-ph].

[23] Luca Vecchi. "A dangerous irrelevant UV-completion of the composite Higgs". In: *JHEP* 02 (2017), p. 094. DOI: 10.1007/JHEP02(2017)094. arXiv: 1506.00623 [hep-ph].

[24] Francesco Sannino et al. "Fundamental partial compositeness". In: *JHEP* 11 (2016), p. 029. DOI: 10.1007/JHEP11(2016)029. arXiv: 1607.01659 [hep-ph].

[25] Giacomo Cacciapaglia et al. "Minimal Fundamental Partial Compositeness". In: *Phys. Rev. D* 98.1 (2018), p. 015006. DOI: 10.1103/PhysRevD.98.015006. arXiv: 1704.07845 [hep-ph].

[26] Alessandro Agugliaro and Francesco Sannino. "Real and Complex Fundamental Partial Compositeness". In: *JHEP* 07 (2020), p. 166. DOI: 10.1007/JHEP07(2020)166. arXiv: 1908.09312 [hep-ph].

[27] Giacomo Cacciapaglia, Claudio Pica, and Francesco Sannino. "Fundamental Composite Dynamics: A Review". In: *Phys. Rept.* 877 (2020), pp. 1–70. DOI: 10.1016/j.physrep.2020.07.002. arXiv: 2002.04914 [hep-ph].

[28] Florian Goertz, Álvaro Pastor-Gutiérrez, and Jan M. Pawlowski. "Flavour hierarchies from emergent fundamental partial compositeness". In: (July 2023). arXiv: 2307.11148 [hep-ph].

[29] Kaustubh Agashe, Roberto Contino, and Alex Pomarol. "The Minimal composite Higgs model". In: *Nucl. Phys. B* 719 (2005), pp. 165–187. DOI: 10.1016/j.nuclphysb.2005.04.035. arXiv: hep-ph/0412089.

[30] Brando Bellazzini, Csaba Csáki, and Javi Serra. "Composite Higgses". In: *Eur. Phys. J. C* 74.5 (2014), p. 2766. DOI: 10.1140/epjc/s10052-014-2766-x. arXiv: 1401.2457 [hep-ph].

[31] Curtis G. Callan Jr. et al. "Structure of phenomenological Lagrangians. 2." In: *Phys. Rev.* 177 (1969), pp. 2247–2250. DOI: 10.1103/PhysRev.177.2247.

[32] Sidney R. Coleman, J. Wess, and Bruno Zumino. "Structure of phenomenological Lagrangians. 1." In: *Phys. Rev.* 177 (1969), pp. 2239–2247. DOI: 10.1103/PhysRev.177.2239.

[33] David B. Kaplan. "Flavor at SSC energies: A New mechanism for dynamically generated fermion masses". In: *Nucl. Phys. B* 365 (1991), pp. 259–278. DOI: 10.1016/S0550-3213(05)80021-5.

[34] Savas Dimopoulos and Leonard Susskind. "Mass Without Scalars". In: *Nucl. Phys. B* 155 (1979). Ed. by A. Zichichi, pp. 237–252. DOI: 10.1016/0550-3213(79)90364-X.

[35] Kenneth Lane. "Two Lectures on Technicolor". In: (Feb. 2002). arXiv: hep-ph/0202255.

[36] Giuliano Panico et al. "On the Tuning and the Mass of the Composite Higgs". In: *JHEP* 03 (2013), p. 051. DOI: 10.1007/JHEP03(2013)051. arXiv: 1210.7114 [hep-ph].

[37] Riccardo Barbieri and G. F. Giudice. "Upper Bounds on Supersymmetric Particle Masses". In: *Nucl. Phys. B* 306 (1988), pp. 63–76. DOI: 10.1016/0550-3213(88)90171-X.

[38] Csaba Csaki, Teng Ma, and Jing Shu. "Maximally Symmetric Composite Higgs Models". In: *Phys. Rev. Lett.* 119.13 (2017), p. 131803. DOI: 10.1103/PhysRevLett.119.131803. arXiv: 1702.00405 [hep-ph].

[39] Csaba Csáki et al. "Emergence of Maximal Symmetry". In: *Phys. Rev. Lett.* 124.24 (2020), p. 241801. DOI: 10.1103/PhysRevLett.124.241801. arXiv: 1810.07704 [hep-ph].

[40] Simone Blasi and Florian Goertz. "Softened Symmetry Breaking in Composite Higgs Models". In: *Phys. Rev. Lett.* 123.22 (2019), p. 221801. DOI: 10.1103/PhysRevLett.123.221801. arXiv: 1903.06146 [hep-ph].

[41] Simone Blasi, Csaba Csaki, and Florian Goertz. "A natural composite Higgs via universal boundary conditions". In: *SciPost Phys.* 10.5 (2021), p. 121. DOI: 10.21468/SciPostPhys.10.5.121. arXiv: 2004.06120 [hep-ph].

[42] Hsin-Chia Cheng and Yi Chung. "A More Natural Composite Higgs Model". In: *JHEP* 10 (2020), p. 175. DOI: 10.1007/JHEP10(2020)175. arXiv: 2007.11780 [hep-ph].

[43] Gauthier Durieux, Matthew McCullough, and Ennio Salvioni. "Gegenbauer Goldstones". In: *JHEP* 01 (2022), p. 076. DOI: 10.1007/JHEP01(2022)076. arXiv: 2110.06941 [hep-ph].

[44] Armen Tumasyan et al. "Search for pair production of vector-like quarks in leptonic final states in proton-proton collisions at $\sqrt{s}$ = 13 TeV". In: *JHEP* 07 (2023), p. 020. DOI: 10.1007/JHEP07(2023)020. arXiv: 2209.07327 [hep-ex].

[45] Morad Aaboud et al. "Combination of the searches for pair-produced vector-like partners of the third-generation quarks at $\sqrt{s} = 13$ TeV with the ATLAS detector". In: *Phys. Rev. Lett.* 121.21 (2018), p. 211801. DOI: 10.1103/PhysRevLett.121.211801. arXiv: 1808.02343 [hep-ex].

[46] Georges Aad et al. "Search for pair-production of vector-like quarks in pp collision events at s=13 TeV with at least one leptonically decaying Z boson and a third-generation quark with the ATLAS detector". In: *Phys. Lett. B* 843 (2023), p. 138019. DOI: 10.1016/j.physletb.2023.138019. arXiv: 2210.15413 [hep-ex].

[47] Albert M Sirunyan et al. "Search for pair production of vectorlike quarks in the fully hadronic final state". In: *Phys. Rev. D* 100.7 (2019), p. 072001. DOI: 10.1103/PhysRevD.100.072001. arXiv: 1906.11903 [hep-ex].

[48] Georges Aad et al. "Search for single production of a vectorlike T quark decaying into a Higgs boson and top quark with fully hadronic final states using the ATLAS detector". In: *Phys. Rev. D* 105.9 (2022), p. 092012. DOI: 10.1103/PhysRevD.105.092012. arXiv: 2201.07045 [hep-ex].

[49] Roberto Contino, Leandro Da Rold, and Alex Pomarol. "Light custodians in natural composite Higgs models". In: *Phys. Rev. D* 75 (2007), p. 055014. DOI: 10.1103/PhysRevD.75.055014. arXiv: hep-ph/0612048.

[50] Oleksii Matsedonskyi, Giuliano Panico, and Andrea Wulzer. "Light Top Partners for a Light Composite Higgs". In: *JHEP* 01 (2013), p. 164. DOI: 10.1007/JHEP01(2013)164. arXiv: 1204.6333 [hep-ph].

[51] David Marzocca, Marco Serone, and Jing Shu. "General Composite Higgs Models". In: *JHEP* 08 (2012), p. 013. DOI: 10.1007/JHEP08(2012)013. arXiv: 1205.0770 [hep-ph].

[52] Alex Pomarol and Francesco Riva. "The Composite Higgs and Light Resonance Connection". In: *JHEP* 08 (2012), p. 135. DOI: 10.1007/JHEP08(2012)135. arXiv: 1205.6434 [hep-ph].

[53] Adrian Carmona and Florian Goertz. "A naturally light Higgs without light Top Partners". In: *JHEP* 05 (2015), p. 002. DOI: 10.1007/JHEP05(2015)002. arXiv: 1410.8555 [hep-ph].

[54] Simone Blasi, Julian Bollig, and Florian Goertz. "Holographic composite Higgs model building: soft breaking, maximal symmetry, and the Higgs mass". In: *JHEP* 07 (2023), p. 048. DOI: 10.1007/JHEP07(2023)048. arXiv: 2212.11007 [hep-ph].

[55] Jogesh C. Pati and Abdus Salam. "Lepton Number as the Fourth Color". In: *Phys. Rev. D* 10 (1974). [Erratum: Phys.Rev.D 11, 703–703 (1975)], pp. 275–289. DOI: 10.1103/PhysRevD.10.275.

[56] H. Georgi and S. L. Glashow. "Unity of All Elementary Particle Forces". In: *Phys. Rev. Lett.* 32 (1974), pp. 438–441. DOI: 10.1103/PhysRevLett.32.438.

[57] A. Zee. *Group Theory in a Nutshell for Physicists*. USA: Princeton University Press, 2016. ISBN: 978-0-691-16269-0.

[58] H. Georgi, Helen R. Quinn, and Steven Weinberg. "Hierarchy of Interactions in Unified Gauge Theories". In: *Phys. Rev. Lett.* 33 (1974), pp. 451–454. DOI: 10.1103/PhysRevLett.33.451.

[59] Michael E. Peskin. "Beyond the standard model". In: *The 1996 European School of High-Energy Physics (formerly CERN / JINR School of Physics)*. May 1997, pp. 49–142. arXiv: hep-ph/9705479.

[60] Harald Fritzsch and Peter Minkowski. "Unified Interactions of Leptons and Hadrons". In: *Annals Phys.* 93 (1975), pp. 193–266. DOI: 10.1016/0003-4916(75)90211-0.

[61] Howard Georgi and Dimitri V. Nanopoulos. "Ordinary Predictions from Grand Principles: T Quark Mass in O(10)". In: *Nucl. Phys. B* 155 (1979), pp. 52–74. DOI: 10.1016/0550-3213(79)90355-9.

[62] Peter Minkowski. "$\mu \to e\gamma$ at a Rate of One Out of 10^9 Muon Decays?" In: *Phys. Lett. B* 67 (1977), pp. 421–428. DOI: 10.1016/0370-2693(77)90435-X.

[63] Tsutomu Yanagida. "Horizontal gauge symmetry and masses of neutrinos". In: *Conf. Proc. C* 7902131 (1979). Ed. by Osamu Sawada and Akio Sugamoto, pp. 95–99.

[64] Murray Gell-Mann, Pierre Ramond, and R. Slansky. "Color Embeddings, Charge Assignments, and Proton Stability in Unified Gauge Theories". In: *Rev. Mod. Phys.* 50 (1978), p. 721. DOI: 10.1103/RevModPhys.50.721.

[65] Rabindra N. Mohapatra and Goran Senjanovic. "Neutrino Mass and Spontaneous Parity Nonconservation". In: *Phys. Rev. Lett.* 44 (1980), p. 912. DOI: 10.1103/PhysRevLett.44.912.

[66] J. Schechter and J. W. F. Valle. "Neutrino Masses in SU(2) x U(1) Theories". In: *Phys. Rev. D* 22 (1980), p. 2227. DOI: 10.1103/PhysRevD.22.2227.

[67] David Tong. *Lecture notes on Particle Physics*. 2021.

[68] A. Takenaka et al. "Search for proton decay via $p \to e^+\pi^0$ and $p \to \mu^+\pi^0$ with an enlarged fiducial volume in Super-Kamiokande I-IV". In: *Phys. Rev. D* 102.11 (2020), p. 112011. DOI: 10.1103/PhysRevD.102.112011. arXiv: 2010.16098 [hep-ex].

[69] Andrei Angelescu et al. "SU(6) gauge-Higgs grand unification: minimal viable models and flavor". In: *JHEP* 04 (2023), p. 012. DOI: 10.1007/JHEP04(2023)012. arXiv: 2208.13782 [hep-ph].

[70] Lawrence J. Hall, Yasunori Nomura, and David Tucker-Smith. "Gauge Higgs unification in higher dimensions". In: *Nucl. Phys. B* 639 (2002), pp. 307–330. DOI: 10.1016/S0550-3213(02)00539-4. arXiv: hep-ph/0107331.

[71] Gustavo Burdman and Yasunori Nomura. "Unification of Higgs and Gauge Fields in Five Dimensions". In: *Nucl. Phys. B* 656 (2003), pp. 3–22. DOI: 10.1016/S0550-3213(03)00088-9. arXiv: hep-ph/0210257.

[72] Naoyuki Haba et al. "Dynamical symmetry breaking in gauge Higgs unification on orbifold". In: *Phys. Rev. D* 70 (2004), p. 015010. DOI: 10.1103/PhysRevD.70.015010. arXiv: hep-ph/0401183.

[73] C. S. Lim and Nobuhito Maru. "Towards a realistic grand gauge-Higgs unification". In: *Phys. Lett. B* 653 (2007), pp. 320–324. DOI: 10.1016/j.physletb.2007.07.053. arXiv: 0706.1397 [hep-ph].

[74] Nobuhito Maru and Yoshiki Yatagai. "Improving fermion mass hierarchy in grand gaugeHiggs unification with localized gauge kinetic terms". In: *Eur. Phys. J. C* 80.10 (2020), p. 933. DOI: 10.1140/epjc/s10052-020-08485-8. arXiv: 1911.03465 [hep-ph].

[75] Nobuhito Maru and Yoshiki Yatagai. "Fermion Mass Hierarchy in Grand Gauge-Higgs Unification". In: *PTEP* 2019.8 (2019), 083B03. DOI: 10.1093/ptep/ptz083. arXiv: 1903.08359 [hep-ph].

[76] Yutaka Hosotani and Naoki Yamatsu. "GaugeHiggs grand unification". In: *PTEP* 2015 (2015), 111B01. DOI: 10.1093/ptep/ptv153. arXiv: 1504.03817 [hep-ph].

[77] Atsushi Furui, Yutaka Hosotani, and Naoki Yamatsu. "Toward Realistic Gauge-Higgs Grand Unification". In: *PTEP* 2016.9 (2016), 093B01. DOI: 10.1093/ptep/ptw116. arXiv: 1606.07222 [hep-ph].

[78] Lisa Randall and Raman Sundrum. "A Large mass hierarchy from a small extra dimension". In: *Phys. Rev. Lett.* 83 (1999), pp. 3370–3373. DOI: 10.1103/PhysRevLett.83.3370. arXiv: hep-ph/9905221.

[79] Ignatios Antoniadis et al. "New dimensions at a millimeter to a Fermi and superstrings at a TeV". In: *Phys. Lett. B* 436 (1998), pp. 257–263. DOI: 10.1016/S0370-2693(98)00860-0. arXiv: hep-ph/9804398.

[80] Nima Arkani-Hamed, Savas Dimopoulos, and G. R. Dvali. "The Hierarchy problem and new dimensions at a millimeter". In: *Phys. Lett. B* 429 (1998), pp. 263–272. DOI: 10.1016/S0370-2693(98)00466-3. arXiv: hep-ph/9803315.

[81] H. Davoudiasl, J. L. Hewett, and T. G. Rizzo. "Bulk gauge fields in the Randall-Sundrum model". In: *Phys. Lett. B* 473 (2000), pp. 43–49. DOI: 10.1016/S0370-2693(99)01430-6. arXiv: hep-ph/9911262.

[82] V. A. Rubakov. "Large and infinite extra dimensions: An Introduction". In: *Phys. Usp.* 44 (2001), pp. 871–893. DOI: 10.1070/PU2001v044n09ABEH001000. arXiv: hep-ph/0104152.

[83] Csaba Csaki. "TASI lectures on extra dimensions and branes". In: *Theoretical Advanced Study Institute in Elementary Particle Physics (TASI 2002): Particle Physics and Cosmology: The Quest for Physics Beyond the Standard Model(s)*. Apr. 2004, pp. 605–698. arXiv: hep-ph/0404096.

[84] Raman Sundrum. "Tasi 2004 lectures: To the fifth dimension and back". In: *Theoretical Advanced Study Institute in Elementary Particle Physics: Physics in D $\geqq$ 4*. Aug. 2005, pp. 585–630. arXiv: hep-th/0508134.

[85] Csaba Csaki, Jay Hubisz, and Patrick Meade. "TASI lectures on electroweak symmetry breaking from extra dimensions". In: *Theoretical Advanced Study Institute in Elementary Particle Physics: Physics in D $\geqq$ 4*. Oct. 2005, pp. 703–776. arXiv: hep-ph/0510275.

[86] Tony Gherghetta. "Les Houches lectures on warped models and holography". In: *Les Houches Summer School on Theoretical Physics: Session 84: Particle Physics Beyond the Standard Model*. Jan. 2006, pp. 263–311. arXiv: hep-ph/0601213.

[87] Adam Falkowski. "About the holographic pseudo-Goldstone boson". In: *Phys. Rev. D* 75 (2007), p. 025017. DOI: 10.1103/PhysRevD.75.025017. arXiv: hep-ph/0610336.

[88] Tony Gherghetta. "A Holographic View of Beyond the Standard Model Physics". In: *Theoretical Advanced Study Institute in Elementary Particle Physics: Physics of the Large and the Small*. 2011, pp. 165–232. DOI: 10.1142/9789814327183_0004. arXiv: 1008.2570 [hep-ph].

[89] Roberto Contino. "The Higgs as a Composite Nambu-Goldstone Boson". In: *Theoretical Advanced Study Institute in Elementary Particle Physics: Physics of the Large and the Small*. 2011, pp. 235–306. DOI: 10.1142/9789814327183_0005. arXiv: 1005.4269 [hep-ph].

[90] Florian Goertz. "Higgs Physics in Warped Extra Dimensions". In: *46th Rencontres de Moriond on Electroweak Interactions and Unified Theories*. May 2011, pp. 491–494. arXiv: 1105.6070 [hep-ph].

[91] Kaustubh Agashe and Geraldine Servant. "Baryon number in warped GUTs: Model building and (dark matter related) phenomenology". In: *JCAP* 02 (2005), p. 002. DOI: 10.1088/1475-7516/2005/02/002. arXiv: hep-ph/0411254.

[92] Kaustubh Agashe and Geraldine Servant. "Warped unification, proton stability and dark matter". In: *Phys. Rev. Lett.* 93 (2004), p. 231805. DOI: 10.1103/PhysRevLett.93.231805. arXiv: hep-ph/0403143.

[93] Alex Pomarol. "Grand unified theories without the desert". In: *Phys. Rev. Lett.* 85 (2000), pp. 4004–4007. DOI: 10.1103/PhysRevLett.85.4004. arXiv: hep-ph/0005293.

[94] Juan Martin Maldacena. "The Large N limit of superconformal field theories and supergravity". In: *Adv. Theor. Math. Phys.* 2 (1998), pp. 231–252. DOI: 10.4310/ATMP.1998.v2.n2.a1. arXiv: hep-th/9711200.

[95] S. S. Gubser, Igor R. Klebanov, and Alexander M. Polyakov. "Gauge theory correlators from noncritical string theory". In: *Phys. Lett. B* 428 (1998), pp. 105–114. DOI: 10.1016/S0370-2693(98)00377-3. arXiv: hep-th/9802109.

[96] Edward Witten. "Anti-de Sitter space and holography". In: *Adv. Theor. Math. Phys.* 2 (1998), pp. 253–291. DOI: 10.4310/ATMP.1998.v2.n2.a2. arXiv: hep-th/9802150.

[97] Herman L. Verlinde. "Holography and compactification". In: *Nucl. Phys. B* 580 (2000), pp. 264–274. DOI: 10.1016/S0550-3213(00)00224-8. arXiv: hep-th/9906182.

[98] Steven S. Gubser. "AdS / CFT and gravity". In: *Phys. Rev. D* 63 (2001), p. 084017. DOI: 10.1103/PhysRevD.63.084017. arXiv: hep-th/9912001.

[99] Erik P. Verlinde and Herman L. Verlinde. "RG flow, gravity and the cosmological constant". In: *JHEP* 05 (2000), p. 034. DOI: 10.1088/1126-6708/2000/05/034. arXiv: hep-th/9912018.

[100] Nima Arkani-Hamed, Massimo Porrati, and Lisa Randall. "Holography and phenomenology". In: *JHEP* 08 (2001), p. 017. DOI: 10.1088/1126-6708/2001/08/017. arXiv: hep-th/0012148.

[101] R. Rattazzi and A. Zaffaroni. "Comments on the holographic picture of the Randall-Sundrum model". In: *JHEP* 04 (2001), p. 021. DOI: 10.1088/1126-6708/2001/04/021. arXiv: hep-th/0012248.

[102] Manuel Perez-Victoria. "Randall-Sundrum models and the regularized AdS / CFT correspondence". In: *JHEP* 05 (2001), p. 064. DOI: 10.1088/1126-6708/2001/05/064. arXiv: hep-th/0105048.

[103] Roberto Contino et al. "Warped/composite phenomenology simplified". In: *JHEP* 05 (2007), p. 074. DOI: 10.1088/1126-6708/2007/05/074. arXiv: hep-ph/0612180.

[104] J. Wess and B. Zumino. "Consequences of anomalous Ward identities". In: *Phys. Lett. B* 37 (1971), pp. 95–97. DOI: 10.1016/0370-2693(71)90582-X.

[105] Edward Witten. "Global Aspects of Current Algebra". In: *Nucl. Phys. B* 223 (1983), pp. 422–432. DOI: 10.1016/0550-3213(83)90063-9.

[106] Chong-Sun Chu, Pei-Ming Ho, and Bruno Zumino. "NonAbelian anomalies and effective actions for a homogeneous space G/H". In: *Nucl. Phys. B* 475 (1996), pp. 484–504. DOI: 10.1016/0550-3213(96)00322-7. arXiv: hep-th/9602093.

[107] Giuliano Panico and Andrea Wulzer. "The Discrete Composite Higgs Model". In: *JHEP* 09 (2011), p. 135. DOI: 10.1007/JHEP09(2011)135. arXiv: 1106.2719 [hep-ph].

[108] Sidney R. Coleman and Erick J. Weinberg. "Radiative Corrections as the Origin of Spontaneous Symmetry Breaking". In: *Phys. Rev. D* 7 (1973), pp. 1888–1910. DOI: 10.1103/PhysRevD.7.1888.

[109] G. F. Giudice et al. "The Strongly-Interacting Light Higgs". In: *JHEP* 06 (2007), p. 045. DOI: 10.1088/1126-6708/2007/06/045. arXiv: hep-ph/0703164.

[110] Pouya Asadi et al. "Oblique Lessons from the *W* Mass Measurement at CDF II". In: (Apr. 2022). arXiv: 2204.05283 [hep-ph].

[111] James D. Wells and Zhengkang Zhang. "Effective theories of universal theories". In: *JHEP* 01 (2016), p. 123. DOI: 10.1007/JHEP01(2016)123. arXiv: 1510.08462 [hep-ph].

[112] R. L. Workman et al. "Review of Particle Physics". In: *PTEP* 2022 (2022), p. 083C01. DOI: 10.1093/ptep/ptac097.

[113] Andrei Angelescu et al. "Restoring Naturalness via Conjugate Fermions". In: (Sept. 2023). arXiv: 2309.05698 [hep-ph].

[114] Roberto Contino and Alex Pomarol. "Holography for fermions". In: *JHEP* 11 (2004), p. 058. DOI: 10.1088/1126-6708/2004/11/058. arXiv: hep-th/0406257.

[115] Albert M Sirunyan et al. "Search for pair production of vector-like quarks in the bW$\bar{\text{b}}$W channel from proton-proton collisions at $\sqrt{s} = 13$ TeV". In: *Phys. Lett. B* 779 (2018), pp. 82–106. DOI: 10.1016/j.physletb.2018.01.077. arXiv: 1710.01539 [hep-ex].

[116] A. M. Sirunyan et al. "Search for pair production of vector-like T and B quarks in single-lepton final states using boosted jet substructure in proton-proton collisions at $\sqrt{s} = 13$ TeV". In: *JHEP* 11 (2017), p. 085. DOI: 10.1007/JHEP11(2017)085. arXiv: 1706.03408 [hep-ex].

[117] Albert M Sirunyan et al. "Search for vector-like T and B quark pairs in final states with leptons at $\sqrt{s} = 13$ TeV". In: *JHEP* 08 (2018), p. 177. DOI: 10.1007/JHEP08(2018)177. arXiv: 1805.04758 [hep-ex].

[118] Albert M Sirunyan et al. "Search for vector-like quarks in events with two oppositely charged leptons and jets in proton-proton collisions at $\sqrt{s} = 13$ TeV". In: *Eur. Phys. J. C* 79.4 (2019), p. 364. DOI: 10.1140/epjc/s10052-019-6855-8. arXiv: 1812.09768 [hep-ex].

[119] M. Aaboud et al. "Search for pair production of heavy vector-like quarks decaying to high-p_T W bosons and b quarks in the lepton-plus-jets final state in pp collisions at $\sqrt{s} = 13$ TeV with the ATLAS detector". In: *JHEP* 10 (2017), p. 141. DOI: 10.1007/JHEP10(2017)141. arXiv: 1707.03347 [hep-ex].

[120] Morad Aaboud et al. "Search for pair production of vector-like top quarks in events with one lepton, jets, and missing transverse momentum in $\sqrt{s} = 13$ TeV *pp* collisions with the ATLAS detector". In: *JHEP* 08 (2017), p. 052. DOI: 10.1007/JHEP08(2017)052. arXiv: 1705.10751 [hep-ex].

[121] Morad Aaboud et al. "Search for new phenomena in events with same-charge leptons and b-jets in pp collisions at $\sqrt{s} = 13$ TeV with the ATLAS detector". In: *JHEP* 12 (2018), p. 039. DOI: 10.1007/JHEP12(2018)039. arXiv: 1807.11883 [hep-ex].

[122] Morad Aaboud et al. "Search for pair production of heavy vector-like quarks decaying into high-p_T W bosons and top quarks in the lepton-plus-jets final state in pp collisions at $\sqrt{s} = 13$ TeV with the ATLAS detector". In: *JHEP* 08 (2018), p. 048. DOI: 10.1007/JHEP08(2018)048. arXiv: 1806.01762 [hep-ex].

[123] M. Aaboud et al. "Search for pair production of heavy vector-like quarks decaying into hadronic final states in pp collisions at $\sqrt{s} = 13$ TeV with the ATLAS detector". In: *Phys. Rev. D* 98.9 (2018), p. 092005. DOI: 10.1103/PhysRevD.98.092005. arXiv: 1808.01771 [hep-ex].

[124] Morad Aaboud et al. "Search for pair production of up-type vector-like quarks and for four-top-quark events in final states with multiple b-jets with the ATLAS detector". In: *JHEP* 07 (2018), p. 089. DOI: 10.1007/JHEP07(2018)089. arXiv: 1803.09678 [hep-ex].

[125] Morad Aaboud et al. "Search for pair- and single-production of vector-like quarks in final states with at least one Z boson decaying into a pair of electrons or muons in pp collision data collected with the ATLAS detector at $\sqrt{s} = 13$ TeV". In: *Phys. Rev. D* 98.11 (2018), p. 112010. DOI: 10.1103/PhysRevD.98.112010. arXiv: 1806.10555 [hep-ex].

[126] John R. Ellis, Mary K. Gaillard, and Dimitri V. Nanopoulos. "A Phenomenological Profile of the Higgs Boson". In: *Nucl. Phys. B* 106 (1976), p. 292. DOI: 10.1016/0550-3213(76)90382-5.

[127] Aleksandr Azatov and Jamison Galloway. "Light Custodians and Higgs Physics in Composite Models". In: *Phys. Rev. D* 85 (2012), p. 055013. DOI: 10.1103/PhysRevD.85.055013. arXiv: 1110.5646 [hep-ph].

[128] Z. Chacko, Hock-Seng Goh, and Roni Harnik. "The Twin Higgs: Natural electroweak breaking from mirror symmetry". In: *Phys. Rev. Lett.* 96 (2006), p. 231802. DOI: 10.1103/PhysRevLett.96.231802. arXiv: hep-ph/0506256.

[129] Michael Geller and Ofri Telem. "Holographic Twin Higgs Model". In: *Phys. Rev. Lett.* 114 (2015), p. 191801. DOI: 10.1103/PhysRevLett.114.191801. arXiv: 1411.2974 [hep-ph].

[130] Riccardo Barbieri et al. "The Composite Twin Higgs scenario". In: *JHEP* 08 (2015), p. 161. DOI: 10.1007/JHEP08(2015)161. arXiv: 1501.07803 [hep-ph].

[131] Matthew Low, Andrea Tesi, and Lian-Tao Wang. "Twin Higgs mechanism and a composite Higgs boson". In: *Phys. Rev. D* 91 (2015), p. 095012. DOI: 10.1103/PhysRevD.91.095012. arXiv: 1501.07890 [hep-ph].

[132] A. D. Sakharov. "Violation of CP Invariance, C asymmetry, and baryon asymmetry of the universe". In: *Pisma Zh. Eksp. Teor. Fiz.* 5 (1967), pp. 32–35. DOI: 10.1070/PU1991v034n05ABEH002497.

Acknowledgements

Above all I want to thank Dr. Florian Goertz who allowed me to spend the last year in his research group, an experience I thoroughly enjoyed. Thank you for all the offered possibilities, and always being available for advice. Additional thanks go to Prof. Joerg Jaeckel, who agreed to be the second examiner of this thesis.

For the every day work at the institute I thank Andreas Bally and Andrei Angelescu for answering the many questions I brought to them. For sure my experience would have been very different without you. In general, this holds for many people of the Max–Planck Lindner division, who made the atmosphere both scientifically fruitful and socially welcoming.

Furthermore I thank Dr. Javier Rubio and his students Joan Bachs Esteban, Giorgio Laverda and Matteo Piani for hosting me and making me part of your group whenever I come to visit, be it in Lisbon or in Madrid.

I also thank my parents, my sister and Giorgio for supporting me and being there for me.